International Committee for Future Accelerators
Sponsored by the Particles and Fields Commission of IUPAP

Beam Dynamics Newsletter

No. 30

Issue Editors

Jie Wei and Lia Merminga

April 2003

Contents

1: Forewords

1.1 From the Chairman

John M. Jowett John.Jowett@cern.ch CERN

This issue of the ICFA Beam Dynamics Newsletter has been edited in a collaboration between Dr Jie Wei of Brookhaven National Laboratory and Dr Lia Merminga of Jefferson Lab. They have chosen the special theme of Electron-Ion Colliders. Regular readers will have noticed a small change in our editorial policy. In view of the continually shifting composition of the editorial team, it no longer makes much sense to list a half-dozen or so editors on the front cover. From now on, only the editors who compiled the current issue will be listed, together with the editors-in-chief who maintain overall continuity. Any member of the Beam Dynamics Panel may edit an issue, possibly in collaboration with other colleagues. The next issue will be edited by Dr Y. Funakoshi of KEK and will feature the topic of High Luminosity e^+ e^- colliders.

1.1.1 Changes in the Beam Dynamics Panel

Prof. Chuang Zhang of IHEP, Beijing, has expressed his wish to retire from the Panel after several years of valuable service. On behalf of the Panel and, I feel sure, the wider beam dynamics community, I would like to thank him for his efforts to promote beam dynamics activities and communications in the Asian region and worldwide. With his special expertise in e^+ e^- collider rings, he has played a particularly important role in our working groups and workshops in this area.

Prof. Kohji Hirata of Sokendai Graduate University (and formerly KEK) has also expressed his wish to retire from the Panel in summer 2003. Most readers will not need to be reminded that Kohji was Chairman of the Panel for several years, up to the end of 2001 and we owe him a considerable debt. Under his stewardship, the Panel's profile rose considerably, as it grew into the international institution we now know. The ICFA Beam Dynamics Newsletter was fully established, with regular publication and wide distribution and readership. Following the emergence of the World-Wide-Web, the Panel was quick to establish its presence there too. The total number of ICFA Advanced Beam Dynamics Workshops rose to 20; the quality control implicit in their approval procedure ensuring their prestige, topicality and a valuable legacy of published proceedings.

Surveying the topics of these workshops—or comparing the lists of attendees—it is evident that the field of beam dynamics covers several distinct specialities, from synchrotron light sources through high intensity hadron beams to lepton linear colliders. And, as usual in science, there is some risk that over-specialisation may inhibit those critical steps forward that, as often as not, involve some breaking down of barriers. While practitioners have plenty of opportunities to *communicate* nowadays, they may not have so many occasions to *work together* on advanced topics that overlap their sub-fields. As attested by the endorsement of ICFA, these opportunities are important for medium- and long-term progress in particle accelerators. The ICFA workshops are a vital means for the accelerator laboratories to husband their intellectual capital *especially while they are constrained* to focus on small numbers of specialised projects over periods of many years. Kohji's unceasing efforts to gain recognition of the value of beam dynamics *in itself* were a key to establishing the series and winning acceptance of these principles. While thanking him for what he achieved, it would be unwise to think that we can now take them for granted.

At its meeting in Tsukuba, Japan on 13 February 2003, ICFA approved Dr JiuQing Wang of IHEP, Beijing, as a new Panel member. In addition it approved Dr Junji Urukawa of KEK who will

assume his Panel membership in summer 2003. On behalf of the Panel, I would like to welcome these new Panel members.

1.1.2 Working group on Remote Experiments in Accelerator Physics (REAP)

At its meeting on 13 February 2003, ICFA also approved the formation of a new working group under the auspices of the Beam Dynamics Panel. Approval was based on a proposal prepared by Dr David Rice, in consultation with persons active in the field of remote operations

The mission statement of this group reads:

To promote collaborative accelerator physics experiments carried out using the evolving techniques of remote operation. It is intended that web based communication and collaborative decision-making will be an important part of the effort.

A link to the group's home page can be found on the Beam Dynamics Panel home page and reports on its activities will appear in this newsletter.

On behalf of the Panel, I would like to thank David Rice for his efforts to formulate the proposal bringing the working group into being and wish him and the other members of the new working group every success in their projects.

1.1.3 Summary of Partial Panel meeting

A partial meeting of the Beam Dynamics Panel was held at KEK on 12 February 2003.

Present: Y. Funakoshi, K. Hirata, S. Kamada, J.M. Jowett (Chair), E. Perevedentsev (representing Y. Shatunov), D. Rice.

J.M. Jowett presented a review of the Panel's activities. More details are available on the Panel's Web page: http://wwwslap.cern.ch/icfa/

Newsletter: Readers have welcomed recent issues of the Beam Dynamics Newsletter, featuring new issue editors and special themes. However there are often delays in printing and distribution of the paper edition and there is some need to update and coordinate the distribution lists maintained by the regional distributors. . Since the printing location changes with each issue, the teething problems have to be dealt with afresh each time. There was some discussion of ways to improve this. S. Kamada suggested that it may be faster and cheaper to print the newsletter locally in each region rather than shipping it in quantity from a single printing location. While it is still felt that the paper edition is a necessary means to reach important segments of our readership, new readers are generally directed towards the electronic edition. As always, Panel members and others are encouraged to write, propose and solicit articles of the usual types.

Working groups: the three existing working groups continue their activities, including mini-workshops, as reported elsewhere.

ICFA Advanced Beam Dynamics Workshops: 4 workshops were held in 2002 and have been reported on in the Beam Dynamics Newsletter. One workshop has already been held in 2003 and two more are scheduled. Proceedings are either already published or in preparation.

David Rice presented the proposal for a new working group on "Remote Experiments in Accelerator Physics" that was to be proposed to ICFA the following day (see the notice of approval above), outlining the expected membership and aims.

There was some discussion as to whether the subject was appropriate for the Beam Dynamics Panel. However this was precisely one of the reasons for limiting the scope of what had originally been conceived as a working group on the broader subject of "Remote Operation" to something falling squarely within our activities.

Y. Funakoshi discussed activities of the Panel in the Asian region. Panel members from the Asian region are well represented in the Panel's working groups, particularly the one on High Luminosity e^+ e^- colliders. Accelerator laboratories throughout the region are strongly encouraged to participate in the Panel's activities, particularly through contributions to the Newsletter.

Y. Funakoshi has volunteered to edit the August 2003 issue of the Beam Dynamics Newsletter.

K. Hirata expressed his wish to retire from the Panel in the summer.

The next meeting of the ICFA Beam Dynamics Panel will be held at the Particle Accelerator Conference in Portland, Oregon, USA, on 13 May 2003.

2: Letters to the Editors

2.1 From A. M. Sessler: Professional Ethics

Andrew M. Sessler amsessler@lbl.gov Lawrence Berkeley Laboratory

Through the years many of my colleagues have approached me with various ethical questions. To some of you that may seem reasonable, but I suspect that to the majority of you, it is surprising to learn that in our rather "dry field" there are ever any questions of ethics.

The questions, more accurately the "concerns" fall into two general categories of unethical behavior. The first has to do with "stealing an idea". Someone has learned of the work of my colleague — perhaps through a third party, or perhaps through an informal conversation, or perhaps by reading a "technical note" (not a "real publication"). This person decides it is a very interesting thought, and immediately does lots of analytic work (or perhaps has numerical programs that can immediately be "turned on") and in very short order writes a paper. My colleague feels very hurt. Often a third party is needed to establish a collaboration, or delay publication so my colleague's paper can appear "side by side" with the other paper, or – at least – have proper reference inserted as to the origin of the idea.

A related ethical concern – an annoyance, but not a major infraction of ethical behavior – is the repeated publishing of the same idea. That is rather easy to do in this modern age, where contributions to Conference Proceedings are not refereed. Repeated publication is often done because travel approval to the Conference requires that a paper be presented and the poor person has nothing new to report. Presenting new work, detailed work not suitable for a refereed journal, is very useful. Significant new work, should, of course, be published in refereed journals, but many "don't get around to it". As a result of repeated publication in non-refereed Proceedings, listing these publications on one's cv means little; even if it should. We are experiencing, unfortunately, a general "watering down" of the scientific literature.

The second has to do with authorship. It sometimes takes the form that the leader of the group desires to have his name on a paper my colleague is writing. Perhaps the leader wants to (still) be known as an active physicist or, perhaps, the leader feels that since he brought in the money for the research and made presentations on it to the funding agents and laboratory officials, he deserves to be a co-author. Telling your boss, "no" is not easy and it is even difficult for a third party. Sometimes the case of authorship that I am asked about concerns marginal contributions by a person who has explicitly asked to be a co-author. Usually, in these cases, a third party can be effective.

The American Physical Society has an ethics statement about authorship that is very clear: "Authorship should be limited to those who have made a significant contribution to the concept, design, execution or interpretation of the research study. All those who have made significant contributions should be offered the opportunity to be listed as authors. Other individuals who have contributed to the study should be acknowledged, but not identified as authors." This statement can often be used to good advantage in handling authorship problems.

Now, a new ethical subject has entered our field; namely, out-and-out fraud. Sure, we have long had misguided physicists who advocate, write papers, give talks, on various crazy things. We know how to handle them, and these guys do no damage. But the recent two cases of fraud are very different; they have caused almost unmeasurable harm, embarrassment, poor publicity, extensive time and effort, and monetary resources. One case was in condensed matter physics, but the other is much closer to home; namely the fabrication of data that led to the (incorrect) announcement of

the discovery of element 118.

In both cases, one person was responsible for the data analysis, fabricated the data, and his work was not checked by the other co-authors. Obviously, fraud is unethical, but also the co-authors bear some responsibility. They didn't exercise (understandably in these first cases of fraud) proper professional behavior. This has led the APS at its Council Meeting (last November), after much discussion and deep consideration, to augment its ethics statement. The additions bear the attention of each of us, for they delineates behavior that generally has not been the practice. The additions:

"SUPPLEMENTARY GUIDELINES ON RESPONSIBILITIES OF
COAUTHORS AND COLLABORATORS

All collaborators share some degree of responsibility for any paper they co-author. Some co-authors have responsibility for the entire paper as an accurate, verifiable, report of the research. These include, for example, co-authors who are accountable for the integrity of the critical data reported in the paper, carry out the analysis, write the manuscript, present major findings at conferences, or provide scientific leadership for junior colleagues.

Co-authors who make specific, limited, contributions to a paper are responsible for them, but may have only limited responsibility for other results. While not all co-authors may be familiar with all aspects of the research presented in their paper, all collaborations should have in place an appropriate process for reviewing and ensuring the accuracy and validity of the reported results, and all co-authors should be aware of this process.

Every co-author should have the opportunity to review the manuscript before its submission. All co-authors have an obligation to provide prompt retractions or correction of errors in published works. Any individual unwilling or unable to accept appropriate responsibility for a paper should not be a co-author.

SUPPLEMENTARY GUIDELINE ON RESEARCH RESULTS

Collaborations are expected to have a process to archive and verify the research record; to facilitate internal communication and allow all authors to be fully aware of the entire work; and respond to questions concerning the joint work and enable other responsible scientists to share the data. All members of a collaboration should be familiar with, and understand, the process."

The full APS Statements on Ethics and Values can be found at:

http://www.aps.org/statements/02.2.html

It is perhaps unfortunate, but understandable, that we must be concerned with ethics. I believe that more of us need to be overtly conscious of the subject. We need, in instructing young workers and students, not only to teach them mathematical methods, numerical procedures, experimental techniques, but also proper professional behavior. All of these elements are necessary for the further advancement of our beloved field of physics.

3: Special Section - Electron-Ion Colliders

3.1 Introduction

Lia Merminga merminga@jlab.org CASA, Jefferson Lab, Newport News, VA 23606 USA

Jie Wei jwei@bnl.gov Collider-Accelerator Department, Brookhaven National Laboratory, Upton, NY 11973, USA

Thirty years after the establishment of QCD as the theory of the strong nuclear interaction, and despite significant achievements in our knowledge of the structure of hadronic matter in the intervening decades, understanding how QCD works in practice remains one of the great puzzles in nuclear physics. Some crucial questions in the field remain open and involve the role and behavior of quarks and gluons in atomic nuclei. There are still gaps in our understanding of how quarks and gluons provide the binding and the spin of the nucleon, of how quarks and gluons evolve into hadrons via the dynamics of confinement, and of how the nuclear binding arises from QCD. Further, there is interest in exploring a new class of physical phenomena, including the hypothesized new state of matter called "Color Glass Condensate." The nuclear physics community worldwide has suggested that a polarized electron-ion collider with variable center-of-mass energy in the range of 20 to 100 GeV and luminosity at or above 10^{33} cm^{-2} sec^{-1} would be a powerful new microscope to probe the hadronic structure of matter, and provide answers to these questions.

This issue of the Beam Dynamics Newsletter devotes a special section to recent work on electron-ion colliders and electron cooling, which, as we will see below, is an integral part of future designs of electron-ion colliders.

Two accelerator design scenarios are being explored for a high luminosity, high polarization collider: the scheme of colliding storage rings and the linac-ring scheme, with the electron beam generated from a polarized source and accelerated in a superconducting, energy recovering linac (ERL). A critical challenge of the storage ring scenario is related to the complexity of preserving and manipulating the electron spin, while the challenge of the linac-ring option stems from the necessity to generate, accelerate and energy recover a high bunch charge, high average current polarized electron beam.

Detailed initial parameters have been worked out for eRHIC, which is based on the existing RHIC machine and would require the construction of a 5-10 GeV electron accelerator (either a storage ring or an ERL), and for ELIC, which is based on CEBAF, and would require the construction of a 50-100 GeV ion storage ring.

To achieve luminosities above10^{32} cm^{-2} sec^{-1} in all these schemes, electron cooling is required to overwhelm intrabeam scattering (IBS), in both transverse and longitudinal degrees of freedom. Electron cooling at such high energies can only be conceived in the context of superconducting RF (SRF) ERLs, and BNL, in collaboration with Budker Institute and JLab, is pursuing the development of an electron cooling prototype for the heavy ions at RHIC. A luminosity increase of RHIC by an order of magnitude is expected through cooling.

The section on electron-ion colliders opens with a comprehensive report on experience with an existing electron-proton collider, HERA at DESY. The storage ring scenario of eRHIC is discussed next, followed by a description of the two ERL-based schemes, eRHIC and ELIC. The following section is devoted to electron cooling, with an introduction to the subject by Skrinsky, reports on electron cooling activities from Fermilab and BNL, and a concluding contribution by Derbenev, presenting an outlook of the ultimate luminosity potential of these colliders under electron cooling. The last section is a collection of physics and technology challenges and R&D topics that the

designers of the future electron-ion colliders are facing and exploring. These topics include high current and high polarization electron sources, polarized ion sources, ERLs, including a short description of the recent GeV-scale demonstration of energy recovery that took place at CEBAF. The concept of circulator rings, which promises to ease photoinjector and ERL requirements in the ERL-based designs is introduced, and the current thinking and recent progress on spin dynamics, interaction region issues, beam-beam, electron cloud and IBS are presented.

3.2 Experiences with the HERA beams

Georg Hoffstaetter gh77@cornell.edu Cornell University, Ithaca, New York, USA
Mathias Vogt mathias.vogt@desy.de DESY, Hamburg, Germany
Ferdinand Willeke ferdinand.willeke@desy.de DESY, Hamburg, Germany

(for the HERA Luminosity Upgrade Group)

After the design luminosity of the electron-proton collider HERA had been exceeded [1,2], the interaction regions were rebuilt to obtain smaller β* at the two interaction points (IPs) [3,4,5]. Spin rotators on both sides of the IPs were installed to achieve collisions with longitudinal electron or positron polarization. Since the new interaction regions incorporate combined function magnets within the experimental solenoids' fringe fields, it is not trivial to achieve the longitudinal spin alignment with the precision required to avoid depolarization of the beam. Data is here presented, illustrating that this precision has been achieved. The desired increase in specific luminosity was quickly obtained after the upgrade of the interaction regions (IRs), but operating the detectors with full beam currents has not been possible due to too large background signals in H1 and in ZEUS. Currently a number of improvements are being implemented to reduce this background. The tests that are presented here show how the planed increase of the beam currents should translate into an increased absolute luminosity. In this context, experiences with the beam-beam force in HERA are important and will be described.

3.2.1 HERA

With a length of 6335 m, HERA is the largest accelerator at DESY in Hamburg. It provides collisions between a 920 GeV proton beam and a 27.5 GeV polarized electron or positron beam and supplies four high energy physics experiments. Since all data that will be shown has been obtained with positrons, we only refer to positrons in the following, even though HERA can also accelerated electrons. H1 and ZEUS are the world's only high-energy e/p collider experiments; HERMES and HERA-B have a fixed target. HERA-B scrapes the proton halo with wires, and HERMES has a polarized gas storage cell target in the polarized electron or positron beam to analyze the polarized quark-gluon-structure of the nucleons. Before the IR-upgrade, HERMES was the only experiment which could take advantage of the typically 60% polarization of the electron or positron beam, since only around this experiment spin rotators brought the spins in a longitudinal direction. Now, 6 spin rotators align the positron polarization longitudinally in H1 and ZEUS as well.

3.2.2 HERA Upgrade

For equal proton emittances $\varepsilon_{px} = \varepsilon_{py}$ and assuming that the proton beam sizes at the interaction point can always be matched by the positron beam ($\sigma_{ex/y} = \sigma_{px/y}$), the following equation

Table 3.1: HERA operations and upgrade parameters.

Parameters	HERA I		Design goal HERA II		Achieved	
	e-ring	p-ring	e-ring	p-ring	e-ring	p-ring
E(GeV)	27.5	920	27.5	920	27.5	920
I(mA)	50	106	58	140	10-40	20-100
$N_{ppb}(10^{10})$	3.5	7.3	4.0	10.3	1-3.5	4-7.5
n_{tot}	189	180	189	180	10-189	10-180
n_{col}	174	174	174	174	10-174	10-174
β_x*(m)	0.90	7.0	0.63	2.45	0.63	2.45
β_y*(m)	0.60	0.5	0.26	0.18	0.26	0.18
ε_x(nm)	41	5000/$\beta\gamma$	20	5000/$\beta\gamma$	20	4000/$\beta\gamma$
$\varepsilon_y/\varepsilon_x$	10%	1	17%	1	15%	1
$\sigma_x/\sigma_y(\mu$m)	192/50	189/50	112/30	112/30	113/25	
σ_z(mm)	11.2	191	10.3	191	-	150-200
$2\Delta\nu_x$	0.024	0.0026	0.068	0.0031	-	-
$2\Delta\nu_y$	0.060	0.0007	0.103	0.0009	-	-
Polarization	60%	0%	45%	0%	50%	0%
Ls	$6.70{\cdot}10^{29}$		$17.9{\cdot}10^{29}$		$24{\cdot}10^{29}$	
L	$0.172{\cdot}10^{32}$		$0.744{\cdot}10^{32}$		$0.27{\cdot}10^{32}$	

$$L = \frac{N^p_{ppb}}{\in_{px}} \frac{I_e}{4\pi e} \frac{1}{\sqrt{\beta^*_{px}\beta^*_{py}}}$$

shows that the luminosity can be increased by boosting the brightness $N^p_{ppb}/\varepsilon_{px}$ of the p beam, by increasing the e current I_e, or by a decrease of the proton beta functions $\beta^{\rm q}_{px}$ and $\beta^{\rm q}_{py}$ at the collision points. These three measures have been found to be about equally expensive, but modifying the interaction region for obtaining smaller betas was themethod of choice. In order to focus the proton beam stronger in the experimental region, the positron beam has to be separated from the proton beam as early as possible [3,4,5,6]. Whereas the first proton quadrupole had been 26 m after the IP, this distance is now 11m. Additionally the upgrade project included 60 m long spin rotators at both sides of the H1 and ZEUS detectors. The complete upgrade involved 448 m of new vacuum pipes, 4 superconducting magnets for early separation of the e and p beams inside the detectors with a distance of only 2 m from the IP, and 54 normal conducting magnets. The superconducting magnets have been built by BNL, and the Efremov Institute in St. Petersburg has built the normal conducting magnets.

Important parameters of previous HERA operation and the design parameters of the upgraded HERA are shown in Table 3.1. The achieved polarization and the achieved luminosities are discussed below. Since the specific and the absolute luminosities **L**s and **L** were not obtained with the same set of parameters, the last two columns are only partially filled.

3.2.3 Polarization

Before the IRs were rebuilt, 60% positron polarization were routinely obtained. Due to the radiative Sokolov-Ternov buildup of polarization, the radiation is vertical in HERA's arcs. While a pair of dipole spin rotators rotated the polarization to the longitudinal direction in HERMES already since 1994 [7], the polarization in H1 and ZEUS used to be transverse. The experimental

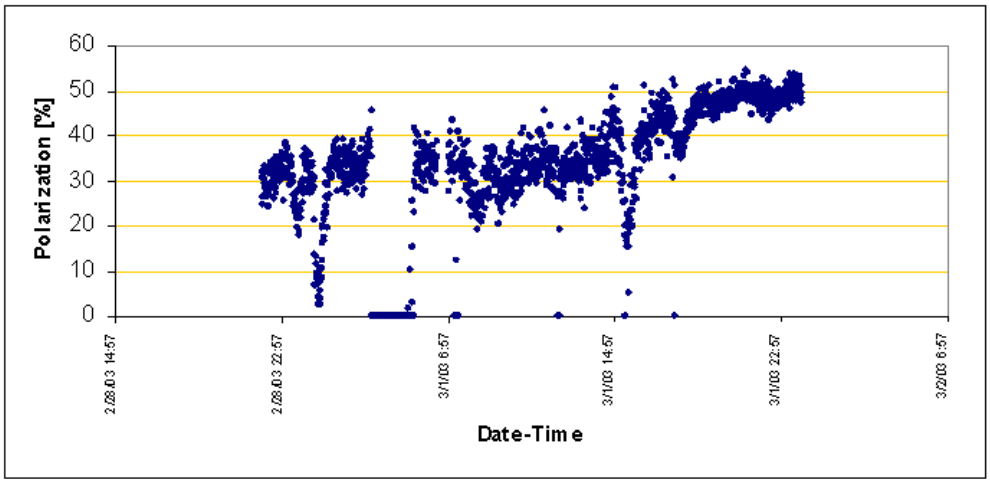

Figure 3.1: Polarization optimizations with 3 pairs of spin rotators in HERA-e on the 1st of March 2003. A polarization of 54% was ultimately obtained.

solenoids rotated this polarization around the longitudinal direction, but a counter solenoid subsequently compensated this perturbing effect so that the vertical polarization coming from one arc arrived vertical at the following arc after passing through the IR. For lack of space, the new IRs do not have counter solenoids and a vertical spin coming from one arc would not arrive vertically at the next arc if it were not rotated first, to be longitudinal in each IP's have counter solenoids and a vertical spin coming from one arc would not arrive vertically at the next arc if it were not rotated first, to be longitudinal in each IP's solenoid. With the new IRs, an accurate setting of the newly installed spin rotators right and left of H1 and ZEUS is therefore essential to obtain a polarized beam in HERA [8]. Obtaining such an accurate setting is not trivial since the spins move in the superimposed fields of combined function magnets and the fringe fields of the solenoids, which are not very accurately know. Nevertheless, 54% polarization was quickly achieved after all 3 pairs of spin rotators of HERA were switched on. Figure 3.1 shows the successful optimization of polarization.

3.2.4 Luminosity

The required specific luminosity was reached relatively early on [9,10], when the polarization was not optimized and when the beam currents were low, so that the background in the detectors was not a limiting factor. Figure 3.2 shows that specific luminosities were reached that are higher than the design goal. For typical proton beam intensities as reached during the year 2000 running, the specific luminosity is close to the design value.

The highest absolute luminosity of $2.7 \cdot 10^{31}/\mathrm{cm}^2/\mathrm{s}$ that has been reached is illustrated in Fig. 3.3 (left). It is shown that the achieved luminosity varies linearly with the product of the proton bunch current and the total positron current. The right hand side of Fig. 3.3 shows the luminosity that would be expected if one scales to 174 colliding bunches, as a function of the product of the bunch currents. Up to values corresponding to the year 2000 bunch intensities, there is also a linear dependence. This indicates that the beam-beam force does not pose a limit up to this level of intensity. Up to now, the product of the proton and the positron beam current has been limited by the detector backgrounds, but after the installation of improved shielding by the end of June 2003 [11,12], nominal beam currents should be achievable. Figure 3.3 suggests that without

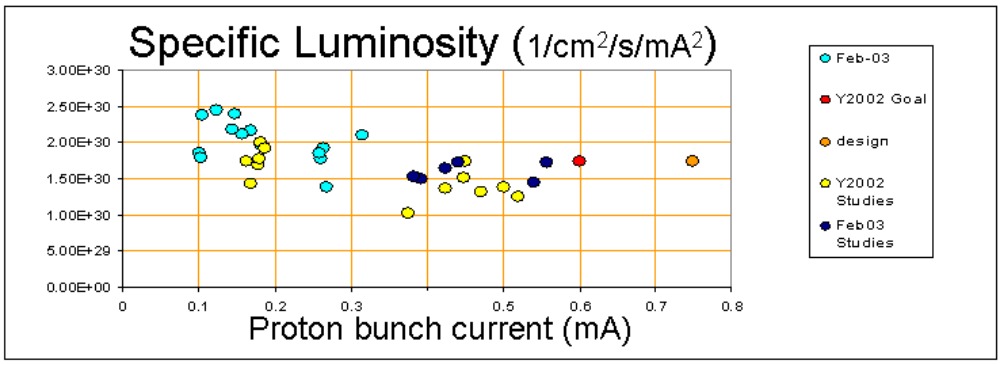

Figure 3.2: Specific luminosity versus proton bunch current.

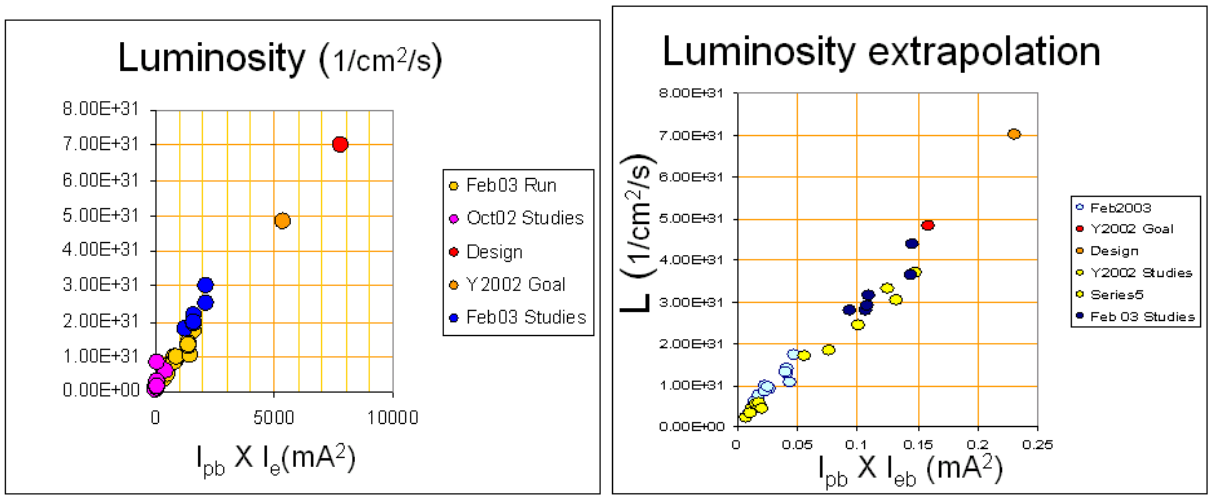

Figure 3.3: Achieved absolute luminosity as a function of the product of the proton bunch current and the total positron current (left). Expected luminosity when the positron current is scaled to its design value. Note that this does not change the beam-beam force for the positrons.

this limitation on the total beam currents, a luminosity of about $5{\cdot}10^{31}/\mathrm{cm}^2/\mathrm{s}$ should therefore be achievable. No luminosity data are available yet for proton bunch intensities that exceed the year 2000 values.

3.2.5 Observations about the Beam-Beam Interaction

While it has been observed that the proton lifetime decreases and the halo production, as measured by the wire of the HERA-B target, increases with increasing positron bunch current [13,14], the luminosity has not been shown to be deteriorated strongly by the beam-beam force acting on the protons. This indicates that the nonlinear beam-beam force affects protons with large transverse amplitudes, whereas it does not yet deteriorate the core of the proton bunches. Furthermore the resonance strength of proton dynamics including the influence of the hourglass effect on the proton's beam-beam force has been studied for the parameters of the new IRs [15,16].

Before HERA's IRs were changed, it was investigated whether the beam-beam force deteriorates the positron beam so that the specific luminosity would diminish with increasing positron bunch current. As shown in Fig. 3.4, such a correlation was not observed when plotting the specific

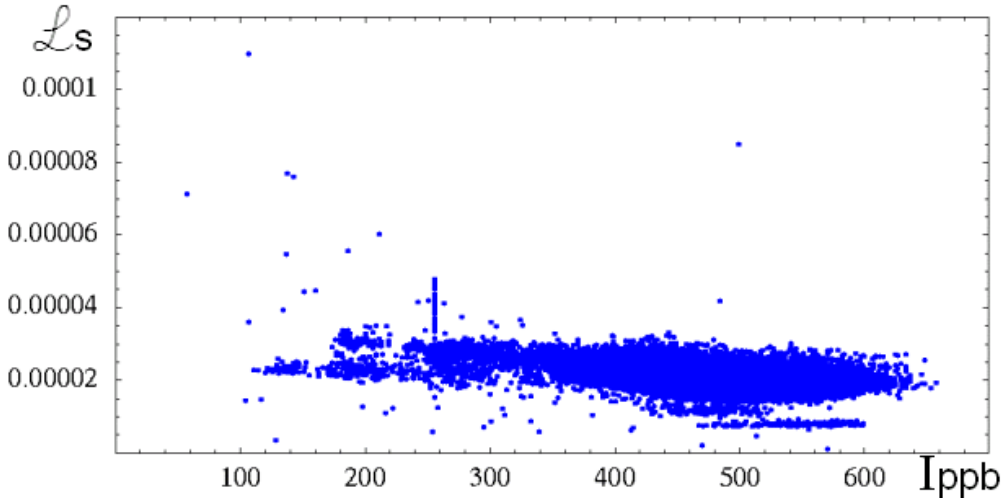

Figure 3.4: The specific luminosity Ls (arbitrary units) for each colliding bunch against the proton bunch current I_p(A) as obtained by H1.

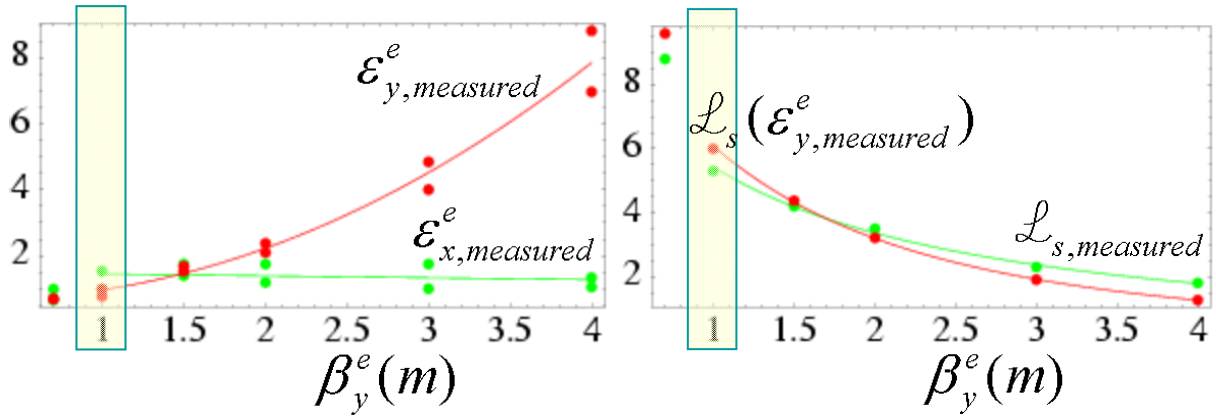

Figure 3.5: Measured emittances of the positron beam as a function of vertical beta function (left). Measured and computed specific luminosity (right).

luminosities as a function of proton bunch current for all runs of the first four months of the year 2000.

Since the vertical beam-beam tune shift of the lepton beam will increase by 50% compared to the year 2000 operation, when nominal proton currents are filled, the tune shift limit has been explored with the old IRs by increasing the positrons' β^*_{ey} [17]. Values of β^*_{ex}= 2.5 m (corresponding to the expected horizontal tune shift with 140 mA of protons) and β^*_{ey}=1 m, 1.5 m, 3 m, and 4 m have been implemented and collided with a 90 mA proton beam. The e and p beam sizes were not matched. We observed a monotonically increasing blow-up of the vertical lepton emittance with increasing β^*_{ey} by factors up to 8 as shown in Fig. 3.5 (left). At the value of β^*_{ey}=1.5 m which corresponds to a vertical beam-beam tune shift of 0.069, the blow-up factor was 1.5. Figure 3.5 (right) shows the measured specific luminosity and the luminosity computed from the measured beam emittances. The lifetime and operation conditions were good even with the tune shift of 0.5. This is probably due to a depopulation of the bunch center. This is also indicated by the fact that the shift in the coherent oscillation frequency for β^*_{ex}=2.5 m and β^*_{ey}=4 m was measured to

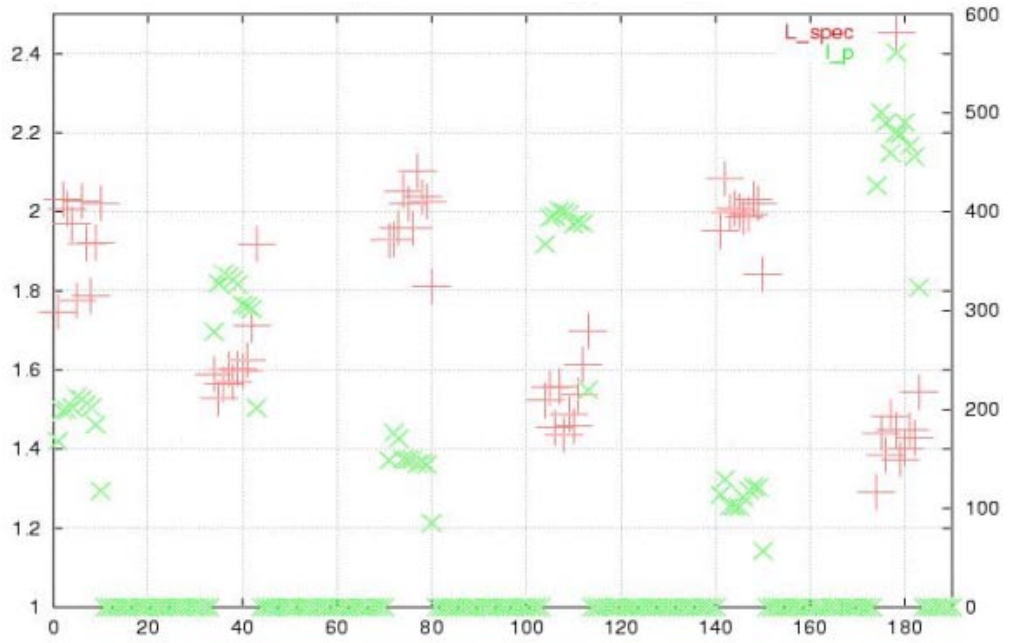

Figure 3.6: Specific luminosity (red, +) for different proton bunch currents (green, X).

be only $\Delta\nu_x$=0.009 and $\Delta\nu_y$=0.013 while it would be $\Delta\nu_x$=0.027 and $\Delta\nu_y$=0.082 if both beams were Gaussian. The latter values were computed with a simple formula for the coherent beam-beam tune shift for Gaussian beams of unequal sizes [13] in the weak-strong limit, i.e. under the assumption that the proton beam acts as a fixed nonlinear lens:

$$\Delta\nu_{ex} = \xi_{ex}\frac{\sigma_{px}(\sigma_{px}+\sigma_{py})}{\Sigma_x(\Sigma_x+\Sigma_y)}, \quad \Delta\nu_{ey} = \xi_{ey}\frac{\sigma_{py}(\sigma_{px}+\sigma_{py})}{\Sigma_y(\Sigma_x+\Sigma_y)},$$
$$\Sigma_x = \sqrt{\sigma_{ex}^2+\sigma_{px}^2}, \quad \Sigma_y = \sqrt{\sigma_{ey}^2+\sigma_{py}^2}\,.$$

Recent simulations with the specified beam parameters have yielded a coherent tune shift of $\Delta\nu_x$=0.003 and $\Delta\nu_y$=0.013. While the horizontal tune shift is close to the resolution of the calculation and therefore not very trustworthy, the agreement of the vertical tune shift with the measurement is quite remarkable [18].

In recent measurements with the new IRs, the beam-beam force on the e beam has influenced the luminosity adversely. Fig. 3.6 shows the specific luminosity and the proton bunch current for each e/p bunch pair for an irregularly filled HERA-p. It is very apparent that the pairs with higher proton current have lower specific luminosity. Furthermore Fig. 3.7 shows that the simple formula, given above, describes the coherent tune shift rather well for low proton bunch currents, indicating that the e beam has a Gaussian distribution. For larger proton bunch currents the tune shift deviates from the simple formula, indicating that the beam-beam force has altered the particle distribution of the e beam. This effect is being studied in more detail.

Since the beam-beam forces on the e beam become relevant, simulation studies of this effect are being continued and optical measures are being analyzed that should minimize the influence of the beam-beam forces in the two IPs.

References

[1] G. H. Hoffstaetter, “Future Possibilities for HERA”, Proceedings EPAC, Vienna (2000)

[2] G. H. Hoffstaetter and F. Willeke, “Future HERA High Luminosity Performance”, Proceedings HEACC01, Tsukuba (2001)

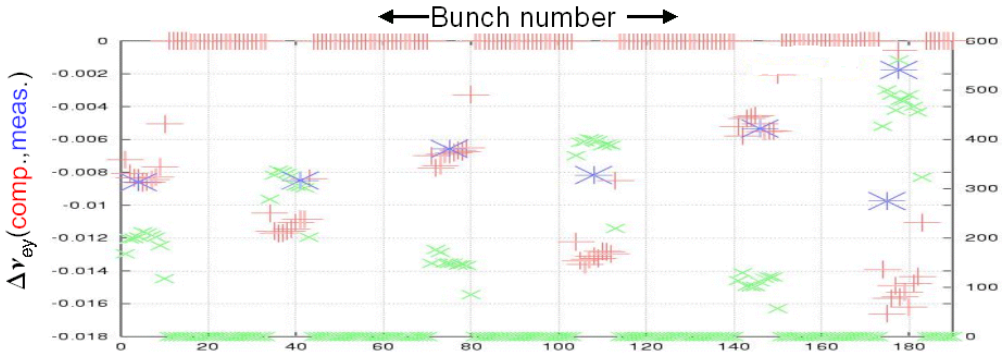

Figure 3.7: The vertical coherent tune shift ν_{ey} per bunch for different proton bunch currents (green, X): computed tune shift for all 60 bunches (red, +) and measured tune shifts for one bunch per train of 10 similar proton bunches (blue, +x).

[3] U. Schneekloth (ed.), "The HERA Luminosity Upgrade", Report DESY-HERA-98-05 (1998)

[4] M. Seidel, "The Upgraded Interaction Regions of HERA", Report DESY-HERA-00-01 (2000)

[5] M. Seidel, "Layout of the Upgraded HERA Interaction Regions", Proceedings of EPAC00, Vienna (2000)

[6] G. H. Hoffstaetter, "Electron Dynamics after the HERA Luminosity Upgrade", Proceedings EPAC 2000, Vienna (2000)

[7] D. P. Barber et al., "The first achievement of longitudinal spin polarization in a high energy electron storage ring", Phys.Letts., B343, p.436 (1995)

[8] M. Berglund, "Spin-orbit maps and electron spin dynamics for the luminosity upgrade project at HERA", Doctoral Thesis, Royal Institute of Technology, Stockholm, June 2001 and Report DESY-Thesis-2001-044 (2001)

[9] G. H. Hoffstaetter, "Luminosity Scans at HERA", Proceedings EPAC 2002, Paris (2002)

[10] M. Dohlus, G. H. Hoffstaetter, M. Lomperski, R. Wanzenberg, "Report from the HERA Taskforce on Luminosity Optimization. Theory and First Luminosity Scans", Report DESY-HERA-2003-01 (January 2003)

[11] "Further Report on Beam-Induced Backgrounds in the H1-Detector", Notes H1-10/02-606, H1-01/03-607 (2003)

[12] "Study of beam-induced backgrounds in the ZEUS detector from 2002 HERA running", Notes ZEUS-02-018, ZEUS-02-020, ZEUS-02-027 (2002)

[13] M. Bieler, E. Gianfelice, G. H. Hoffstaetter, T. Limberg, M.Minty, and F.Willeke, "Experiments about the Beam-Beam Effect at HERA", in [14] (2000)

[14] G. H. Hoffstaetter (ed.), "HERA Accelerator Studies 1999", Report DESY-HERA-00-02 (May 2000)

[15] G. H. Hoffstaetter and F. Willeke, "Beam-Beam Limit with Hourglass Effect in HERA", Proceedings EPAC 2002, Paris (2002)

[16] G. H. Hoffstaetter and F. Willeke, "Future HERA High Luminosity Performance", Proceedings of HEACC 2001, Tsukuba (2001)

[17] G. H. Hoffstaetter (ed.), "HERA Accelerator Studies 2000", Report DESY-HERA-00-07 (2000)

[18] Jack Shi, University of Kansas, Private communication (2002)

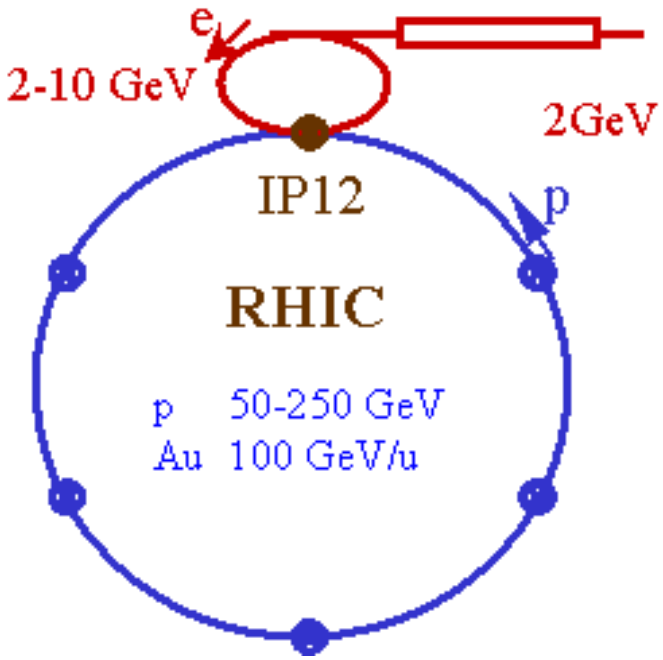

Figure 3.8: The general layout of the e-ring installed into the RHIC complex.

3.3 Storage Ring Options

3.3.1 Ring-Ring option of eRHIC

A. V. Otboev Budker Institute of Nuclear Physics, Novosibirsk, 630090, Russia

Yu. M. Shatunov shatunov@inp.nsk.su Budker Institute of Nuclear Physics, Novosibirsk, 630090, Russia

V. Ptitsyn vadimp@bnl.gov Brookhaven National Laboratory, Upton, NY 11973 USA

3.3.1.1 Introduction

In Brookhaven National Laboratory experiments at the new collider RHIC have successfully started with both ion-ion and polarized proton-proton beams [1]. To enhance the experimental capability of the RHIC complex, different schemes of polarized $e-p$collisions are under discussion at few last years. This paper presents a study of the ring-ring option of EIC, which have been developed in collaboration between BINP (Novosibirsk), BATES-MIT laboratory and BNL. We suggest (see the Fig. 3.8) to construct mainly outside the RHIC tunnel the electron storage ring which will have the circumference 4/15 of the RHIC orbit and an intersection with ions in the one of the existing RHIC experimental area (at 12 o'clock).

The injection into the electron ring will be done from a 2 GeV linac. After that the electron beam is accelerated to collisions energies (5-10 GeV) and acquires its polarization through the process of synchrotron radiation. The radiative polarization of the electron beam and a combination of solenoids and bending magnets will provide high degree of the longitudinal polarization of the electron beam in the IP.

The RHIC ion rings already have dedicated magnet insertions, Siberian Snakes and spin rota-

tors, in order to provide high energy polarized proton beam. In order to create longitudinal proton beam polarization for the e-p collisions additional pair of spin rotators should be installed around the e-p interaction region. Besides electron-proton collisions, electron-ion collisions involving fully stripped gold ions of 100 GeV per nucleon energy or lighter ions are interesting opportunity for physics.

3.3.1.2 Radiative Polarization And E-Ring Design

The radiative polarization has been observed at many electron storage rings. According to this experience the energy range of 5–10 GeV is quite comfortable for obtaining the polarization degree about 80 %.

A radiative polarization time strongly depends on the bending field ($\tau_p : B^{-3}$). On the other hand the high magnetic field increases energy losses for the synchrotron radiation ($\Delta E_{turn} : B^2$). We propose to use so-called super-bends magnets with relatively high field in a short central part of each magnet. It allows strongly decrease the polarization time at low energies and suppress spin resonances by the relatively minimal energy losses. The possible optimum is to use high field in the super-bends at low energy (so to keep the polarization time at the level of 15 minutes at 5 GeV) and the uniform field at 10 GeV.

We considered the e-ring which consists of two arcs with regular FODO structure and two straight sections: one for the beams collisions and other for a technical usage. To deliver spin longitudinal into the IP we need to install two spin rotators on both sides of the interaction area. We found a scheme of the focusing structure, that contains only regular quadrupoles inside the solenoid insertions and cancels the betatron coupling as well as creates the spin transparency.

To minimize the reconstruction of the RHIC rings while adding the new electron ring two possible schemes of the interaction region arrangement are proposed: so-called horizontal “dog-leg” scheme and vertical one [5]. After the solenoids spin precess around the vertical magnetic field (in case of horizontal “dog-leg” scheme) or around the horizontal magnetic field (in case of vertical “dog-leg” scheme), becoming at the medium energy 7.5 GeV purely longitudinal at the IP. Spin-transparency conditions which are needed for obtaining sufficient polarization degree in electron beam have been found for both options of the IP layout.

Calculations with the ASPIRRIN code [6] give the equilibrium polarization degree about 90% and the polarization time about 500 s at 10 GeV (in case of horizontal “dog-leg” scheme). But in the vertical “dog-leg” variant, despite of the spin transparency, the vertical bend initiates some spin resonances even in the ring without any imperfections. The situation is dramatically changed due to random vertical fluctuations of the arc quadrupoles positioning. The polarization does not exceed 50 percents with the RMS shift 0.5 mm [7]. The correction schemes to improve the polarization, like the harmonic correction developed and used successfully at HERA, should be considered in this case [8].

3.3.1.3 The Luminosity Consideration

Achieving the high luminosity value up to 1×10^{33} cm^{-2}s^{-1} needs a special consideration that has to take into account both a world wide experience of many machines, either electron’s and proton’s, and results of beam-beam interaction simulations. In particular, the simulations predict a number of advantages for round beam geometry by the collision due to a conservation of the angular momentum [2]. To satisfy the last requirement we should meet 2 conditions: equal beam sizes and equal tunes of betatron oscillations. Since origins of a forming of the beam emittances (ϵ_e; ϵ_i) are quite different, so as their dependences on the energy, lattices of the electron and ion

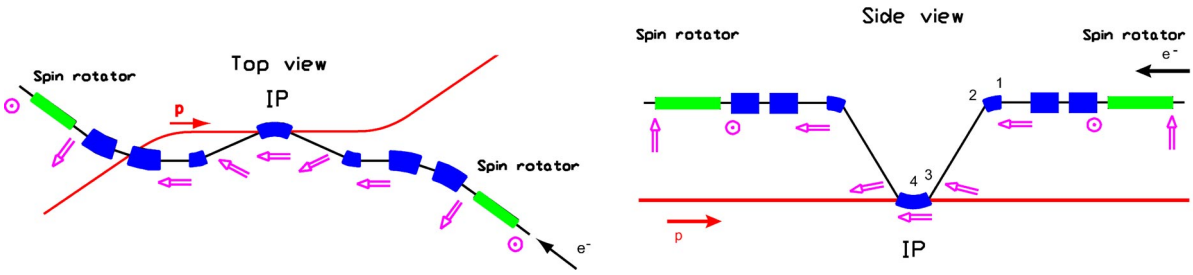

Figure 3.9: The layout of the e-ring interaction region.

Table 3.2: General parameters of the eRHIC.

Parameter	e-ring	ion ring	
		P	Au
Circumference, m	1022	3833	
Energy, GeV	5–10	250	100/u
Number of bunches	96	360	
Bunch population	$1 \cdot 10^{11}$	$1 \cdot 10^{11}$	$1 \cdot 10^{9}$
Beam current, A	0.45	0.45	
Beta function at IP, cm	10	27	
Beam size at IP, mm	0.07–0.05	0.07–0.05	
Beam-beam parameter	≤ 0.05	≤ 0.005	
Luminosity, cm^{-2}s^{-2}		(0.5-0.9)·10^{33}	(0.5-0.9)·10^{31}

rings have to provide some flexibility to control β^*-functions in the IP.

The world-wide experience shows that achievable values of the space charge parameters due to the beam-beam effects do not exceed 0.05 for electrons and 0.005 for protons. For electrons the most severe intensity threshold is set by the head-tail transverse mode-coupling instability, that limits the one bunch population. The modern accelerator experience (for instance, in both B-factories or LEP collider), tells us, that $N_e = 10^{11}$ is more or less a safe number. The proton bunch population is admitted to $N_p = 10^{11}$, which is based on BNL and FNAL experimental results.

The main parameters of the eRHIC for the current variants of electron and ion ring lattices are listed in the Table 3.2 for the cases of e-p and e-Au collisions.

In order to achieve and maintain during collisions the required Au beam emittance an electron cooling system should be developed and installed to the ion rings. A cooling also would be required for experiments involving proton beam with the energy below 200 GeV.

3.3.1.4 Conclusion

The present study shown that the ring-ring option of the electron-proton collider is able to provide the luminosity up to 0.9·10^{33} in the SCM energy range 15–100 GeV. The project of the electron ring with the super bend magnets and the solenoidal spin rotators performs to obtain not less 70 percents of the longitudinal polarization in the IP.

Two possible layouts of the interaction region are considered. The scheme with flat electron ring (horizontal “dog leg”) looks preferable for the electron polarization. A serious consideration of a new RHIC final focus design for the low beta is needed.

References

[1] D.Trbojevic *et al.*, in: *Proc. of EPAC 2002*, Paris, (2002), p.380; T. Roser *et al.*, in: *Proc. of EPAC 2002*, Paris, (2002), p.290.

[2] A.N. Filippov *et al.*, in: *Proc. 15th Int. Conf. High Energy Accelerators*, Hamburg (Germany), (1992), p.1145.

[3] Ya. Derbenev, A.M. Kondratenko, A.N. Skrinsky, *Sov. Phys. JETP*, **33**, 658 (1971).

[4] Ya.S. Derbenev, A.M. Kondratenko and A.N. Skrinsky, "Radiative polarization at ultra-high energies"', in *Particle Accelerators*, **9**, 247 (1979).

[5] The scheme suggested by B. Parker.

[6] E.A. Perevedentsev, V.I. Ptitsyn and Yu. M. Shatunov, *Proc. of 5th Int. Workshop on High Energy Spin Physics*, Protvino, 1994, 281.

[7] From polarization analysis done by D.P. Barber.

[8] D.P. Barber et al., Nucl. Instr. Meth. **A338**, 166 (1994).

3.4 Linac-Ring Options

3.4.1 Linac-Ring Designs of Electron-Ion Colliders

Ilan Ben-Zvi benzvi@bnl.gov Brookhaven National Laboratory, Upton, NY 11973 USA

Lia Merminga merminga@jlab.org CASA, Jefferson Lab, Newport News, VA 23606 USA

Yaroslav Derbenev derbenev@jlab.org CASA, Jefferson Lab, Newport News, VA 23606 USA

Electron-ion colliders with center of mass energies between 20 and 100 GeV range, luminosities equal or greater than 10^{33} cm^{-2}sec^{-1} with both beams longitudinally polarized at 80% in the interaction region, promise great scientific potential towards the understanding of the hadronic structure. Two different schemes have been proposed for the realization of an electron-ion collider: the "*storage ring option*," described in the previous section, which uses an electron storage ring and the electron beam is polarized by the synchrotron radiation, and the "*linac-ring option*," [1] described in this section, in which the electrons are generated from a polarized source and accelerated in a superconducting linac. Although the linac-ring option is not as well understood and developed as the classic storage ring option, it appears to allow for higher luminosities, while it presents significant advantages with respect to preserving and manipulating the electron spin. For the linac-ring option to be feasible, RF power and beam dump considerations require that the electron linac is an energy recovering linac (ERL), technology demonstrated at high power in the Jefferson Lab's IR FEL

A generic linac-ring scheme for an electron-ion collider [2] might have the following layout: Longitudinally polarized electrons are generated from a high current polarized source and are injected into an ERL for acceleration. To ease the high current polarized photoinjector and ERL requirements, a circulator ring (CR) may be used [3]. In this scenario, the electrons are injected into the circulator ring, after acceleration in the ERL, and circulate for $\sim$100 revolutions while they continuously collide with the ions. They are subsequently extracted, transported back to the ERL for deceleration and energy recovery, and are dumped at approximately their injection energy. The average current requirement on the polarized injector is lower by the number of revolutions in the CR. Different filling patterns of the CR are being considered [4,5]. The CR configuration can be easily operated as a single pass ERL. At the same time, the tolerance of the CR to beam-beam interactions and disruption is lowered in some proportion to the number of circulations, thus the simplification of the electron injector and the luminosity limitation due to beam-beam must be

balanced.

For the ion complex of the linac-ring scheme, one can envision using the existing RHIC storage ring, as in the eRHIC scheme [1], which is described in the next section, or a green-field design, as described in the ELIC scheme [6].

In either case, it has been determined that electron cooling of the protons/ions is required for luminosity above $\sim 10^{32}$ cm^{-2} sec^{-1} to overwhelm intrabeam scattering, in both transverse and longitudinal degrees of freedom [2]. Cooling of the intense ion bunches contemplated here requires high electron beam current (hundreds of mA). Electron cooling at such high energy can only be conceived in the context of superconducting rf ERLs. The BNL is seriously pursuing the design and prototyping of an ERL-based electron cooling device for RHIC [7] in collaboration with BINP and Jefferson Lab. The electron beam energy will be 54 MeV and the electron beam current will be approximately 280 mA.

Although luminosities up to 10^{35} cm^{-2} sec^{-1} look possible with a linac-ring scenario, there are a number of significant technical challenges that need to be resolved. These challenges include the demonstration of high energy electron cooling of protons/ions briefly discussed above, the demonstration of high average current polarized electron source, high current, high energy demonstration of energy recovery and integration of the IR design with real detector geometry.

A significant technological challenge for the realization of the linac-ring scenario is the high average current polarized electron source. The highest average current that has been demonstrated to date is approximately 1 mA at Jefferson Lab [8]. The circulator ring concept appears promising in easing this requirement.

Energy recovery has been demonstrated reliably at the JLab IR FEL with average current up to 5 mA and energy up to 50 MeV. Establishing feasibility and high-efficiency operation of ERLs at an average current of order 300 mA, as required both for the electron cooling device and for the collider itself, and at an energy of several GeV, requires the experimental investigation and understanding of a number of issues. An energy recovery experiment at CEBAF has been proposed and is being planned for March 2003 [9]. CEBAF-ER aims to investigate the ability for phase space management and to quantify beam quality degradation in GeV scale ERLs. Further, the experimental investigation of high average current effects [10] is planned at the JLab FEL Upgrade, presently under commissioning, and designed to accelerate10 mA of cw beam current up to $\sim$200 MeV and energy recover it to $\sim$10 MeV, and in the Cornell/JLab ERL prototype and BNL electron cooling prototype [11].

In summary, the linac-ring scenario offers a number of distinct advantages over a storage ring scenario, which include:

Preservation and manipulation of spin is straightforward, without crossing of spin resonances and without quantum depolarization effects.

The interaction regions are highly simplified allowing for wide energy variability of both beams, without sacrificing the high degree of polarization.

Minimum beam emittance is determined by the electron source, allowing for small collision beam size and increased luminosity.

The limit on the electron beam-beam tune shift, inherent in the storage ring scenarios, is much more relaxed in the linac-ring scenario, even with the CR option.

In the following, two specific linac-ring designs are described in detail: eRHIC, which uses the RHIC storage ring, and ELIC, which uses the CEBAF electron accelerator.

References

[1] I. Ben-Zvi, et al., NIM A, Vol. 463, No. 1-2, (2001) pp. 94-117

[2] L. Merminga, et al., Proc. of HEACC Conf. 2000

[3] Ya. Derbenev, Proceeding of EPAC 2002

[4] V. Litvinenko, Private Communication
[5] A. Hutton, Private Communication
[6] L. Merminga et al., Proceeding of EPAC 2002
[7] V. Parkhomchuk and I. Ben-Zvi, C-A/AP/47, 2001
[8] C. K. Sinclair, Proceeding of PAC Conference 1999
[9] http://casa.jlab.org/internal/research/er/er.shtml
[10] L. Merminga, Proceeding of FEL Conference 2001
[11] I. Ben-Zvi et al., Proceedings of PAC'01 and PAC'03.

3.4.2 eRHIC Linac-Ring Version

Ilan Ben-Zvi benzvi@bnl.gov Brookhaven National Laboratory, Upton, NY 11973 USA
Jörg Kewisch jorg@bnl.gov Brookhaven National Laboratory, Upton, NY 11973 USA
Vladimir Litvinenko vl@phy.duke.edu Duke University, USA

In this section we would like to explore the performance of a linac-ring version of eRHIC, the electron-ion collider based on the RHIC machine. One may expect that various improvements may be done to the luminosity of the RHIC machine by lowering β* the beta function in the IP (by placing the final focus quadrupoles closer than the present rather large 25.36 meters) or storing more bunches or shorter bunches by modifications to its RF system. However, for the sake of this discussion, we shall assume the demonstrated performance, allowing us to assume only two possible changes: a slight increase (a factor of two) in ion bunch population and electron cooling. As for the electron cooling, we assume a modest emittance improvement of a factor of two and a smaller β* function because of cooling. The purposes of these "upgrade" variations are to demonstrate the latent improvement in luminosity that is the characteristic of the linac-ring version.

We can express the highest luminosity that an electron-ion collider can achieve mostly in terms of the ion ring parameters, by using the ion machine beam-beam parameter to replace the number of electrons per bunch:

$$L = \frac{c}{l}\frac{10^{-4}A}{Zr_p}\frac{N_i\gamma_i\xi_i}{\beta_i^*}F\left(\frac{\sigma_i}{\beta_e^*}\right)$$

L is the luminosity in inverse square cm*second including the hourglass factor, all other parameters are in MKS. c is the velocity of light, l is the bunch spacing, A and Z the ion mass number and charge, r_p is the classical radius of the proton, N_i is the number of ions per bunch, γ_i is the ions energy, ξ_i is the ion ring's beam-beam parameter, β_i^* is the ion's IP beta function, σ_i is the ion bunch rms bunch length. $\beta_e^*$is the only electron machine parameter, which enters in the hourglass effect function F. Since in RHIC the ions bunch rms length is 0.2 m, we set it to β_e^*=0.5 m, which is a minimal value needed to avoid luminosity loss due to the hourglass effect.

Since the RHIC ion machine parameters are fairly well known, it makes sense to express the luminosity in this way and then see what it implies for the electron accelerator. We will assume a bunch spacing of 10.65 m. The maximum ion's beam-beam parameter is taken as 0.005. The electron energy can vary over a very wide range, say 2 to 10 GeV, without sacrificing performance. For the purpose of the calculations, we will assume 5 GeV.

We calculate the electron machine parameters using the following expressions:

Parameter	Protons (A=1, Z=1, γ=266)				Gold (A=197, Z=79, γ=106)			
N_i (10^9)	Present, 100		Upgrade, 200		Present, 1		Upgrade, 2	
ε_n(rms, μ)	1.4	0.7	1.4	0.7	1.4	0.7	1.4	0.7
β_I^*	0.5	0.3	0.5	0.3	0.5	0.3	0.5	0.3
L (10^{33})	0.460	0.760	0.910	1.500	0.0046	0.0076	0.0091	0.015
Resulting electron linac parameters								
N_e (10^9)	57	29	57	29	140	71	140	71
I_e (A)	0.26	0.13	0.26	0.13	0.64	0.32	0.64	0.32
ε_n(rms, μ)	51	15	51	15	130	39	130	39
ξ_e	0.44	1.5	0.87	2.9	0.14	0.46	0.28	0.92

$$N_e = \frac{4\pi A \xi_i \varepsilon_i \gamma_i}{Z r_p}, \quad \varepsilon_e = \varepsilon_i \frac{\beta_i^*}{\beta_e^*} \quad \xi_e = \frac{N_i Z r_e}{4\pi \varepsilon_e \gamma_e}$$

The results are shown in the table below.

Detailed studies had shown that with proper matching in the ERL case, the tune shifts of $\Delta\nu_e \sim 1$ and disruption parameters ~ 5 cause modes increase of the beam emittance of $\leq$ 20%, which can be easily re-circulated in the ERL. In addition, the proper matching of electron beam into the IP provides for a modest variation of the transverse e-beam size and do not cause additional tune shift spread in the ion beam (see Fig. 3.10).

We see that in order to obtain the maximal luminosity of the ion machine, the electron machine is driven to a high beam-beam parameter, beyond what can be sustained by a storage ring. Thus a linac-ring configuration of eRHIC will produce a higher luminosity. Thus there are a number of compelling advantages for the linac-ring:

- The linac-ring will have a higher luminosity that a ring-ring collider, due to its beam-beam parameter.
- The electrons are used only once, eliminating spin rotators near the IP.
- A linac can operate over a wide energy range without sacrificing performance.
- The polarization of a linac is high and can be rapidly alternated at will.
- The linac's naturally round beam is well matched to the RHIC beam.
- With strong cooling of RHIC, the electron current of the linac will be significantly smaller, reducing synchrotron radiation in the detectors.
- The total electric consumption of the linac is significantly smaller, even if one assumes that its refrigeration does not take advantage of the RHIC refrigerator.
- A linac can be easily upgraded for higher energies.

A possible layout of eRHIC with a linac-ring is shown in Figure 3.11.

Cost saving is realized by circulating the beam twice through the linac, thus halving its length. The use of 703.75 MHz cavities with ferrite HOM power absorbers should allow for stable operation of this configuration up to the maximum current assumed in the calculations above.

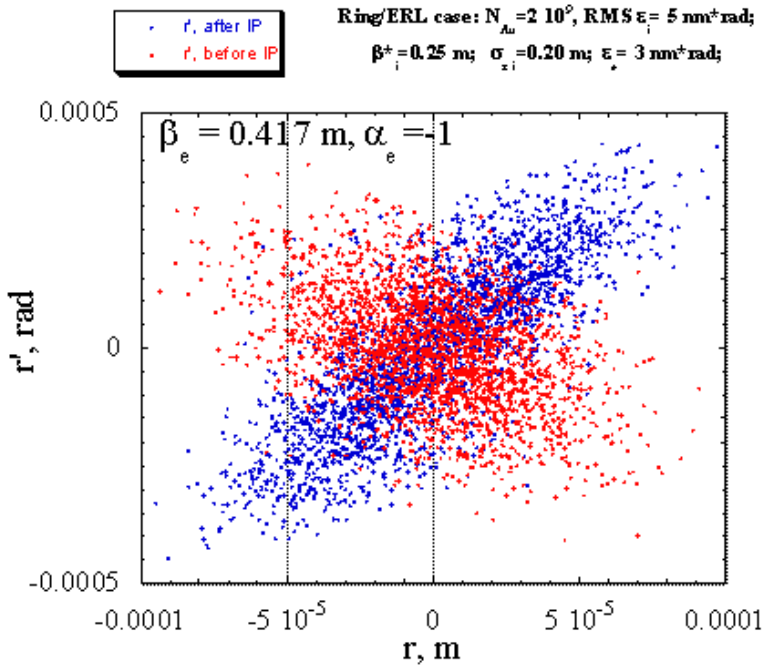

Figure 3.10: Round electron beam from ERL with initial transverse RMS emittance of 3 nm*rad passes through the IP with the disruption parameter 3.61 (tune shift $\Delta\nu$e = 0.6). The figure shows Poincare plots for e-beam distribution before (red) and after (blue) the IP. After removal of r-r' correlations, the emittance growth is 11%, a value that should be easily acceptable for energy recovery in the linac.

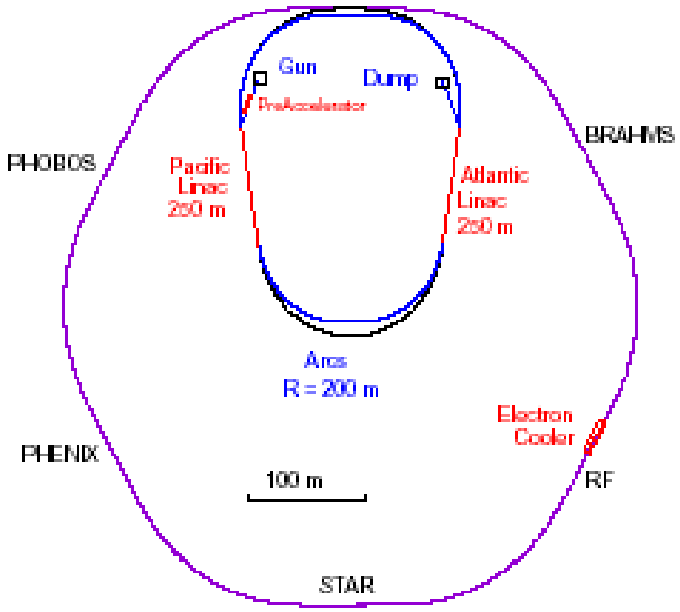

Figure 3.11: A schematic layout of a linac-ring eRHIC. The linac comprises two sections, 2.5 GeV each and beam is passed twice for acceleration and twice for energy recovery through each section, allowing for a 10 GeV energy-recovery linac operation.

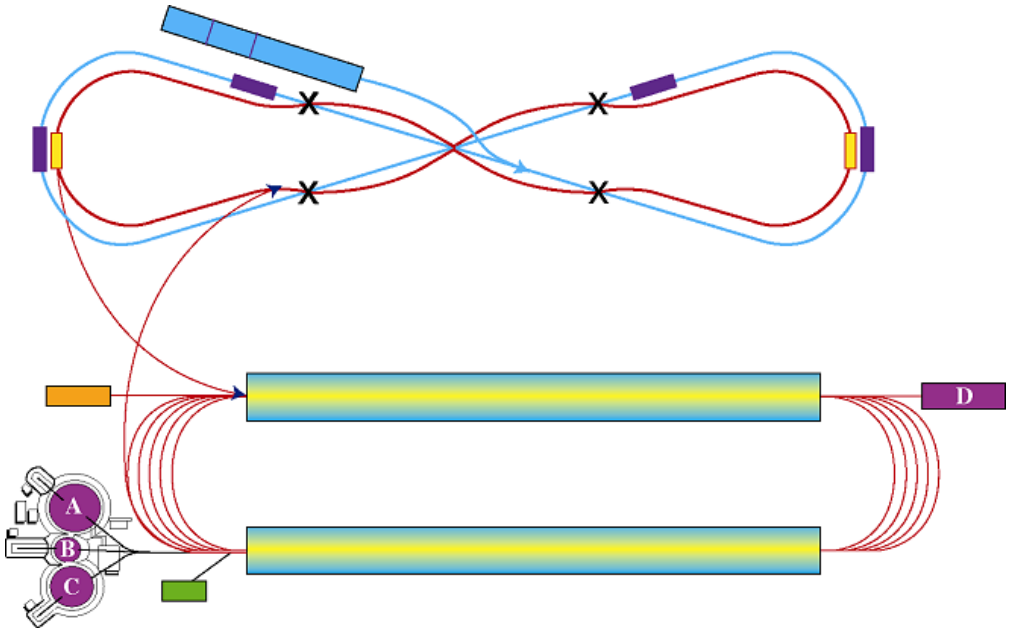

Figure 3.12: ELIC Layout.

References

[1] S. Peggs and W.W. MacKay, editors, Collective Instabilities in RHIC, RHIC/AP/36

3.4.3 ELIC: An Electron-Light Ion Collider at CEBAF

Lia Merminga merminga@jlab.org CASA, Jefferson Lab, Newport News, VA 23606 USA

Yaroslav Derbenev derbenev@jlab.org CASA, Jefferson Lab, Newport News, VA 23606 USA

An Electron Light-Ion Collider (ELIC) based on CEBAF [1] has been proposed as a means of probing the hadronic structure of matter. The luminosity of this collider should be greater than 10^{33} cm^{-2} sec^{-1} with both beams longitudinally polarized at 80% in the interaction region. The center-of-mass energy should be variable between 20 and 65 GeV and ion species should include protons, deuterons and He^3. Spin-flip of both beams is extremely desirable for exclusive measurements. The ELIC proposal is based on the following elements: The CEBAF accelerator in energy recovery mode (for rf power savings and ease of beam dump requirements) is used for the acceleration of electrons. "Figure 8" [2] booster and storage rings are used for the ions for spin preservation and flexible manipulation of all ion species of interest. A circulator ring [2], in which electrons are injected after acceleration in the Energy Recovering Linac (ERL) and circulate for a small number of revolutions (about 100) while colliding with the ion beam, may be used to ease the high current polarized photoinjector and ERL requirements.

Figure 3.12 displays a schematic layout of ELIC. Longitudinally polarized electrons generated from a high current polarized source are injected into the CEBAF accelerator. With CEBAF Upgrade-style cavities, operating at a gradient of $\sim$20 MV/m installed in the tunnel, a single pass recirculation through CEBAF results in electron beam energy of $\sim$5 GeV. In the scenarios that include a circulator ring (CR), the 5 GeV electrons are then injected into the CR where they stay for $\sim$100 turns while they continuously collide with the ions. They are subsequently extracted,

transported back to CEBAF for deceleration and energy recovery, and are dumped at approximately their injection energy. If the polarized source development should become so advanced that the CR does not offer any advantages, the electrons can still follow the same transport, but now circulate only once before being reinjected to CEBAF for energy recovery.

The CR concept greatly eases the requirements on the polarized electron source and the ERL: The ERL injector produces current macropulses of length equal to the ring circumference. Each macropulse is then injected into the CR for $\sim$100 revolutions. During this time the injector current is turned off. After $\sim$100 revolutions, the macropulse is extracted and reinjected into the linac for energy recovery. At the same time a new pulse is being injected into the linac for acceleration, in perfect synchronism with the decelerating pulse for energy recovery to work. The average current requirement on the polarized injector is lower by the number of revolutions in the CR. Different filling patterns of the CR are being considered [3,4].

All ion species are injected longitudinally polarized and accelerated in a conventional ion RF Linac. The circulated ring can also be used as a booster ring bringing the ion energy to 10-20 GeV. The ions are then injected and stored in the "Figure 8" storage ring housed in the same tunnel with the CR. The "Figure-8" storage ring is used for the ions for its zero spin tune, thus intrinsic spin resonances and spin resonance-crossing are avoided. Longitudinal polarization for all ion species at all energies is possible by introducing solenoids in the straight sections or horizontal dipoles in the arcs. Spin rotators around the interaction points would not be needed. For protons, up to 4 simultaneous interaction regions (IRs) can exist with longitudinal polarization. For D and He up to 2 simultaneous IRs can exist with longitudinal spin. To ensure that the electron spin remains longitudinal at the IRs, a Wien filter in the injector plus one or two Siberian snakes is required for two IRs, and a Wien filter plus 2 Siberian snakes, or three Siberian snakes without the Wien filter for 4 IRs.

Consistent sets of parameters have been developed for four point designs for ELIC (Table 3.3). Point Design 0 (PD0) is a baseline design based on presently achieved parameters (not necessarily simultaneously) assuming no electron cooling of the ions. Under these assumptions, the maximum achieved luminosity is 10^{32} cm^{-2} sec^{-1}. PD1 assumes electron cooling. Luminosity at 10^{33} cm^{-2} sec^{-1} appears feasible. PD2 gives maximal luminosity of 10^{34} cm^{-2} sec^{-1}. This solution requires, in addition to electron cooling and the associated short ion bunches, a circulator ring and the use of crab crossing for increase of collision frequency and reduction of parasitic collisions, as described in earlier section. The final design (PD3) gives the maximally attainable luminosity. We found that 10^{35} cm^{-2} sec^{-1}is feasible only if the ion energy is 100 GeV or above. Each point design should be viewed as an evolutionary upgrade to the previous design.

3.4.3.1 Integration with 25 GeV Electrons for Fixed-Target Experiments

The same electron accelerator that is used in the collider mode can also provide up to 25 GeV electrons for .xed target experiments for physics. This scheme requires the implementation of a 5-pass recirculator at $\sim$5 GeV per pass as in present CEBAF. It is a subject of further investigation whether the collider and .xed target modes could run simultaneously, or in alternating modes. The emittance growth due to synchrotron radiation in the CEBAF arcs at the higher energies has been addressed with a novel optics design for the higher arcs, resulting in a significant reduction in emittance growth [5]. The beam spot sizes will thus be between 0.3-0.5 mm at 25 GeV.

Table 3.3: ELIC Parameter Table

Parameter	Units	Point Design 0		Point Design 1		Point Design 2		Point Design 3	
		e-	Ions	e-	Ions	e-	Ions	e-	Ions
Energy	GeV	5	50	5	50	5	50	5	50/100
Cooling	-	-	No	-	Yes	-	Yes	-	Yes
Luminosity	cm^{-2} sec^{-1}	1×10^{32}		1×10^{33}		1x 10^{34}		6x10^{34} / 1x10^{35}	
N_{bunch}	ppb	1x10^{10}	2.5x10^{10}	1x10^{10}	2.5x10^{10}	2x10^{10}	5x10^{9}	1x10^{10}	1x10^{10}
f_c	MHz	150		150		500		1500	
I_{ave}	A	0.24	0.6	0.24	0.6	1.6	0.4	2.5	2.5
σ^*	μm	45	45	14	14	6	6	4.5	4.5
ϵ_n	μm	10	2	10	0.2	10	0.2	10	0.1
β^*	cm	200	5	20	5	4	1	2	1
σ_z	cm	0.1	5	0.1	5	0.1	1	0.1	1
ξ_e/ξ_i	-	0.5	0.0006	0.5	0.006	0.1	0.01	0.2	0.01
$\Delta_{\nu L}$	-	-	0.005	-	0.05	-	0.05	-	0.09

3.4.3.2 Accelerator physics and technology challenges

Although luminosities up to 10^{35} cm^{-2} sec^{-1} look indeed promising at the proposed CEBAF-based electron-ion collider facility, and the integration with a 25 GeV fixed target program appears to be straightforward, there are a number of technical challenges that need to be resolved, before construction commences. These challenges include the demonstration of the high average current polarized electron source, high energy electron cooling of the ions, high current and high energy demonstration of energy recovery, and integration of the IR design with a real detector geometry. A significant challenge for the realization of ELIC is the high charge per bunch and the high average current polarized electron source. The highest average current that has been demonstrated to date is approximately 1 mA at Jefferson Lab [6]. The circulator ring concept appears promising in easing this requirement. Cooling of the intense ion bunches contemplated here requires high electron beam current (hundreds of mA). Electron cooling at such high energy can only be conceived in the context of superconducting rf ERLs demonstrated and routinely used in the Jefferson Lab IR FEL. The BNL/BINP collaboration is seriously pursuing the design and prototyping of an ERL-based electron cooling device for RHIC [7]. Jefferson Lab has recently formally joined collaboration with BNL. Energy recovery has been demonstrated reliably at the JLab IR FEL with average current up to 5 mA and energy up to 50 MeV. Establishing feasibility and high-efficiency operation of ERLs at an average current of order 100 mA, as required both for the electron cooling device and for the collider itself, and at an energy of several GeV, requires the experimental investigation and understanding of a number of issues. The experimental investigation of high average current effects is planned at the JLab FEL Upgrade (10 mA), the Cornell/JLab ERL prototype, and the BNL electron cooling prototype (both 100 mA).

3.4.3.3 Conclusions and R&D strategy

An electron-ion collider based at CEBAF yielding 10^{33} to 10^{35} cm^{-2} sec^{-1} luminosity appears feasible. Electron cooling is required in all scenarios. We are investigating the concept of circulator ring, as it promises to ease requirements on polarized electron source as well as high average current issues in the ERL. Other conceptual improvements are being explored. The R&D strategy includes experimental investigation of high average current effects in the JLab IRFEL, Cornell/JLab ERL prototype and BNL electron cooling prototype. Complementary to these efforts is

the energy recovery experiment at CEBAF to address ERL issues in large systems. Electron-ion collider program integrated with a 25-GeV CEBAF-based fixed target program appears feasible.

References:

[1] L. Merminga, et al., Proceedings EPAC 2002
[2] Ya. Derbenev, Proceeding of EPAC 2002
[3] V. Litvinenko, Private Communication
[4] A. Hutton, Private Communication
[5] Y. Chao, JLab TN99-038
[6] C. K. Sinclair, Proceeding of PAC Conference 1999
[7] V. Parkhomchuk and I. Ben-Zvi, C-A/AP/47, 200

3.5 Electron Cooling

3.5.1 Continuous Electron Cooling for High Luminsity Colliders

A. Skrinsky A.N.Skrinsky@inp.nsk.su Budker INP, Novosibirsk, Russia

Now, the Electron Cooling, proposed and developed at Novosibirsk [1-8], is accepted as an important working tool at many laboratories throughout the world [9].

There are different types of experiments and problems to apply Electron Cooling:

- storing of secondary stable and long enough living hadrons, nuclei and ions (maybe in combination with Stochastic Cooling - to rise effective acceptance);
- achieving of very low "temperature" of stored particles;
- suppression of beam blow-up due to diffusive effects of different nature (multiple scattering by "internal targets", external noise, multiple intra-beam scattering, beam-beam effects, ...).

This talk is devoted to the reaching of "highest luminosity at the collision stage" in colliders, when collisions involve hadrons and (stripped) nuclei. I intend to consider colliders, specifically, - not "mergers" or "crossers" with their specificity. Consequently, we have in mind $e^{+/-}p^{+/-}$; $e^{+/-}Z$; $p^{+/-}p^{+/-}$; $p^{+/-}Z$; Z_1Z_2,etc. colliders (where Z is the nuclear charge number; we consider the case of fully stripped ions only, since the loss cross-section for non-stripped ion at collisions is overwhelmingly high). We have in mind colliders of relativistic particles (v$\sim$c) with double ring and single head-on interaction region. All four transversal (geometrical) emittances are considered equal to$g\varepsilon g$geometrical, without π), all four beta functions - equal to β_0, and equal to bunch rms length σ_{long}, equal for both beams. Distance between bunches is equal to D_{bb} - the same for both beams. Transversal space charge effect for ions is considered as limited by the maximal sustainable betatron tune shift $\Delta\nu$, beam-beam effects are considered limited by maximal tune shifts ξ_e and ξ_Z. (The stochastic cooling being quite useful in the collection of secondary heavy particles, is not useful in reaching high luminosity collisions, where high density of particles is needed.)

Let us look, as an example, on the simple formulae for Electron-Nuclei (Z,A) collider, presenting ultimate luminosity for different cases.

If the number of electrons per bunch N_{be} is limited "externally" and ion longitudinal density is limited by space charge tune shift $\Delta\nu$s the ultimate luminosity will be

$$L_{eZ1} = \frac{c}{2\pi r_p} \cdot \frac{A}{Z^2} \cdot \gamma_Z^3 \cdot \frac{\Delta\nu}{R_{Zav} D_{bb}} \cdot N_{be},$$

where R_{zav} is average ion storage ring radius, and γ_Z is ion relativistic factor (ion velocity is assumed close to velocity of light c).

If the limiting factor is the beam emittance (it could be either the fraction of collider acceptance, small enough to ensure good life time, or ion beam emittance affordable for effective electron cooling), number of ions per unit length is limited by space chargesgnd number of electrons per bunch is limited by ion beam-beam tune shift ξ_Z, the ultimate luminosity will be

$$L_{eZ2} = \frac{2c}{r_p^2} \cdot \frac{A^2}{Z^3} \cdot \gamma_Z^4 \cdot \frac{\xi_Z \Delta\nu}{R_{Zav} D_{bb}} \cdot \varepsilon \quad ,$$

in both previous cases independently of IP beta-function.

If the limiting factors are beam emittance and beam-beam tune shifts, the ultimate luminosity will depend on IP beta-function:

$$L_{eZbb} = \frac{4\pi c}{r_e r_p} \cdot \frac{A}{Z^2} \cdot \gamma_e \gamma_Z \cdot \frac{\xi_e \xi_Z}{\beta_0 D_{bb}} \varepsilon,$$

r_e, r_p - classical radii of electron and proton.

In this case, the proper value of beam emittances should be produced not by beam-beam interaction itself, but "externally" - to prevent the flip-flop instability (when the diminishing of the transversal size of one beam makes beam-beam tune shift for the other one higher than the critical value and its size grows up; this change produces further diminishing of the first beam size, etc.). The solution for electrons (positrons) is formation of beam emittances needed by quantum fluctuations. For particle beams under ECooling, it is worth to arrange the proper emittances by the relative inclination in the cooling section of particle equilibrium orbit and the guiding longitudinal field by the angle corresponding to its emittance angle (using the so called "monochromatic instability" [2]). In this case, the cooling rate for rms and higher amplitudes is not slowed down, but for smaller amplitude it becomes negative.

The maximal values of tune shifts $\Delta\nu$ and ξ depend on whether strong cooling for the particles involved does exist. A very rough estimation (for optimal operating conditions), based on the "world experience", is:

ξ_Z, $\Delta\nu$= 0.005 - if no cooling,

and

ξ_Z, $\Delta\nu$ = 0.05 - if cooling is "good".

And "good cooling" means that number of collisions (or number of turns for space charge limitation) per cooling time $N_{coll/cool}$ is

$$\text{less than} \sim \quad 3 \cdot 10^6.$$

(It is necessary to be cautious with this estimation, since it is based on the experience with radiation cooling, for which the cooling power grows with oscillation amplitude; for ECooling at collider parameters of interest the dependence is just opposite. The subject needs careful simulation and experimental study.)

The "good cooling" prevents diffusion, and hence beam emittance and luminosity degradation, due to "non-linearities" in beam-beam interaction or in particle motion under combined action of space charge and machine imperfections, or due to multiple intra-beam scattering. The latter diffusion is active for ions if

$$\gamma_Z > \frac{\beta_R}{D_R} \quad ;$$

for quasi-symmetric collider this condition transforms in to operation "above critical energy", or in to

$$\gamma_Z > Q_R.$$

For even higher energies - in dependence of beam emittance and linear density - the multiple intra-beam scattering heating becomes too slow to care about.

In many cases, the same high and long-living luminosity can be reached without cooling, but would require much higher intensities and emittances. These smaller emittances under good cooling lead to much smaller transversal spot size at collision and allow to observe the life-length of reaction products much more efficient. The correspondingly smaller angular spread at collision gives possibility to study much smaller momentum transfers. In some cases, the much better monochromaticity under cooling is also important for physics.

Discussing future e-cooling based colliders, we need do not forget - up to now, the highest electron energy used for cooling was not higher than 300 keV, hence for ion energies below 600 MeV/A, the most recent and perfectly operating ECooling device was developed and constructed by INP for SIS Heavy Ions Synchrotron at GSI [10].

For electron energies up to, say, 5 MeV (E_Z¡10 MeV/A) technically is quite possible to use conventional rectifier based accelerator-recuperator, similar to INP high power electron accelerators used for industrial applications [11-13]. In a special installation of 1 MeV, 1 A continuous operation was achieved [14], with the whole beam path from the gun to the collector immersed in 500 Gs longitudinal magnetic field. The main improvement needed is to diminish rectifier ripples (by switching, probably, to the higher power supply frequency - from 400 Hz to few kHz) and to stabilize better the average electron energy. The Van-de-Graaf type electrostatic accelerators, also considered as potential candidates for this energy range, have excellent energy stability, but provide much smaller ("active") currents. Thus, the long-term reliability of operation could be more difficult to achieve, due to higher sensitivity to the sudden current losses (caused by ion and secondary electrons processes in high current electron beam under recuperation).

For higher energies (starting from few MeV to hundreds of MeV electrons, up to hundreds of GeV/A ion energy) the most promising approach, at least, in my view, is the use of RF accelerators-recuperators, of the type now under construction at INP for Free Electron Laser [15]. The operation of such a device, yet never tested, does not rise doubts in principle.

For even higher energies (if ECooling happens to be useful) the electron storage ring under strong enough synchrotron radiation cooling can become of interest.

The important step - very much desirable from technical and economic points of view - is the switching from continuous guiding longitudinal magnetic field, in use in all the ECooling devices up to now, to the "interrupted field" approach: to immerse in longitudinal field the gun and the cooling section, only. To keep electrons properly transversally magnetized in cooling section, the radial phase advance between the exit from the gun section magnetic field and the entrance to the cooling section magnetic field should be strictly 2πn (for the same field directions) plus radial magnification should be inversely proportional to the magnitudes of magnetic field - for proper compensation of "coming-out" and "coming-in" rotation kicks (any rotation around the beam axis is not important, of course). A special care should be taken to correct chromatic and other aberrations.

But additionally to the high intensity effects mentioned and other familiar ones, there is also an important phenomenon, which appears in some cases at high intensities of cooling electrons and ions, called "electron heating" [16], the studies of which are started just recently. The suppression of effects of this origin might require additional sectioning of the cooling section, fast feedbacks, and/or proper radius of beams merging, etc. The very preliminary estimations show, this kind of instability should not hamper the collider options presented below.

Prior to giving the sets of parameters for potential colliders, let us present the simplest formulae for ECooling, multiple intra-beam scattering, recombination rate and life-times as a background for these rough sketches.

The cooling time for reasonably high beams energy (γ_Z¿¿1) and the longitudinal magnetic field of finite value $H_{long}$is given by the familiar formula [2, 5]:

$$\tau_{cool} = \frac{1}{2\pi r_e r_p c^4} \cdot \frac{A}{Z^2} \cdot \frac{1}{L_{Ccool}} \cdot \frac{\gamma_Z^2}{n_e \eta} \cdot (\sum_n v_n)^{\frac{3}{2}} \quad .$$

Here, n_e - the cooling electron density (in lab system), η - fraction of the collider perimeter occupied by cooling section, v_n - relative electron-ion velocities of different nature (in their rest frame), L_{Ccool} - the effective Coulomb logarithm for "magnetized" collisions [5, 17, 18]:

$$L_{Ccool} = \ln \left[\frac{\left[\sqrt{2\pi r_e \cdot \frac{n_e}{\gamma_Z^3}} + \frac{1}{\sqrt{2} L_{cool}} \right]^{-1} \cdot \sqrt{\frac{\varepsilon}{\beta_{Zcool}}} + \frac{m_e c}{e} \cdot \frac{v_{etr}}{H_{long}}}{\frac{m_e c}{e} \cdot \frac{v_{etr}}{H_{long}} + \frac{r_e}{2} \cdot \frac{\beta_{Zcool}}{\gamma_Z^2 \varepsilon}} \right] \quad .$$

If L_{Ccool} is a unit or more (this requires high enough longitudinal magnetic field in the cooling section), the transverse electron velocities enter to the cooling rate via this logarithm, only. Hence, the expansion of electron beam by diminishing longitudinal magnetic field in the cooling section relative to the field at the electron gun makes cooling slower - because the influence of the electron density decrease is much stronger.

For high energy colliders, the main contribution to velocities in the cooling section v_n are: ion transverse velocities corresponding to the ion beam emittance ε

$$v_Z = \sqrt{2c^2 \cdot \frac{\varepsilon \gamma_Z^2}{\beta_{Zcool}}} \mathrm{g},$$

and longitudinal electron velocities induced by relative energy spread Δ_{eE}(for example, due to energy modulation along the electron bunch appearing at RF acceleration)

$$v_{elong} = c\Delta_{eE} \quad .$$

The latter velocity should be smaller than v_ε for not slowing the cooling.

The multiple intra-ion-beam scattering (MIBS) can blow-up the beam emittance and "kill" the collider luminosity. To prevent the degradation, the increase due to MIBS in transversal ion velocities v_{MIBS} collected during τ_{cool} should be smaller than v_ε, where

$$v_{MIBS} = \sqrt{\frac{r_p^2 c^3}{\pi} \cdot \frac{Z^4}{A^2} \cdot \Lambda \cdot \frac{\beta_{Zav}^{\frac{5}{2}}}{\gamma_Z R_{Zav}^2 \beta_{Zcool} \beta_0} \cdot \frac{N_{bZ}}{\varepsilon^{\frac{3}{2}}} \cdot \tau_{cool}} \quad ,$$

$$\Lambda = \frac{\pi}{2} \ln \left(\gamma_Z \cdot \sqrt{\frac{\pi \varepsilon^{\frac{3}{2}} A}{2 r_p Z^2}} \right) \mathrm{g},$$

β_{Zav} - the average beta-function in ion ring, β_{Zcool}- the ion beta-function at the cooling section, N_{bZ} - number of ions per bunch.

If we prevented beams blow-up, the luminosity would decrease with time due to losses of particles. The electron beam losses are caused in most cases by single bremsstrahlung at counter

ions; cross-section of the process grows fast with ion charge. As a result, electron beam life-time is

$$\tau_{elife} = \frac{N_{\Sigma e}}{L_{eZ}\sigma_{\gamma 0} Z^2} \quad ,$$

where $N_{\Sigma e}$. - the total number of electrons, $\sigma_{\gamma 0} = 4 \cdot 10^{-25}$ - the singlegremsstrahlung cross-section of electron at unit charge.

The ion life-time, additionally to the usual processes in collisions, is limited by (radiative) recombination events with cooling electrons. The life-time due to this process is

$$\tau_{Zrec} = \frac{1}{30\alpha r_e^2 c^2} \frac{\gamma_Z^2}{Z^2 n_e \eta \ln\left(\frac{Z\alpha c}{v_{etr}}\right)} \cdot v_{etr}$$

(α - the fine structure constant).

Here, I want to underline especially the proportionality of the recombination life-time to v_{etr}: for high Z ions this life-time could become uncomfortably short, but we have possibility to increase it very substantially almost without damaging the cooling rate (keeping the L_{Ccool} bigger than 1). The other option of "hollow electron beam", proposed and developed at Novosibirsk recently, solves the problem probably even more efficiently.

The previous discussion confirm, in my understanding, a very interest in further development and active use of Electron Cooling for elementary particle physics, as well as for nuclear and atomic studies.

References:

[1] G. Budker: Atomnaya Energiya, 22, 346 (1967); Proc. Intern. Symposium Electron and positron Storage Rings, Saclay, 1966, p. II-I-I

[2] Ya. Derbenev, A. Skrinsky: preprint No 225, INP, Novosibirsk, 1968; Particle accelerators, 1977, v.8, p.1

[3] G. Budker, N. Dikansky, V. Kudelainen, I. Meshkov, V. Parkhomchuk, D. Pestrikov, A. Skrinsky, B. Sukhina: IEEE Transaction on Nuclear Science, NS-22, No5, 2093 (1975); Particle Accelerators,V.7, No 4, 1976

[4] G. Budker, A. Skrinsky: Soviet Uspekhi Fiz. Nauk, 1978, v.124, No4, p.561

[5] Ya. Derbenev, A. Skrinsky: Sov. Phizika plazmy, 1978, v. 4, p. 492

[6] V. Parkhomchuk, A. Skrinsky: Particle and Nucl. Physics, JINR, Dubna, 1981, v.12, issue 3, pp 557-613

[7] V. Parkhomchuk, A. Skrinsky: Reports on Progress in Physics, IPJ-EPS.v.54, No 7, pp 919-947

[8] N. Dikansky, V. Kudelainen, V. Lebedev, I. Meshkov, V. Parkhomchuk, A. Sery, A. Skrinsky, B. Sukhina: preprint No 88-81, INP, Novosibirsk, 1988.

[9] I. Meshkov, Electron cooling with circulating electron beams in GeV energy range, Workshop on Electron Cooling and Related Topics, incorporating the 5-th Workshop on Medium Energy Electron Coling, Uppsala, Sweden, May 19-22, 1999.,

[10] M. Steck et al.: Workshop on Electron Cooling and Related Topics, incorporating the 5-th Workshop on Medium Energy Electron Coling, Uppsala, Sweden, May 19-22, 1999.

[11] R. Salimov, N. Kuksanov et al.: Chapter 3 in the book "Environmental Applications of Ionizing Radiation"; John Willy & Sons, Inc., New York, 1998, pp 47-63.

[12] N. Kuksanov, R. Salimov et al.: Radiation Physics & Chemistry, v. 35, No 4-6, 1990.

[13] R. Salimov, N. Kuksanov et al.: Radiation Physics and Chemistry, v.46, 1995.

[14] M. Veis, B. Korabelnikov, N. Kuksanov, R. Salimov: EPAC'88, Rome, 1988

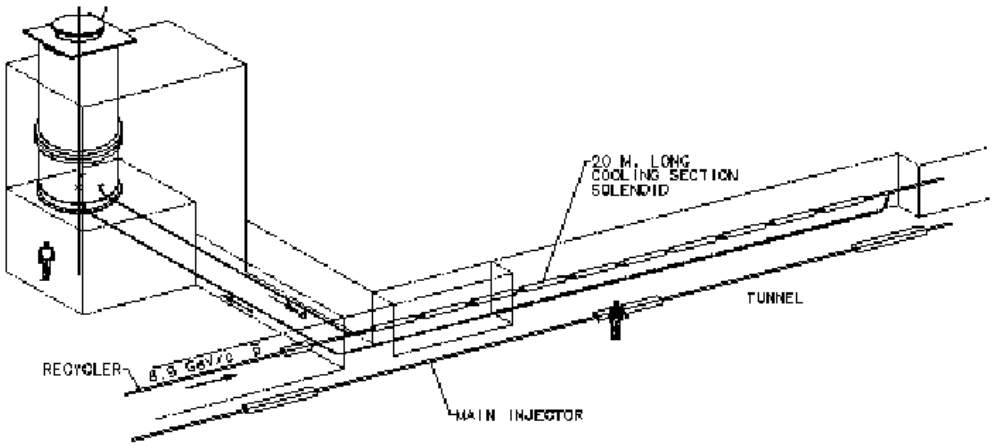

Figure 3.13: Schematic layout of the Recycler electron cooling system.

[15] Vinokurov N. A. et al.: Second Asian Simposium on Free Electron Laser, 1995, Novosibirsk, Russia

[16] V. Parkhomchuk: Workshop on Electron Cooling and Related Topics, incorporating the 5-th Workshop on Medium Energy Electron Coling, Uppsala, Sweden, May 19-22, 1999.

[17] V. Parkhomchuk: private communication.

[18] Conceptual Design Study of the GSI Electron-Nucleon Collider; INP Report 97-51, Novosibirsk; GSI Report 97-07, Darmstadt.

3.5.2 Electron Cooling At Fermilab

S. Nagaitsev nsergei@fnal.gov Fermi National Accelerator Laboratory, USA

3.5.2.1 Background

In 1995 Fermilab started to investigate the application of electron cooling to 8.9 GeV/c antiprotons in the Recycler ring as a promising component of an upgrade of Tevatron luminosity [1]. Purposes of a Recycler beam cooling system (stochastic or electron) are:

- To re-cool the recycled beam during a time period of the collider store;
- To aid beam stacking in the Recycler during frequent transfers from the Accumulator;
- To counteract various beam heating mechanisms, such as residual-gas and intra-beam scattering.

The Recycler electron cooler, discussed here, will be installed in one of the sections of the Recycler ring and is schematically shown in Figure 3.13.

The ultimate goal is to realize a peak luminosity of 3×10^{32} cm^{-2}s^{-1} in the Tevatron collider by supplying a larger flux of antiprotons. Our conceptual design studies demonstrate that this can be accomplished by providing longitudinal emittance cooling rates in the Recycler of 80 eV·s/h or higher (in conjunction with the transverse stochastic cooling). The specific technical goal for the Recycler with the electron cooling system is to deliver 5×10^{12} antiprotons with a 50 eVs (or less) longitudinal phase-space area (98%) and 10 μm transverse emittance (95%, norm.) in 8 hours.

Table 3.4: Electron Cooling System Parameters

Parameter	**Design value**	**Achieved or installed**	**Units**
Electrostatic Accelerator			
Terminal Voltage	4.36	4.36/3.5	MV
Electron Beam Current	0.5	0.5/1.0	A
Terminal Voltage Ripple	500	500	V (FWHM)
Cathode Radius	2.5	2.5	mm
Gun Solenoid Field	$\leq$ 600	600	G
Cooling Section			
Length	20	18	m
Solenoid Field	$\leq$ 150	150	G
Vacuum Pressure	0.1	wip	nTorr
Electron Beam Radius	6	wip	mm
Electron Beam Divergence	$\leq$ 80	wip	μrad

3.5.2.2 Research And Development Goals

To date, electron cooling at relativistic energies remains an unproven technology, and thus constitutes a high-risk segment of the luminosity upgrade plan. To address the R&D issues and to achieve the required system parameters Fermilab has created an electron cooling R&D facility at one of the fixed-target lab buildings. A 5-MV Van de Graaff accelerator (Pelletron) has been purchased and installed in this building. This accelerator together with an electron beamline forms an R&D facility. The beamline closely resembles the final beamline. Most of its elements will be reused in the Recycler tunnel. In addition, all of the Pelletron equipment will be reused. The purpose of this R&D program is to develop a system ready to be installed in the Recycler tunnel.
wip – work in progress

Table 3.4 presents important parameters of the Recycler electron cooling system. It was determined that the most effective way to attain these parameters was to conduct the development in two stages by: (1) demonstrating the beam current, voltage and necessary stability in a short 10-m long beamline and (2) commissioning the full-scale 60-m long beam line prototype. At present, the R&D program is in transition between the first and second stages. The successful completion of the first stage of the program allowed us to proceed with the civil construction of a building near the Recycler tunnel, where the electron cooler will be housed. The new building is scheduled to be completed in March, 2004, at which time the electron cooling equipment will be moved to its final location. The cooling section installation is scheduled for the summer of 2004.

The following section briefly outlines the issues that might be important for anyone designing a similar or scaled-up cooling system, based on a dc electron beam.

The amount of stored electrostatic energy in the high-voltage terminal is high enough so that a full-voltage spark can damage both the inside electronics and the vacuum electrodes. All internal systems should be carefully protected against sparks and the amount of energy deposited by charged particles in vacuum should be minimized. We were able accomplish this through a number of hardware and software modifications [2].

We found that while without any beam the accelerating gradient can be as high as 16 kV/cm, with the dc electron beam in excess of 10 mA the stable operating gradient drops to 12 kV/cm [2]. This prompted us to plan an upgrade for the Pelletron from 5 to 6 MV maximum rating by extending the acceleration tube. This upgrade will be implemented when the Pelletron is moved to

its final location. Table 3.4 shows the achieved results for two voltages – 4.36 and 3.5 MV. While at 4.36 MV we were able to demonstrate the design current of 0.5 A, the stable beam operation was frequently interrupted by beam-induced sparks (every 4 minutes or so) with eventual high-voltage de-conditioning such that the Pelletron was no longer capable of holding 4.36 MV. At a lower 3.5-MV voltage the beam-induced sparks occurred on average every 20 minutes and did not cause any de-conditioning to the accelerating tube such that it took on average 20 seconds to restore the beam operation after the interruption. Such a duty cycle was determined to be acceptable for electron cooling.

Early in the design stage we determined that the best way to focus the electron beam in the 20-m long cooling section is to use a weak 150-G solenoid. Such a solenoid becomes effective only if the electron beam enters it with a matched angular momentum to cancel the solenoid edge effects. The only way to impart an angular momentum onto the electron beam is to immerse the electron gun in a solenoidal magnetic field. Naturally, such a solenoid can only be of limited length because of high-voltage restrictions in the Peletron terminal. Thus, we designed a beam transport line in which a beam is produced by a 5-mm diameter cathode in a 600-G magnetic field and then propagated to the cooling section, where it is injected into a 150-G solenoid. The beam exits the gun solenoid at a fairly low energy (about 500 keV) and rapidly expands due to its angular momentum. While the defocusing effect of the angular momentum is reduced by further beam acceleration, nevertheless, it remains to be a driving term in the envelope equation – by far greater than both the emittance and space-charge terms. We called this beam transport regime an angular-momentum dominated regime [4]. This regime will be fully tested during the second stage of the R&D program.

Finally, the cooling section solenoid is unlike the solenoids that are presently used in all of the low-energy electron coolers. Because of its low magnetic field (about 100 G) and high electron beam energy, the field quality requirement is set on the transverse field integral rather than on the value of the transverse field itself. Thus, short-range (30 cm or less) field fluctuations become less important than the long-range alignment. Details of our solenoid design can be found in Ref. [3].

References

[1] J. MacLachlan (editor), ”Prospectus for an electron cooling system for the Recycler”, Fermilab-TM-2061, http://www-lib.fnal.gov/archive/1998/tm/TM-2061.html

[2] J. Leibfritz et al., ”Status of the Fermilab Electron Cooling Project”, EPAC-2002, p. 1094, http://accelconf.web.cern.ch/AccelConf/e02/PAPERS/WEPRI032.pdf

[3] A. Burov et al., ”Optical Principles of Beam Transport for Relativistic Electron Cooling”, Phys. Rev. ST-AB, Vol. 3, 094002 (2000).

[4] S. Nagaitsev et al., ”Field Measurements in the Cooling Section Solenoid for the Recycler Cooler”, EPAC-2002, p. 2373, http://accelconf.web.cern.ch/AccelConf/e02/PAPERS/TUPDO012.pdf

3.5.3 Electron Cooling For RHIC

Ilan Ben-Zvi benzvi@bnl.gov Brookhaven National Laboratory, Upton, NY 11973 USA

Jörg Kewisch jorg@bnl.gov Brookhaven National Laboratory, Upton, NY 11973 USA

Vasily Parkhomchuk Budker Institute of Nuclear Physics, Novosibirsk, 630090, Russia

Electron-cooling of the Relativistic Heavy Ion Collider (RHIC) is essential for eRHIC and for the luminosity upgrade of RHIC. This project has a number of new features as electron coolers go: It will cool use 54 MeV electrons; it will be the first attempt to cool a collider at storage-energy;

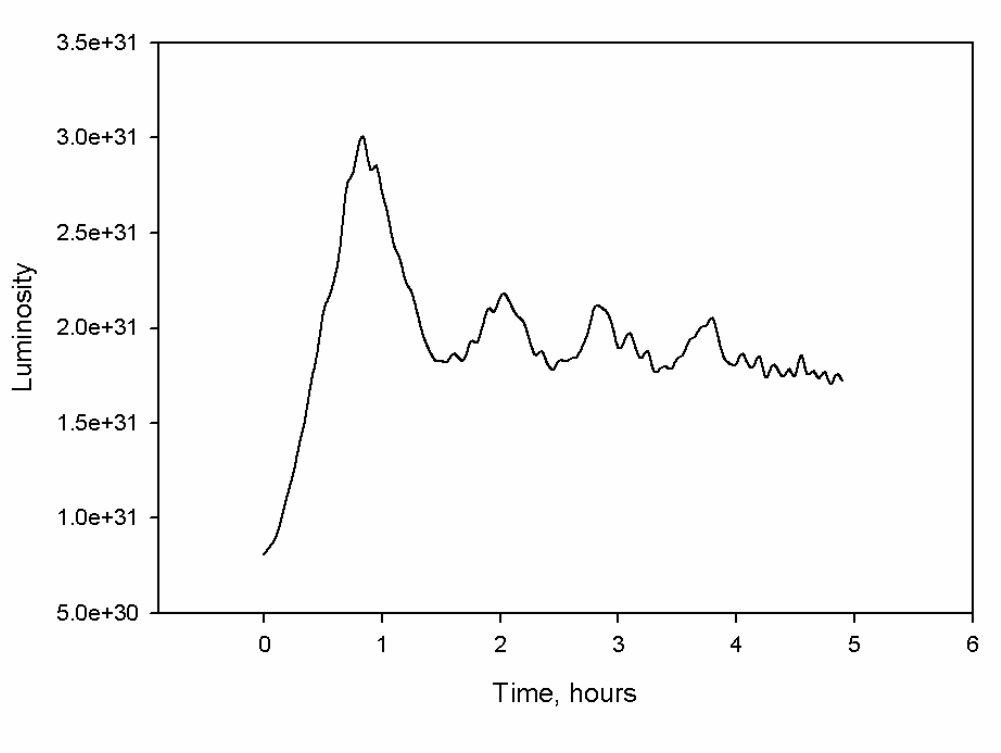

Figure 3.14: The luminosity as a function of time.

and it will be the first cooler to use a bunched beam and a linear rf accelerator as the electron source. The linac will be superconducting with energy recovery. The electron source will be based on a photocathode gun. The project is carried out by the Collider-Accelerator Department at BNL in collaboration with the Budker Institute of Nuclear Physics and Jefferson National Accelerator Facility.

An initial feasibility study, Electron Cooling for RHIC Design Report [1], indicated that cooling RHIC at full energy for gold ions and some intermediate energy for protons are feasible. The study defined the necessary electron beam and solenoid parameters for the cooler, dealt with the transport of magnetized electrons and showed the significance of electron-ion recombination and beam breakup in the IP. The first is not a problem with protons, and the second is not a problem in electron-ion collisions. Recombination affects the performance of eRHIC with gold ions since the ion population decays by about 30% over 5 hours.

The RHIC gold beam evolution is dominated by Intra-Beam Scattering (IBS), which leads to emittance growth and beam loss. Cooling has to be done during the storage phase of the machine to keep IBS in check. Protons can be cooled at an intermediate energy and then accelerated to the top energy. The solenoid of the cooler is a particularly challenging device, a 30 m superconducting solenoid at a field of 1 T, with a required precision of 8 parts per million.

The parameters of the electron beam for the eRHIC electron cooler are as follows: Bunch charge 10 nC, average current 280 mA, energy 54 MeV, rms normalized emittance 40 μm, energy spread 0.02%. The performance of the cooler was simulated with a computer code Simcool [2]. The performance of eRHIC for a gold beam is shown in Figure 3.14.

We start with 2x10^9 gold ions and a normalized emittance of 2.6 μm rms. The initial electron current is 0.28 amperes. As the emittance is reduced the luminosity grows, and the beam parameter grows. The program starts reducing the electron cooling current as soon as the beam-beam

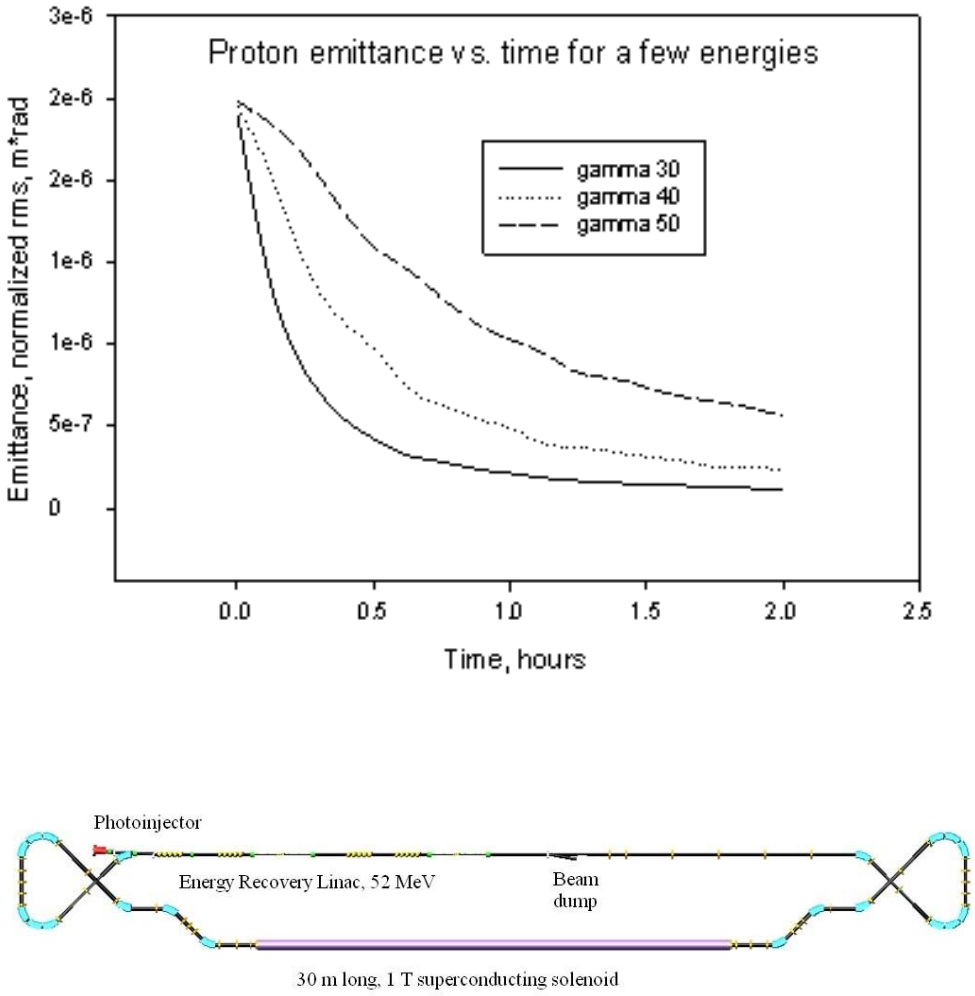

Figure 3.15: Schematic diagram of the high-energy electron cooler for RHIC.

parameter passes the preset value of 0.005, bringing the luminosity down as well. The electron current at 5 hours is 30% of its initial value, and the emittance stabilizes at about 0.7 μm. We can see that eRHIC provides a stable luminosity of about 2x10^{31} per nucleus (or 4x10^{33} per nucleon), limited only by the RHIC beam-beam parameter. Recombination is no problem, at the end of 5 hour the number of ions drops only to 1.5x10^{9}.

For protons, up to a γ of 50 or 60, cooling can be done at storage energy. For higher energies quick cooling can be done at a γ of 30 to 40, followed by acceleration to collision energies. Since the IBS strength for protons at high energy is low, this technique should work quite well.-beam

The schematic layout of the RHIC high-energy cooler is shown in Figure 3.15. The electron beam will be produced with a cw photoinjector (laser photocathode RF gun). The cathode of the gun will be immersed in a magnetic field to produce a ‘magnetized’ electron beam.

Following the initial acceleration in the gun to about 2.5 MeV the beam will be injected into a superconducting energy recovery linac. The accelerated beam will be debunched in order to increase it bunch length from about 12 mm to about 50 mm. The purpose of the debunching is

twofold: To reduce the space-charge interaction of the electron and ion beams to a safe level and to reduce the energy spread of the beam. The beam transport has to preserve the magnetization of the beam in the transport with discontinuous magnetic field. The magnetized electron beam, which is velocity matched to the ion beam, is then introduced into the 1 T cooling solenoid, overlapping the ion beam. Since the ion beam is much longer than the electron beam, the phase of the electron beam will be modulated in order to cool the required longitudinal extent of the ion beam. Other modulations (in energy and radial coordinates) may be introduced to shape the ion beam in phase-space. Emerging from the 30 m long cooling solenoid, the electron beam will be separated from the ion beam, rebunched (to match the linac acceptance) and decelerated to recover its energy. The beam will be dumped at about 2.5 MeV.

The 1 T, 30 m long ultra-high precision solenoid is another challenge. The required precision is of the order of the ions' angular spread, $\Delta\theta$, given by:

$$\Delta\theta := \sqrt{\frac{\epsilon_{ni}}{\beta\gamma\beta_{cool}}} \tag{3.1}$$

where ε_{ni} is the ions' normalized emittance and β_{cool} is the beta function in the cooler solenoid. In our case $\Delta\theta$ is about 10^{-5}.

We are pursuing R&D on a number of system elements: The photoinjector (including its laser and photocathode deposition system), a high-current superconducting cavity for the 54 MeV ERL of the cooler, beam dynamics of the complete system, electron cooling simulation codes and the high-precision superconducting solenoid.

References

[1] Electron Cooling for RHIC Design Report, V.V. Parkhomchuk and I. Ben-Zvi, 2001.

[2] The code Simcool was written by Vasily Parkhomchuk with some modification made by Ilan Ben-Zvi.

3.5.4 Luminosity Potentials of EIC With Electron Cooling

Yaroslav Derbenev derbenev@jlab.org CASA, Jefferson Lab, Newport News, VA 23606 USA

Electron cooling of ion beam is considered an inevitable component of a high luminosity electron-ion collider. Below we discuss and illustrate possible design advances that may have a positive impact on the efficiency of EIC.

3.5.4.1 Attainability of Short Ion Bunches

Electron bunch length of EIC is quite small, about 1 cm in storage rings and up to 1mm in ERL and, perhaps, in circulator rings, while bunch length in proton rings is settled usually between 10 to 30 cm. Conventionally, the luminosity increase in a collider with beam cooling is associated with decrease and maintenance of transverse emittance of hadron beams. Cooling effect on longitudinal emittance that may lead to bunch shortening, hence, to design of a low beta-star, was not emphasized at earlier conceptual studies of colliders with cooling; a general reason for this was an insufficient strength of RF field bunching the beam. With high field superconducting resonators available today the ion bunch length 1 cm or even shorter seems feasible at use of electron cooling [1,2].

Note, that a large increase of the synchrotron tune that results from implementation of high frequency superconducting resonators might significantly improve the ion beam stability against both the beam-beam and intra-beam space charge interaction. It also might prevent the development of microwave longitudinal instabilities of ion bunches.

Table 3.5: Cooled proton bunches in a ring with SRF resonators

Beam energy	GeV	150
Resonators frequency	GHZ	1.5
Integrated RF voltage amplitude	MV	100
Ring circumference	Km	1.2
Compaction factor		$4*10^{-3}$
Synchrotron tune		0.06
Energy acceptance	%	0.3
Energy spread, rms	%	0.03
Bunch length, rms	mm	5

Table 3.6: Final focus of EIC with short bunches (proton/electron)

Beam energy	GeV	150/7
Bunch length, rms	mm	5/5
Final focal length	m	4/4
Large beta	km	3.2/3.2
Beta-star	mm	5/5
Transverse emittance, norm	mcm	1/100
Beam size at large beta, rms	mm	5/6
Beam size at star point, rms	mm	6/6

3.5.4.2 Attainability of Low Beta-Star

The correspondently low beta-star for electron and ion beam can be achieved, according to well-known final focus design principle, by a necessarily large beams transverse extension before the final focusing quadrupoles. This challenge relaxes of decrease of ion beam emittances by the electron cooling, in the limits determined by the optics imperfections and beam alignment control. An illustration is presented in Table 3.6.

Crab Crossing Colliding Beams

Short bunches also would make feasible crab crossing interaction points. In this method colliding beams intersect at a large crossing angle, while the bunches are tilted off beam directions by half of this angle becoming parallel to each other; thus, the parasitic collisions avoided without loss of luminosity [3,2]. For example, tilt angle 50 mrad proton beam with above shown energy and final focus length can be created by 1.5 GHz SRF cavities of integrated transverse magnetic field amplitude 0.1 TM installed in section of beam extension. Arrangement of crab crossing would allow for a high collision rate (up to 1.5 GHz) while leaving a necessary space for detectors.

Traveling Ion Focus

If the ion bunches are still much longer than the electron ones, one may attempt to arrange the traveling focus for ion beam, with beta-star approaching the e-bunch length while making the ion focus point traveling with electron bunch [4]. The traveling effect can be achieved using the same SRF kicker as for crab crossing and introducing a gradient of final focus parameter by mean of sextupole field [2]. Estimated strength of sextupole magnets is about of 10-20 % with respect to that of the quadrupole magnets.

EIC With Flat Beams

Electron cooling has to be introduced to ion ring in order to suppress the beam blowing up by IBS and maintain beam emittances near the limits determined by the beam-beam space charge

interaction. At energies above the transition value, energy exchange at intra-beam collisions leads to the horizontal emittance growing up due to the basic energy-orbit coupling, and vertical emittance – due to x-y coupling. Since the luminosity is determined by the product of two emittances, reduction of transverse coupling to a minimum while conserving the beam area would benefit one with a decrease of energy scattering, hence, decrease of the whole the IBS impact on luminosity. Electron cooling then leads to a flat equilibrium with a large aspect ratio [5]. A flat ion beam should collide with a correspondently flat electron beam. Electron beam can be naturally flat in a storage ring. In linac-ring EIC, flat beam can be obtained from injector with magnetized electron gun, using vortex-plane beam adapters [6].

3.5.4.3 Conditioned Electron Cooling

Transverse rate of high energy electron cooling, conventionally, is low comparatively to the longitudinal one due to a large ratio of the related temperatures. This deficiency can be corrected by organizing the dispersive cooling [5,7], a mechanism of which similar in basic principle to the radiation decrements redistribution in electron synchrotrons and storage rings. Flat cooling beam can be obtained using the *elliptic beam adapters* [6] to match between round beam in solenoid of electron gun and flat beam in solenoid of cooling section.

Ion Equilibrium And Luminosity Lifetime

Considering the IBS-beam-beam-space charge-electron cooling balance, it is important to distinguish between *multiple IBS* and *single scattering* or Touschek effect. Multiple scattering has a relatively large probability and responsible for (or contributing to) ion *Fokker-Planck equilibrium* i.e. beam core, while single scattering kicks the particles out of the core. To overwhelm the multiple IBS, current of the cooling beam must well exceed a critical value, obviously proportional to the ion current [5]. After the cooling starts, the ion beam will shrink to the Focker-Plank equilibrium. Following this stage, an interplay between Touschek scattering and particle damping due to electron cooling beyond the core will determine the core i.e. luminosity lifetime. At ion energies far above the transition value, area of cooling beam should frequently exceed that of the ion beam, in order to extend the ion core lifetime. Using this phenomenology at a proper choice of luminosity lifetime, one can estimate an optimum set of parameters for a maximum average luminosity of a collider.

Feasibility of Electron Cooling For High Luminosity EIC

Considerations of feasibility and design of relativistic electron cooling for hadron colliders [5,8,9] and EIC are based on breakthroughs of recent years in accelerator technology: beam transport with discontinuous solenoid [10,11], adapting optics [6], and realization of superconducting energy recovering linacs (ERL) [12]. Conditioned electron cooling as above discussed would allow for a significant reduction of critical electron current needed to overwhelm the IBS.

High ion current that is needed for high luminosity EIC requires a large average current in electron cooler that might be difficult to attain with modern state of art electron sources. Recovery of such high current might also be quite challenging. This issue can relax drastically of use of electron circulator-cooler ring, similar in idea to the circulator-collider ring [1,2] but designed for electron energy smaller than ion energy by a factor of mass ratio. Use of electron circulator ring as a complementary to accelerator line was earlier meant as an option of beam transport for medium energy relativistic electron cooling [13]. Optical scheme of a circulator ring matched with magnetized electron gun through an RF accelerator line have been developed at conceptual studies of electron cooling of proton beam in PETRA for HERA [14]. Circulator-cooler ring can work in conjunction with ERL, as well; the only considerable addition to a CW single loop scheme would be fast kickers for switching the electron bunches between ERL and circulator. Estimations

Table 3.7: Initial electron cooling (p/e)

Beam energy	GeV/MeV	20/10
Cooling section length	m	12
Proton emittance, norm	mcm	3
Energy spread	%	0.03/0.03
Bunch length	cm	5/3
Number of particles/bunch	10^9	2/10
Bunch spacing	cm	20
Beam current	A	0.5/25
Cooling time	min	10
Cooled emittance, norm	mcm	1
Cooled bunch length	cm	1
Space charge tune shift		0.06

Table 3.8: High luminosity colliding beams (p/e)

Beam energy	GeV	150/7
Energy of cooling beam	MeV	75
Bunch collision rate	GHz	1.5
Number of particles/bunch	10^{10}	0.2/1
Beam current	A	0.5/2.5
Horizontal emittance, norm	mcm	1/100
Vertical emittance, norm	mcm	0.01/1
Number of interaction points		4
Total beam-beam tune shift		0.04/0.16
Space charge tune shift in proton beam		0.02
Luminosity over 4 interaction points	10^{35} cm^2.s	2
Cooling/IBS time in proton beam core	min	5
Core and luminosity Touschek's lifetime	h	20

indicate that, typically, electron bunches can stay in circulator during 100 revolutions, at least, before the dilution of beam quality due to the intra and inter-beam scattering leads to a significant reduction of cooling rates.

Electron cooling time grows with beam energy in the first or second power and with normalized beam emittances - in the third power. Therefore, it seems critically important to organize the cooling process in two stages: cool the ion beam initially at injection energy after stacking it in collider ring (in parallel or after re-bunching), and continue the cooling during and/or after acceleration to a high energy. Electron beam area could be then varied with time in an optimum way to minimize the time of beam shrinkage to equilibrium and maximize the lifetime as above discussed. Tables 3.7 and 3.8 together with Tables 3.7 and 3.8 present basic set of estimated parameters of high luminosity EIC with electron cooling.

Note, that, if the possibilities for shortening the ion beta-star are still not exhausted, then the luminosity potential shown in Table 3.8 could be even increased by introduction of traveling ion focus, as above discussed, at a correspondent reduction of electron emittances and bunch length.

It should also be noted that some of the above discussed advances could also be addressed to hadron colliders when considering the luminosity upgrade with electron cooling. More comprehensive analysis, simulations, optimization and experiments studies should forego the working out

of recommendations for practical design.

References

[1] L. Merminga, et al., Proc. of EPAC 2002
[2] Ya. Derbenev, Proc. of EPAC 2002
[3] R Palmer, SLAC SLAC-PUB-4707, Stanford 1988
[4] R.Brinkmann, and M.Dohlus, DESY-M-Report 95-11 (1995)
[5] Ya.Derbenev, Proc. of EPAC 2000
[6] A.Burov et al., Phys.Rev.E 66:016503,2002
[7] Ya.Derbenev and A.Skrinsky, Sov.Phys.Rev., 1 (1981) 165
[8] P.Wesolowski et al., proc. of EPAC 2000
[9] I.Ben-Zvi and V.Parkhomchuck, this ICFA Letter
[10] A.Burov et al., Rev. ST- Accel. Beams, Vol.3, 094002 (2000)
[11] S. Nagaitsev et al., this ICFA letter
[12] L. Merminga et al., on ERL
[13] G. Budker and A. Skrinsky, Sov. Phys. Usp. 21 (1978) 277 [14]
[14] Yu. Martirosyan et al., Proc. of EPAC 2000

3.6 Technology Demonstration Initiatives

3.6.1 Prospects On High-Intensity Optically-Pumped Polarized H^-, D^-, and $^3He^{++}$ Ion Source Development

A. Zelenski zelenski@bnl.gov Brookhaven National Laboratory, Upton, NY 11973 USA
J. Alessi alessi@bnl.gov Brookhaven National Laboratory, Upton, NY 11973 USA

The OPPIS technique is based on spin-transfer proton (or atomic hydrogen) collisions in an optically-pumped alkali metal vapor cell. The modern technologies involved – a superconducting solenoid, a 28 GHz microwave generator, and high power solid state tunable lasers – are essential to the OPPIS technique. The general polarization method is similar for all polarized ion sources. In the first step, electron spin polarized atoms are produced; in the second step, the electron polarization is transferred to the nuclei by means of the hyperfine interaction; and in the last step, the nuclear spin polarized atoms are ionized [1].

An advantage of the OPPIS in comparison with the conventional atomic beam source (ABS) technique is the use of fast beams (of several keV beam energy). Therefore, ionization to the H^- ion species can be easily done by passing the atomic beam through an alkali-metal vapor ionizer cell. The intensity of the fast DC polarized atomic beam is about $2{\cdot}10^{17}$ atoms/s within the ionizer acceptance. In contrast to the ABS, where the atomic beam intensity is limited due to intrabeam scattering and cannot be increased significantly in pulsed operation, an atomic beam intensity of $3 \cdot 10^{18}$ atoms/s and corresponding 40 mA H^- ion current within 2 π mm mrad normalized emittance was demonstrated in a pulsed OPPIS [2].

Polarization in the OPPIS is the result of a multi-step angular momentum transfer process. The primary source of angular momentum is the high-power lasers. The first step is the optical pumping of an alkali-metal vapor. Rb and Cs vapor are the best choices since the required laser wavelengths are in the operational range of Ti:sapphire and Cr:LISAF lasers (a 795-900 nm range is also ideal for semiconductor laser application). The TRIUMF laser system includes two commercial Ti:sapphire lasers of 5 W power each, which produce electron-spin polarized Rb atoms at a rate of up to $3 \cdot 10^{19}$ atoms/s [3]. The optical pumping rate determines the scale of polarized beam

intensity. In a pulsed mode, in excess of 1 kW of laser power can be easily obtained, which means that multi-ampere polarized beams are feasible. For accelerator applications the useful beam current is limited by the acceptance of the accelerators, which usually does not exceed 1-2 π mm mrad.

The second step is polarization transfer in H^+-Rb collisions, or spin-exchange polarization in H^0-Rb collisions. Due to the large cross-section, a Rb cell thickness of about 10^{14}atoms/cm^2 is sufficient for charge-exchange polarization. A higher thickness of about 10^{15} atoms/cm^2 is required for efficient spin-exchange polarization to occur. In the combined charge- and spin-exchange scheme an optically pumped Rb cell thickness of $5{\cdot}10^{14}$ atoms/cm^2 will be sufficient to produce an H electron polarization in excess of 90% /3/. In the third step, polarization is transferred from the electron to the H nucleus by the Sona transition or by an RF-transition unit. Polarized atoms are then ionized to H^- ions in the alkali metal vapor ionizer cell (the ionization efficiency is about 10% in sodium vapor), or to protons in the He-gaseous cell (ionization efficiency of about 80%).

In the BNL OPPIS, an ECR-type source produces a primary proton beam of a 2.0 – 3.0 keV energy, which is converted to electron-spin polarized H atoms by electron pick-up in an optically pumped Rb vapor cell. A pulsed Cr:LISAF laser of a 1 kW peak at 450 μs pulse duration is used for optical pumping. The nuclear polarized H atoms are then negatively ionized in a Na-jet vapor cell to form nuclear polarized H^-ions. This source produces in excess of 1.6 mA polarized $\overline{H}^-$ion current at 80% polarization [4].

The ECR has a comparatively low emission current density and high beam divergence. This limits further current increase and gives rise to inefficient use of the available laser power for optical pumping. In pulsed operation, suitable for application at high-energy accelerators and colliders, the ECR source limitations can be overcome by using instead a high brightness proton source outside the magnetic field. Following neutralization in hydrogen, the high brightness 1.0 – 5.0 keV atomic H beam is injected into a superconducting solenoid, where both a He-ionizer cell and optically-pumped Rb cell are situated in the same 25-30 kG solenoidal field, which is required to preserve the electron-spin polarization. The injected H atoms are ionized in the He-cell with 80% efficiency to form a small emittance, intense proton beam that then enters the polarized Rb vapor cell /5/. The protons pick up polarized electrons from the Rb atoms to become a beam of electron-spin polarized H atoms. The equilibrium fraction of neutral H beam after the He ionizer cell is about 20%. These residual atoms can be polarized in spin-exchange collisions between atomic H beam and Rb vapor. Depolarization during electron to proton spin transfer can be reduced to less than 5%; therefore an $\overline{H}^-$nuclear polarization in excess of 80% is expected. The feasibility of 10 mA polarized $\overline{H}^-$beam has been already demonstrated in experiments at TRIUMF with a possible increase to the 50 mA range [1]. The ECR-source replacement with an atomic hydrogen injector will provide the high intensity beam for polarized RHIC luminosity upgrade and for future RHIC facilities.

3.6.1.1 Optically-Pumped D^- Ion Sources

A replacement of the hydrogen by a deuterium gas bottle in the OPPIS will produce vector polarized D- ions with theoretical 66% (practical $\sim$55%) vector polarization. The D^- beam intensity will be similar to the above discussed H^- beam. The tensor polarization must be zero, which makes such a source attractive for experiments on the deuteron electric dipole moment search [5]. Higher (100% theoretical) vector polarization can be obtained in a dual optical pumping scheme [6]. A 300 μA polarized D- ion current of a 70% vector polarization was achieved in the KEK OPPPIS with dual pumping [7]. To produce maximal tensor polarization an additional RF transition would be required [5].

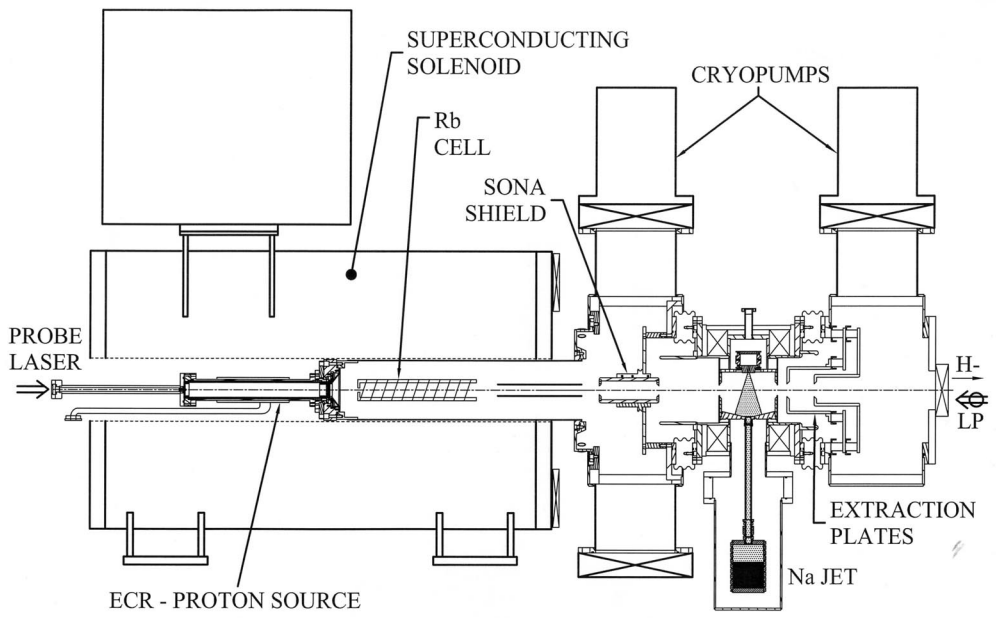

Figure 3.16: The BNL OPPIS general layout.

3.6.1.2 Polarized $^3He^{++}$ Sources

Spin–transfer collisions can be also used for polarized $^3He^{++}$ production. This scheme is under development at RCNP (Osaka, Japan) [8]. It requires a very high thickness optically-pumped alkali-metal vapor cell and high current primary He^{++} ion source.

There exist two very well developed ^{3}He nuclear polarization techniques: metastability-exchange optical pumping, and spin-exchange collisions with optically-pumped Rb vapor in a high-pressure gas cell. A ^{3}He atom production rate of about 10^{18}-10^{19} atoms/sec of 50-70% polarization was achieved in both techniques. Possible polarized $^3He^{++}$ acceleration in RHIC (and also for a future RHIC upgrade to an electron-ion collider eRHIC) will require about $2{\cdot}10^{11}$ ^{3}He ions in the source pulse and about 10^{11} ions in a RHIC bunch. We propose the use of an EBIS (Electron-Beam Ion Source) to produce $^3He^{++}$ by ionization of the polarized ^{3}He gas. An appropriate EBIS is under development at BNL as an alternative to the Tandem heavy ion injector for RHIC [11]. The ionization in the EBIS is produced in a 50 kG magnetic field, which is essential to preserve nuclear ^{3}He polarization while in the intermediate single-charged $^3He^+$ state. The ionization efficiency to double-charged $^3He^{++}$ will be close to 100% and the number of ions is limited to maximum charge which can be confined in the EBIS. From experiments with the Au^{32+} ion production, one expects about $2.5{\cdot}10^{11}$ $^3He^{++}$ ions to be produced and extracted for subsequent acceleration and injection to RHIC.

References

[1] A.Zelenski, Proc.SPIN 2000, **AIP 570**, p.179, (2000).

[2] A.Zelenski et al., DESY-PROC-1999-03, p.177, (1999).

[3] A.Zelenski et al., NIM **A402**, p.185, (1998).

[4] A.Zelenski et al., “Polarization optimization studies in the RHIC polarized source “, will be published in Proc.SPIN 2002 conference, BNL 2002.

[5] Y.K. Semertzidis private communications.

[6] M.B.Schneider and T.B.Clegg, NIM **A254**, p.630, (1987).

[7] M.Kinsho, Y.Mori et al., Proc. Int Workshop on polarized sources and targets, Cologne,

1995, World Scientific, Singapore, ed. H.P. Shieck, p.126 (1996).
[8] M.Tanaka et al., Phys. Rev. **A 1**.p.534, (1970).
[9] E.N. Beebe, et. al., Rev. Sci. Instr., **73**, p.899, (2002).

3.6.2 Polarized Ion Sources with Resonant Charge-Exchange Plasma Ionizer for Future Electron Ion Collider

.

A. S. Belov belov@al20.inr.troitsk.ru Institute for Nuclear Research of Russian Academy of Sciences, Moscow, Russia

V. P. Derenchuk laddie@iucf.indiana.edu Indiana University Cyclotron Facility, Bloomington, USA

Modern day sources of polarized hydrogen or deuterium ions all have a mechanism to form a polarized neutral beam of atoms which feeds into a device that ionizes these atoms. An atom source that forms a beam of polarized atoms with thermal velocities is normally referred to as an atomic beam source or ABS. The ABS is commonly used to provide polarized atoms for targets in accelerator-based experiments as well as for ion sources. Basic principles of the ABS are considered in many reviews, see for example [1] and recently [2].

In the ABS, hydrogen or deuterium atoms are formed by dissociation of molecular gas, typically in a RF discharge. The atomic flux is cooled to a temperature 30K - 80K by passing through a cryogenically cooled nozzle. The atoms escape from the nozzle orifice into a vacuum and are collimated to form a beam. The beam passes through a region with inhomogeneous magnetic field created by sextupole magnets where atoms with electron spin up are focused and atoms with electron spin down are defocused.

Nuclear polarization of the beam is increased by inducing transitions between the spin states of the atoms. The transition units are also used for a fast reversal of nuclear spin direction without change of the atomic beam intensity and divergence. Several schemes of sextupole magnets and RF transition units are used in the hydrogen or deuterium ABS. For atomic hydrogen, a typical scheme consists of two sextupole magnets followed by weak field and strong field RF transition units. In this case, the theoretical proton polarization will reach $P_z = \pm 1$. Switching between these two states is performed by switching between operation of the weak field and the strong field RF transition units. For atomic deuterium, two sextupole magnets and three RF transitions are used in order to get deuterons with vector polarization of $P_z = \pm 1$ and tensor polarization of P_{zz} = +1, -2

Pulsed ABS's produce more intense beams of polarized atoms compared with the DC mode of operation. A peak polarized atomic hydrogen beam intensity of $2 \cdot 10^{17}$ atoms/sec downstream of the sextupole magnets had been achieved at the Institute for Nuclear Research (INR), Moscow [3]. This is approximately 3 times larger than intensity of atomic beam from the best DC atomic beam sources.

Different methods for ionizing polarized atoms and their conversion into negative ions were developed in many laboratories. The techniques depended on the type of accelerator where the source is used and the required characteristics of the polarized ion beam (see ref. [2] for a review of current sources).

For the pulsed atomic beam-type polarized ion source (ABPIS) the most efficient method was developed at INR, Moscow [3-5]. Polarized hydrogen atoms with thermal energy are injected into a deuterium plasma where polarized protons or negative hydrogen ions are formed due to the quasi-resonant charge-exchange reaction:

$$H^0 \uparrow + D^+ \quad \rightarrow H^+ \uparrow + D^0 \ (1)$$

$$H^0 \uparrow + D^- \quad \rightarrow H^- \uparrow + D^0 \ (2)$$

The use of reaction (2) for polarized ion sources has been proposed by W. Haeberli [6]. The cross-section of reaction (1) at a relative energy of colliding particles of about 10 eV is $5{\cdot}10^{-15}$ cm^2 and for reaction (2) it is $10^{-14}cm^2$. These large cross-sections result in the highly efficient ionization of polarized atoms, high intensity polarized beams are produced.

The INR, Moscow source has produced a pulsed polarized proton beam with peak intensity of 6 mA in a normalized emittance of 1.8 π mm·mrad and a polarization of 90% [3,7]. This intensity corresponds to a conversion efficiency of hydrogen atoms into polarized protons of about 20%.

The density of polarized hydrogen atoms in the charge-exchange region of this source was increased by using a storage cell [8]. The storage cell, made from aluminum alloy, was placed into the charge-exchange region of the plasma ionizer. A polarized proton beam with a peak current of 11mA in a normalized emittance of 1.0 π·mm·mrad and a polarization of 80% has been obtained from the source with the storage cell [9]. The ionization efficiency reached about 30% in this type of ionizer.

A source scheme with the resonant charge-exchange plasma ionizer and storage cell can also be used for production of polarized $^3He^{++}$ ions [10]. It is expected that the intensity of polarized $^3He^{++}$ ion beam produced by this method should be in mA region with a normalized emittance of 1 π·mm·mrad and polarization up to 80%.

For the production of polarized negative hydrogen ions the deuterium plasma in the charge-exchange region of the INR source was enriched by unpolarized negative deuterium ions using a specially designed surface-plasma converter [4,5]. The most efficient two-stage converter has been developed recently [11] in which a deuterium plasma jet generated by a pulsed arc-discharge plasma source collides first with the internal surface of a conical shape neutralizer. Positive ions of the plasma jet are converted into hot neutral deuterium atoms in collisions with the neutralizer surface. These hot atoms are injected into the entrance of the charge-exchange region with a solenoidal magnetic field where they collide with the cesiated surface of the converter. Cs is used for catalysis of negative ion formation by decreasing the work function of the converter surface. The hot deuterium atoms are converted into negative ions in collisions with the converter surface with an efficiency about 10%. Polarized H? ion beam with a peak current of 2.5 mA was obtained from the INR, Moscow source with the two-stage surface-plasma converter and respective unpolarized D$^-$ion current was 45 mA [11]. The efficiency of conversion of polarized hydrogen atoms into polarized H$^-$ ions reached about 8% in this source.

Another ABPIS with the resonant charge-exchange plasma ionizer, CIPIOS, has been built by IUCF in collaboration with INR, Moscow [12,13]. The IUCF source CIPIOS is the most versatile and high brightness pulsed source of polarized H$^-$ and D$^-$ ions. Switching from polarized H$^-$ to polarized D$^-$ operation is a matter of switching the feed gas at the dissociator from hydrogen to deuterium, the gas at the plasma source from deuterium to hydrogen and installing additional transition units. The CIPIOS ionizer is also used as a source of unpolarized H$^-$ and D$^-$ ions with a peak current up to 40 mA.

CIPIOS operated from 1999 to 2002 and averaged over 4,000 hours of beam delivery time per year. The maximum beam peak current for polarized H and D$^-$(3 states) reached 2.2 mA in a normalized emittance of 1.2 π·mm·mrad with a polarization of 85% to 90%. The typical ion beam pulse duration is 200 μs at a repetition rate of 2 Hz. Operation with a longer pulse duration of up to 500 μs has been demonstrated [14]. D$^-$ion polarization states available are listed in Table 3.9.

Table 3.9: IUCF D^- Polarization Results

State Name	Nominal Pz	Measured	Nominal Pzz	Measured
+ Vector	+1	0.909 (31)	+1	0.891 (13)
- Vector	-1	-0.684 (30)	+1	0.695 (14)
+ Tensor	0	0.003 (32)	+1	0.875 (13)
- Tensor	0	0.020 (33)	-2	-1.591 (13)

The source performed very reliably and often ran without any failures for 6 weeks between maintenance periods. Consumption of Cs is only about 100 mg per 1000 hrs of operation and does not create a problem in the operation of the source or RFQ.

To compare polarized ion sources, it is useful to use a figure of merit, $P^2 \cdot I/\varepsilon_n^2$. Here, I is the polarized beam current, P is its polarization and ε_n is normalized emittance. This value is equivalent to brightness for unpolarized beams. For polarized H^- and D^- ions CIPIOS has world record figure of merit value: 1 mA/(mm·mrad)^2 and 2.4 mA/(mm·mrad)^2 respectively.

A further intensity increase of the ABPIS with a resonant charge-exchange ionizer is possible. For a source of polarized positive ions, a cooled storage cell, an increase of plasma flux through the cell and use of higher field sextupoles should result in about 30 mA peak of polarized proton and deuteron beam. For polarized negative ions, a beam intensity **up to 10 mA** may be possible by using super-conducting sextupoles in the ABS, improving the plasma density in the ionizer and with better handling of space charge in the extraction region [15].

References

[1] Haeberli W., Ann. Rev. Nucl. Sci. **17,** 373 (1967).

[2] Clegg Thomas B., "Polarized Ion Sources Progress: Past Achievements! Future Aspirations?", Proc. of Ninth International Workshop on Polarized Sources and Targets 2001, eds. V. P. Derenchuk and B. v. Przewoski, World Scientific, 2002, pp. 183-193.

[3] Belov A.S. et. al., Nucl. Instr. and Methods in Phys. Res. **A255**, 442 (1987).

[4] Belov A.S. et. al., Nucl. Instr. and Methods in Phys. Res. **A333**, 256 (1993).

[5] Belov A.S. et. al., Rev. Sci. Instr. **67**, 1293 (1996).

[6] Haeberli W., Nucl. Instr. and Methods **62,** 355 (1968).

[7] Belov A.S. et. al., "Intense Polarized Proton Source at Moscow INR", in Proc. of International Workshop on Polarized Ion Sources and Polarized Gas Jets", KEK, Tsukuba, Japan, 1990, KEK Report 90-15, p. 69.

[8] Belov A.S. et. al., "Polarized ions from a storage cell", in Proc. of Seventh International Workshop on Polarized Gas Targets and Polarized Beams", Urbana, Il, USA, 1997, AIP Conf. Proc. **421**, 362 (1998).

[9] Belov A.S. et. al., "Polarized Ion Source with Resonant Charge-Exchange Plasma Ionizer", in Proc. of 13^{th} International Symposium on High Energy Spin Physics SPIN 98, 1998, Protvino, Russia, eds. N.E. Tyurin et al.,World Scientific, pp. 622-624.

[10] Belov A.S., Nucl. Instr. and Methods in Phys. Res., **A402**, 205 (1998).

[11] Belov A.S. et. al, "Development of Polarized Negative Hydrogen Ion Source with Resonant Charge-Exchange Plasma Ionizer", in Proc. of 14^{th} International Spin Physics Symposium SPIN 2000, Osaka, Japan, 2000, AIP Conf. Proc. **570**, p.p.835-840.

[12] Derenchuk V.P. and Belov A.S., "A multi-milliampere polarized and unpolarized negative source for IUCF", In proceedings of the 2001 Particle Accelerator Conference, Chicago, USA, 2001, p. 2093-2095.

[13] Derenchuk V.P. and Belov A.S., "Recent Improvements in CIPIOS Intensity and Operation", in Proc. of Ninth International Workshop on Polarized Sources and Targets 2001, eds. V. P.

Derenchuk and B. v. Przewoski, World Scientific, 2002, pp. 210-214.

[14] Derenchuk V.P. and Belov A.S., "Polarized D^- Operation and Development of the IUCF Ion Source CIPIOS", 15^{th} International Spin Physics Symposium SPIN 2002, BNL, US, 2002 (to be published).

[15] Belov A.S. et. al., " Development of Polarized Hydrogen Ion Source with Resonant Charge-Exchange Plasma Ionizer at INR, Moscow", in Proc. of Ninth International Workshop on Polarized Sources and Targets 2001, eds. V. P. Derenchuk and B. v. Przewoski, World Scientific, 2002, pp. 205-209.

3.6.3 Polarized Proton And Ion Issues For eRHIC

V. Ptitsyn vadimp@bnl.gov Brookhaven National Laboratory, Upton, NY 11973 USA

T. Roser roser@bnl.gov Brookhaven National Laboratory, Upton, NY 11973 USA

The physics requirements for EIC call for polarized proton (and ion) beams. In addition the beams should be polarized longitudinally at the collision points. It has always been considered a challenging task to get highly polarized proton beams at high energies. Unlike electrons, protons cannot acquire their polarization through the process of synchrotron radiation. One has to use a polarized ion source and then accelerate the polarized beam to collision energy, minimizing polarization loss during acceleration. The polarization loss comes mainly from first-order spin resonances. The conditions for spin resonances are met when the spin precession tune equals an integer number (imperfection resonances) or the fractional part of the tunes of the betatron orbital motion (intrinsic resonances). For a usual "flat" accelerator, the spin precession tune is equal to $G\gamma$ (with G=1.793 for protons), which means that, during the acceleration, the beam crosses numerous spin resonances.

Among several methods, the use of Siberian Snake presents the most powerful technique to preserve the beam polarization during acceleration. A "full" Siberian Snake is a magnet insertion, which rotates the spin by 180° about an axis lying in the horizontal plane [1]. As a result the spin precession tune becomes independent of the beam energy (1/2 in general case), thus effectively eliminating first-order spin resonances. Early experiments with low energy polarized beam at IUCF confirmed the effectiveness of the Siberian Snake concept [2].

During last year's polarized proton run at the RHIC collider, Siberian Snake insertions (two per RHIC ring) were successfully used to accelerate polarized proton beams up to 100 GeV energy and to store them for experiments with polarized proton-proton collisions [3]. With proton bunch intensities of about 0.7 x 10^{11} protons per bunch a peak luminosity of 1.5×10^{30} $s^{-1}cm^{-2}$ was achieved. The Siberian Snake design, chosen for the RHIC [4], is based on a sequence of helical magnets. This design minimizes the beam orbit distortions inside the Snakes while keeping the orbit undisturbed outside the Snake insertion. The Snakes were constructed using superconducting helical magnets.

However, the application of Siberian Snakes does not guarantee the polarization preservation. With beam energies as high as tens and hundreds of GeVs high-order spin resonances, so-called "snake" resonances [5], can decrease or even destroy the beam polarization, if the beam orbital conditions are not controlled carefully enough. The importance of good orbit control as well as betatron tune and betatron coupling control during the acceleration was clearly seen at the RHIC, where some depolarization was observed from such high-order spin resonances [6]. In the case of RHIC, the precise knowledge of magnet misalignments, either by direct tunnel measurements or extracted from beam-based measurements, is clearly necessary to ensure small enough closed orbit

distortions (rms less than 0.5mm) in order to minimize the depolarization effects. The application of a tune-feedback system as well as dedicated methods of betatron coupling measurements during the acceleration ramp are considered as necessary tools to provide successful polarized beam acceleration to the maximum RHIC proton energy of 250 GeV.

In order to produce, as required for EIC, longitudinal beam polarization at the collision point a pair of longitudinal spin rotators should be installed around the interaction region, transforming transverse beam polarization into the longitudinal polarization and back. Similar spin rotators have already been installed at RHIC at two interaction regions for proton-proton beam experiments. The design of the spin rotators resembles that of Siberian Snakes, since it is also based on superconducting helical magnets in order to minimize beam orbit excursions. The RHIC team is looking forward to the first use of the spin rotators in oncoming polarized proton run.

Besides the application of polarization control devices in the RHIC, as described above, other state-of-the-art techniques and devices are used at the injectors in order to produce and preserve the proton beam polarization. "Optically Pumped Polarized Ion Source", OPPIS produces 10^{12} polarized protons per pulse with up to 80% polarization [7]. In the AGS injector a 5% solenoidal partial snake and rf dipole have been used as tools to artificially increase the spin resonance strength and provide an adiabatic regime (with spin-flip) for resonance crossing, since the use of a Siberian Snake is not reasonable in this low energy range (3-25GeV) [8-10].

The interesting opportunity for EIC physics would be the use of polarized ion beams. The possibility of polarized ion beam acceleration in RHIC has been considered by E.Courant [11]. Polarized deuterons have a G-factor equal to – 0.143, which is more than a factor of ten smaller than for the protons. Because of this there are a considerably smaller number of depolarizing spin resonances that need to be crossed during acceleration. On the other hand, since the efficiency of spin rotation using magnetic fields is also strongly reduced, the application of Siberian Snakes does not look feasible. Therefore, other techniques, like those mentioned above for the AGS accelerator, have to be considered to overcome beam depolarization in this case. However, the polarization preservation for ^{3}He (with G = - 4.191), tritium (G = 7.937) and ^{19}F (G = 4.547) ions can be well controlled using the present RHIC Siberian Snakes. For these ions, the effect of the considerable larger number of spin resonances (a of factor 2 - 5 more numerous than for the protons) should be carefully evaluated. Of course, the development and demonstration of corresponding polarized ion sources is also required.

In summary, the RHIC accelerator complex has a well developed framework for producing high energy polarized proton beams. This framework is being used for experiments with polarized proton-proton beam collisions. It could be naturally used for supplying polarized proton beams for the electron-ion collider, which is considered as a possible future option.

References:

[1] Ya.S.Derbenev et al., Particle Accelerators **8**, 115 (1978).

[2] A. D. Krisch et al., Phys. Rev. Lett. **63**, 1137 (1989).

[3] T. Roser et al., Proceed. of EPAC02, Paris, 209 (2002).

[4] V. Ptitsyn and Yu. M. Shatunov, NIM **A398**, 126 (1997).

[5] S. Y. Lee and S. Tepikian, Phys. Rev. Lett. **56**, 1635 (1986).

[6] V. Ptitsyn, A. Luccio, V. Ranjbar, "The Analysis of Depolarization factors in Last RHIC Run", presented at SPIN2002 Symposium, Upton, (2002).

[7] A. N. Zelenski et al., Proceed. of PAC99, New York, 106 (1999).

[8] T. Roser, Proceed. of SPIN1988 Symposium, Minneapolis, 1442 (1989).

[9] M. Bai, et al., Phys. Rev. Lett. **80**, 4673 (1998).

[10] H. Huang et al., Proceed. of EPAC02, Paris, 335 (2002).

[11] E. D. Courant, AGS/RHIC/SN 066, (1997)

3.6.4 Spin Transports for ELIC

Yaroslav Derbenev derbenev@jlab.org CASA, Jefferson Lab, Newport News, VA 23606 USA

Below, we will discuss in some detail the ion and electron spin transports and manipulation with figure 8 rings, or twisted spin synchrotrons [1] proposed to advance the spin features of the "green field" version of EIC, or Electron-Light Ion Collider [2]. There are two important advantages of such rings: first, ease spin maintenance at beam acceleration in boosters; second, possibility to create a desirable spin polarization, the longitudinal or transverse one, at collision points and manipulate it for all particle species at any beam energy in the collider ring.

3.6.4.1 Spin In Figure 8 Synchrotrons

In twisted rings the spin precession in one arc is cancelled by the reverse precession in the opposite arc, thus, the global spin tune does not change with energy being simply equal to zero. Spin motion on a plane twisted orbit is degenerated, i.e. unstable, but it is easily stabilized by a solenoid introduced in one of two intersecting straights of the orbit, then the spin tune is determined by the spin rotation in solenoid, and the longitudinal polarization in this straight appears the stable one. Spin rotation by solenoid must frequently exceed the spin deviation by the imperfection fields related to orbit excursions. The imperfection effect is proportional to the particle anomalous gyro-magnetic factor, g-2, therefore, spin control by solenoid is especially effective for particles with small g-2 value (d, He^3). Such stabilization is similar in principle to Partial Siberian Snake used successfully at AGS to prevent proton beam depolarization due to crossing the imperfection spin resonances at acceleration [3]. At high energies, when the anomalous spin precession in arcs becomes large, the horizontal spin can be effectively stabilized by transverse magnetic fields associated with vertical excursions of the closed orbit [1].

The intrinsic spin resonances, i.e. resonances between spin precession in vertical field and particle oscillation in focusing quadrupoles, stay away in twisted rings. Thus, the issue of preventing the depolarization due to the intrinsic spin resonances, that challenges operating the proton booster and light ion collider rings [3], disappears in the twisting design. Spin tune spread and high order spin resonances [4,5], or "snake resonances" [3], will be diminished with emittance decrease by electron cooling.

3.6.4.2 Twisted spin transport scheme of ELIC

The proposed ion beam transport of ELIC [2] involves figure 8 collider and booster rings. Optionally, it may include the electron cooling accumulator ring (after $\sim$ 200 MeV ion linac) designed either as twisted ring or conventional ring with Siberian Snake solenoid [2]. After the linac and accumulator ring, longitudinally polarized proton or ion beam can be injected to the straight section of the twisted pre-booster with stable longitudinal spin, accelerated to a few GeV, injected in similar way to large twisted booster (electron circulator-collider ring), accelerated to energy up to 20 GeV and injected to the twisted collider ring. Here, the acceleration can be continued using warm or superconducting solenoid for light ions and type 1 superconducting Siberian Snake (i.e. snake conserving the longitudinal spin, or simply the longitudinal snake) for protons in order to stabilize the spin. In this way, the longitudinal spin can be delivered from the source to the collision points of the twisted collider ring.

Spin steering

Transverse spin for experiments on CP violation can be obtained (after beam acceleration to energy of the experiment) turning the stable spin in horizontal plane from longitudinal direction by

adiabatic ramp of a few or several horizontal dipoles distributed in a proper way around the twisted ring. The strength of stabilizing solenoid or longitudinal snake then should slow down to zero or other optimum value. Here, one has to account for the related orbit excursions. Steering technique also could be used in order to switch the stable spin, either longitudinal or transverse, between two intersecting straights with 4 experiments being hold in total.

Proton beam in twisted ring with longitudinal snakes in arcs

Two full longitudinal snakes installed at the middle of arcs will allow for arrangement of 4 *simultaneously* operated collision points all with the longitudinal or transverse polarization of proton beam stabilized in a way as above discussed. Note, that the helical longitudinal snakes are compact [6]: one snake would occupy a space not longer than 3 m.

3.6.4.3 Flipping the ion spin

Besides the possibilities to alternate the ion polarization over beam pulses from source [7] or to develop and apply an RF-induced flipping technique established for low energy beams [8], one may consider the possibility to use the above described steering technique for periodical reverse of stable ion spin. An additional possibility for each turn flipping transverse proton spin might be the *RF trapped flipping spin* technique [9]. It could work in cooperation with the full longitudinal snake that has to be introduced to one of two intersecting straights of twisted ring in order to make the spin tune in the ring equal to $^1/_2$.

3.6.4.4 Delivering the longitudinal electron spin from polarized source

Bend-related precession of electron spin before injection in a straight of twisted circulator ring can be compensated using either the Wien filter at low energy part in injector or superconducting solenoid as full longitudinal snake settled at a accounted point of beam track. No snakes will be needed in the ring with collision points only in one straight, but two solenoid snakes (about 60 TM each for 5 GeV beam) installed in arcs are needed in order to arrange 2 collision points with repeated turn by turn (longitudinal) polarization in each straight. Since the duration of electron circulation in the ring is quite short (100 revolutions), no more specific measures for spin maintenance would be required.

3.6.4.5 Conclusion

The twisted rings based EIC version should be studied comprehensively as possible way to enhance significantly the capabilities and efficiency of polarized electron-ion collider.

References

[1] Ya. Derbenev, UM HE 96-05, University of Michigan, 1996
[2] L. Merminga and Ya. Derbenev, this ICFA letter
[3] V. Ptitsyn and T. Roser, this ICFA letter
[4] Ya. Derbenev, A. Kondratenko, and A. Skrinsky, Sov. Phys. JETP,33, 658 (1971)
[5] Ya. Derbenev, in DESY-PROC-1999-03, p.225
[6] Ya. Derbenev and A. Kondratenko, AIP Conf. Proc. 51, 292 (1978)
[7] A. Belov, Private communication
[8] B. Blinov et al., PRST AB 3: 104001,2000
[9] V. Anferov and Ya. Derbenev, PRST AB 3: 094001, 2000

Table 3.10: Various scenarios considered for electron-cloud build-up simulations

Case no.	1	2	3	4
Bunch population	2.5x10^{10}	2.5x10^{10}	5x10^{9}	1.0x10^{10}
Bunch spacing	6.7 ns	6.7 ns	2 ns	0.66 ns
Beam energy	50 GeV	50 GeV	50 GeV	100 GeV
Rms bunch length	5 cm	5 cm	1 cm	1 cm
Rms transverse beam size	0.6 mm	0.2 mm	0.2 mm	0.1 mm
Beam pipe radius	2 cm	2 cm	2 cm	2 cm

3.6.5 Electron Cloud in Electron-Ion Colliders

K. Ohmi KEK, Japan
G. Rumolo GSI, Germany
F. Zimmermann Frank.Zimmermann@cern.ch CERN, Switzerland

Many high-intensity proton storage rings operating with short bunches and close spacings have experienced instabilities and steep pressure increases caused by an electron cloud, which is generated via a beam-induced multipacting process. This phenomenon was first seen in the Novosibirsk PSR around 1965 [1], then 1977 in the CERN ISR operated with a bunched beam [2], and since about 1988 it has limited the maximum current in the Los Alamos PSR [3,4]. Recent examples include the CERN SPS [5,6], CERN PS [7], RHIC [8] and the Tevatron [9]. In Los Alamos, the proton bunch is extremely long ($\sim$200 m) and electrons are amplified by multipacting in the decreasing potential at the tail of a bunch ('trailing-edge multipacting' [9]). In the other cases, the number of electrons increases due to multibunch multipacting, where the number of secondary electrons increases from bunch to bunch. It is this second process, which may occur in an ion-electron collider such as ELIC.

Empirical evidence suggests that the bunch current threshold above which multibunch multipacting occurs decreases with shorter bunch spacing, e.g., at the SPS the multipacting threshold for 25 ns spacing is around 5x10^{10} protons per bunch, whereas for a 5 ns spacing it is near 7x10^{9} (this behavior is opposite to what would be expected from the naïve true multipacting condition!). The threshold values improve with progressing surface conditioning, thanks to the multipacting and the electron bombardment itself. The ELIC parameters for various stages [11] listed in Table 3.10 lie between the two SPS examples. Therefore, we expect that the electron cloud may be observed under certain conditions. If an electron cloud is built up, it can induce both coupled-bunch [12] and single-bunch instabilities [13,14].

For our simulations of electron-cloud build up in ELIC, we have considered a rather high value for the maximum secondary emission yield, namely δ_{max}=1.6, and we have assumed that this maximum occurs at an incident energy ε_{max}=270 eV. Elastic reflection of low-energy electrons is included as parametrized in Ref. [15]. The initial number of ionization electrons corresponds to a residual CO pressure of 10 ntorr. The electron cloud build was computed by the codes ECLOUD [16] and PEI [17], and the results are shown in Figs. 3.17, 3.18, and 3.19, respectively. There is no significant electron accumulation in any of the cases considered, except for case 4 with the PEI code (there is a noticeable difference between the two codes). The number of electrons increases linearly and not exponentially (no multipacting) and the absolute level is 3 or 4 orders below those found in simulations for the CERN SPS for example.

From the foregoing discussion, we may conclude that the electron cloud will not be a problem in ELIC. However, in advanced stages of ELIC electron cooling is used to improve the quality of

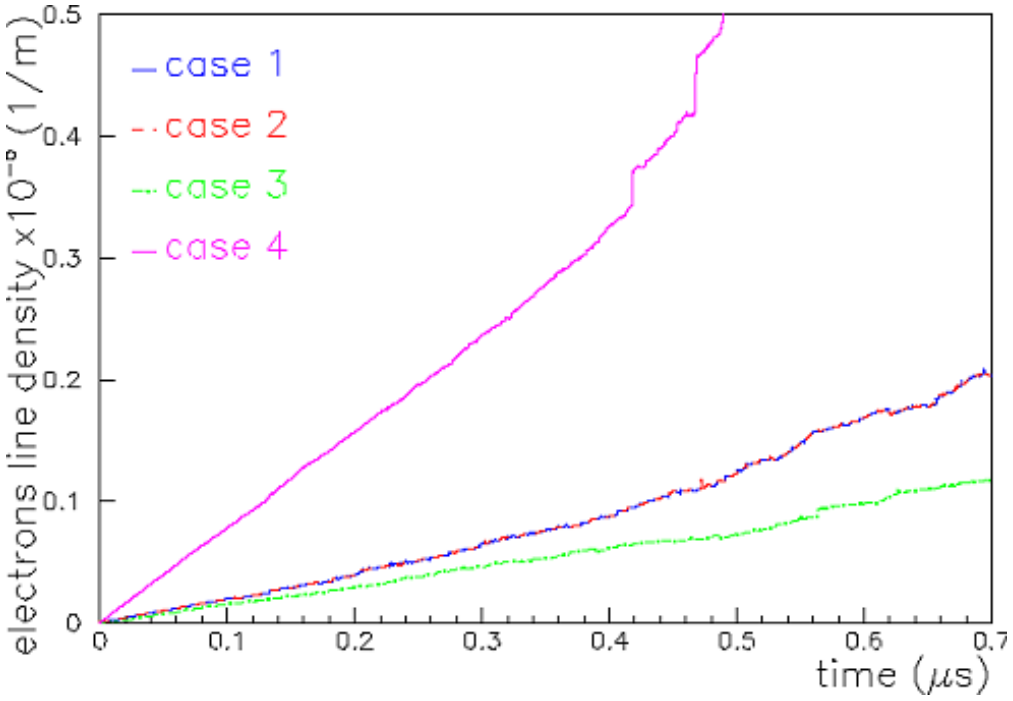

Figure 3.17: Simulated electron line density as a function of time for the 4 ELIC scenarios of Table 3.10, using ECLOUD code.

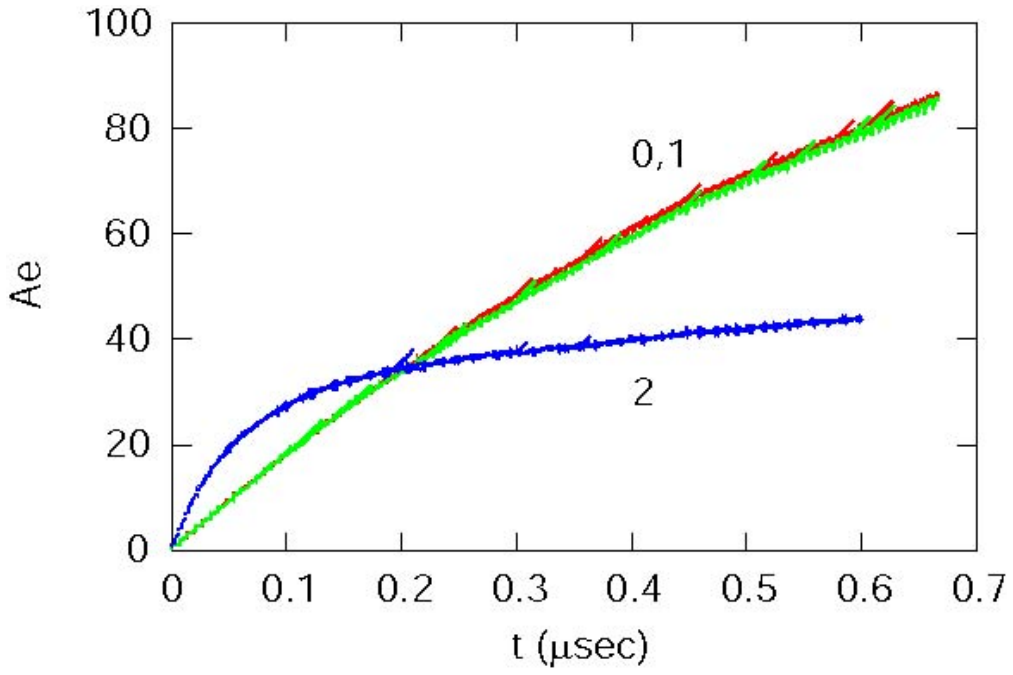

Figure 3.18: Simulated electron line density as a function of time for the first 3 ELIC scenarios of Table 3.10, using PEI code. The vertical coordinate A_e is the number of electrons normalized to the number of primary electrons produced by one bunch.

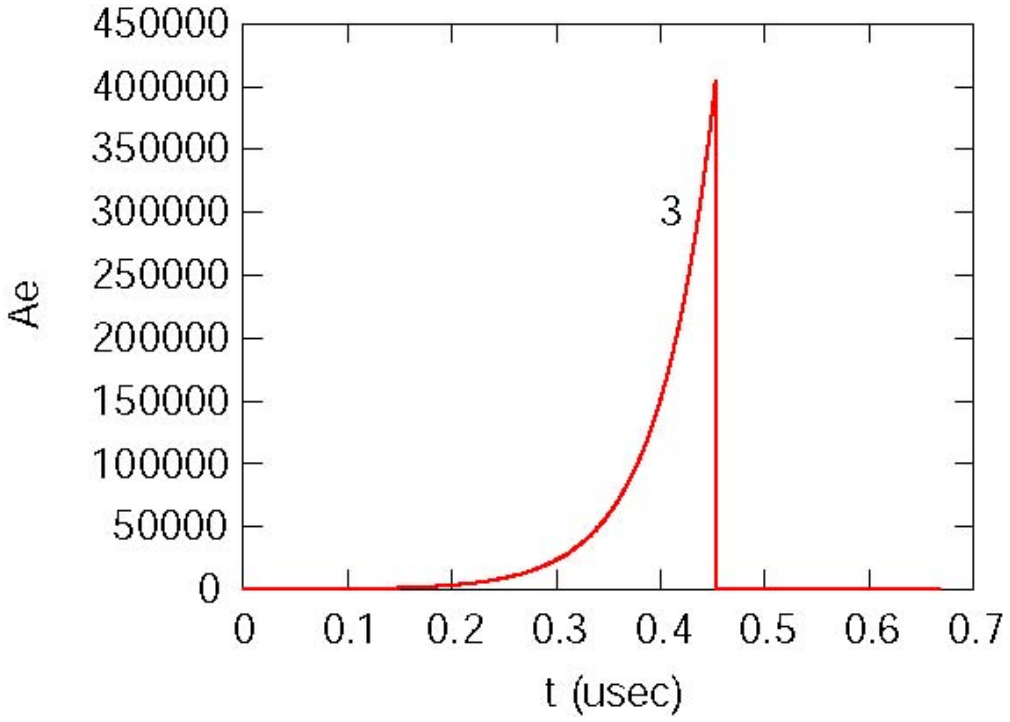

Figure 3.19: Simulated electron line density as a function of time for the last ELIC scenario of Table 3.10, using PEI code. The vertical coordinate A_e is the number of electrons normalized to the number of primary electrons produced by one bunch.

the ion beams, which means that large numbers of electrons are intentionally introduced. In principle the electron cooler can drive a single-bunch instability similar to that caused by the electron cloud [18], but for reasonable solenoid fields in the cooler section this instability is suppressed, according to simulations with the HEADTAIL program [19].

References:

[1] G. Budker, G. Dimov, and V. Dudnikov, et al., Proc.X Internat. Conf. Particle Accelerators, Protvino, 1977, v.2,p.287 (1978).

[2] O. Grobner, Proc. Xth Internat. Conf. on High Energy Accel., Protvino, 1977, p. 277 (1978).

[3] D. Neuffer et al., "Observation of a Fast Transverse Instability in the PSR," published in Nucl.Instrum.Meth.A321:1-12 (1992).

[4] R. J. Macek et al., "New Developments on the ep Instability at the Los Alamos Proton Storage Ring," Tsukuba 2000, Advanced neutron sources, vol. 1, 229-239 (2000).

[5] J. M. Jimenez et al., "Electron Cloud with LHC-Type Beams in the SPS: A Review of Three Years of Measurements," ECLOUD'02, Geneva, Switzerland, 15-18 Apr 2002 (2002).

[6] G. Arduini et al., "Transverse Instabilities of the LHC Proton Beam in the SPS," EPAC 2000, Vienna, 341-343 (2000).

[7] R. Cappi et al., "Electron Cloud build Up and Related Instability in the CERN PS," ECLOUD'02, Geneva, Switzerland, 15-18 Apr 2002, 57-62 (2002).

[8] W. Fischer et al., "Electron-Cloud Measurements and Simulations for RHIC," ECLOUD'02, Geneva, Switzerland, 15-18 Apr 2002, 63-68 (2002).

[9] J. Annala, B. Hanna, unpublished (2002).

[10] J. Wei, R. Macek, "Electron-Cloud Effects in High-Intensity Proton Accelerators," ECLOUD'02, Geneva, Switzerland, 15-18 Apr 2002, 29-40 (2002).

[11] L. Merminga et al., "ELIC and Electron-Light Ion Collider Based at CEBAF," PEAC' 2002, Paris, France (2002).

[12] M. Izawa et al., "The Vertical Instability in a Positron Bunched Beam," Phys. Rev. Lett. 74:5044-5047 (1995).

[13] K. Ohmi, "Beam and Photoelectron Interactons in Positron Storage Rings," Phys. Rev. Lett.75, 1526-1529 (1995).

[14] K. Ohmi, F. Zimmermann, "Head-Tail Instability Casued by Electron Cloud in Positron Storage Rings," Phys.Rev.Lett.85, 3821-3824 (2000).

[15] B. Henrist, N. Hilleret, et al., "Secondary Electron Emission Data for the Simulation of Electron Cloud," ECLOUD'02, Geneva, Switzerland, 15-18 Apr. 02, 75-78 (2002).

[16] G. Rumolo, F. Zimmermann, "Practical User Guide for ECloud," CERN-SL-Note-2002-016 (2002).

[17] K. Ohmi, unpublished; but see Ref. [13].

[18] G. Rumolo et al., "Driving the Electron Cloud by an Electron Cooler," ECLOUD'02, Geneva, Switzerland, 15-18 Apr 2002, 269-274 (2002).

[19] G. Rumolo, F. Zimmermann, "Practical User Guide for HEADTAIL," CERN-SL-Note -2002-036 (2002).

3.6.6 Intrabeam Scattering

Jie Wei jwei@bnl.gov Collider-Accelerator Department, Brookhaven National Laboratory, Upton, NY 11973, USA

Ibtra-beam scattering (IBS) refers to small-angle Coulomb scattering between particles in the same bunch circulating in an accelerator. Beam growth and beam loss caused by intra-beam scattering is of primary concern in heavy-ion storage rings like the Relativistic Heavy Ion Collider (RHIC), since the scattering cross-section is proportional to Z^4/A^2 for particles of charge state Z and atomic number A. For example, at nominal RHIC injection, the IBS growth time for the momentum spread is about 3 minutes. Alternate filling of the two rings, each with about 60 bunches, needs to be done within about 1 minute to prevent difficulty in transition crossing and top-energy RF recapture. At storage, emittance growth occurs in both the transverse and longitudinal dimension. Collimation systems are designed to remove particles escaped from the RF buckets. Methods like stochastic cooling and electron cooling are desired to overcome luminosity degradation caused by IBS [1].

Intra-beam scattering mechanism can be described using the rest frame (x, y, z, t) of the circulating synchronous particle. Measure dimensions in units of the characteristic distance ξ_0 with $\xi_0^3 = r_0\rho^2/\beta^2\gamma^2$, time in units of $\rho/\beta\gamma c$, and energy in units of $\beta^2\gamma^2 Z^2e^2/4\pi\epsilon_0\xi_0$, where $r_0 = Z^2e^2/4\pi\epsilon_0 m_0c^2$ is the classical radius, βc and γm_0c^2 are the velocity and energy of the synchronous particle, and ρ is the radius of curvature in bending regions of magnetic field B_0. The Hamiltonian for particles in a simple system with bending dipoles and focusing quadrupoles of strength $n_1 = -(\rho/B_0)(\partial B_y/\partial x)$ is [2]

$$H = \begin{cases} \frac{1}{2}\left(P_x^2 + P_y^2 + P_z^2\right) + \frac{1}{2}x^2 - \gamma x P_z + V_C & (\text{bending section}) \\ \frac{1}{2}\left(P_x^2 + P_y^2 + P_z^2\right) - \frac{n_1}{2}(x^2 - y^2) + V_C + U_s & (\text{straight section}) \end{cases} \tag{3.2}$$

where U_z is the potential provided by the RF system. The Coulomb potential is non-relativistic in the rest frame:

$$V_C = \sum_j \frac{1}{\sqrt{(x_j - x)^2 + (y_j - y)^2 + (z_j - z)^2}}. \tag{3.3}$$

In terms of dispersion function D and betatron displacements $\beta_{x,y}$, this Hamiltonian is transformed to

$$\bar{H} = \frac{1}{2}\left(P_{\beta_x}^2 + P_{\beta_y}^2\right) + \frac{1 - \gamma^2 F_z}{2} P_z^2 + V_C + U_z, \tag{3.4}$$

where

$$F_z = \begin{cases} D + DD'' + (D')^2 & (\text{bending section}) \\ DD'' + (D')^2 & (\text{straight section}) \end{cases} \tag{3.5}$$

and

$$\langle F_z \rangle = \frac{1}{\gamma_T^2}. \tag{3.6}$$

Below transition energy, $\gamma < \gamma_T$, particles are in a positive-mass regime. In an idealized case that the machine lattice is uniform along the ring circumference, the Hamiltonian in the rest frame is time-independent. The particle system is thus conserved, so does the total temperature of the beam in the rest frame. The heat can be transfered from the high temperature to the low temperature direction. The system eventually reaches an equilibrium state when the temperature (i.e. rest-frame velocity) is the same in all directions.

In an actual alternating-gradient focusing ring, the beam sees a time dependent potential modulated by the ring lattice frequency. The beam structure absorbs "phonons" and heats up [3]. Intra-beam multiple scattering manifests as a mixture of thermal equalization and temperature growth asymptotically approaching equal temperature in all directions in the rest frame.

Above transition energy, $\gamma > \gamma_T$, the beam is in a negative-mass regime. The Hamiltonian (Eq. 3.4) indicates that even in the case of a uniform machine lattice, beam temperature can grow simultaneously in the longitudinal and transverse directions.

Energy exchange and temperature increase in the beam rest frame manifest as variation of beam emittance and momentum spread in the laboratory frame. In the laboratory frame, the rate of emittance and momentum growth is usually obtained [4, 5] assuming multiple small-angle scattering among Gaussian-distributed beams. In the case that $D/\beta_x^{1/2}$ is nearly constant (e.g. for FODO lattice), the growth rate formula can be simplified into the following expression [6, 7],

$$\begin{bmatrix} \frac{1}{\sigma_p}\frac{d\sigma_p}{dt} \\ \frac{1}{\sigma_x}\frac{d\sigma_x}{dt} \\ \frac{1}{\sigma_y}\frac{d\sigma_y}{dt} \end{bmatrix} = \frac{Z^4 N}{A^2} \frac{r_0^2 m_0 c^2 L_c}{8\gamma\epsilon_x\epsilon_y S_{rms}} F(\chi) \begin{bmatrix} n_b(1 - d^2) \\ -a^2/2 + d^2 \\ -b^2/2 \end{bmatrix} \tag{3.7}$$

where $L_C \approx 20$ is the Coulomb logarithm, $\epsilon_{x,y} = \beta\gamma\sigma_{x,y}^2/\beta_{x,y} = \epsilon_N/6$ is the normalized rms transverse emittance, $S_{rms} = \pi m_0 c^2 \beta\gamma\sigma_s\sigma_p/cA = S/6$ is the rms longitudinal bunch area in phase space, $\chi = (a^2 + b^2)/2$, $d = \dfrac{D\sigma_p}{(\sigma_x^2 + D^2\sigma_p^2)^{1/2}}$, $a = \dfrac{\beta_x d}{D\gamma}$, $b = \dfrac{\beta_y\sigma_x}{\beta_x\sigma_y}a$, n_b is equal to 1 if the beam is azimuthally bunched, and is equal to 2 if it is not. For azimuthally bunched beams, σ_s is the rms bunch length and N is the number of particles per bunch; for un-bunched beams, N is the total number of particles and $\sigma_s = \sqrt{\pi}R$. In Eq. 3.7, $F(\chi)$ is an analytic function given by

$$F(\chi) = \frac{-3 + (1 + 2\chi)I(\chi)}{1 - \chi} \tag{3.8}$$

where

$$I(\chi) = \begin{cases} \dfrac{1}{\sqrt{\chi(\chi - 1)}}\mathrm{Arth}\sqrt{\dfrac{\chi - 1}{\chi}} & \chi \geq 1; \\ \dfrac{1}{\sqrt{\chi(1 - \chi)}}\arctan\sqrt{\dfrac{1 - \chi}{\chi}} & \chi < 1 \end{cases} \tag{3.9}$$

The growth rates are linearly proportional to the number of the particle N in the beam, and are strongly dependent ($\sim Z^4/A^2$) on the charge state of the particle. Except for the form factors χ, d, a, and b that depend on the ratio of the beam amplitudes in different dimension, the rates are inversely proportional to the six dimensional phase space area. Below transition energy, the asymptotic distribution corresponds to the condition

$$\langle\frac{\sigma_x}{\beta_x}\rangle \approx \langle\frac{\sigma_y}{\beta_y}\rangle \approx \frac{\sigma_p}{\gamma}, \;\; \gamma \ll \gamma_T.$$

Above transition energy, the asymptotic distribution corresponds to the condition

$$\sqrt{n_b n_c}\langle\sigma_x\rangle \approx \langle D\rangle\sigma_p, \;\; \gamma \gg \gamma_T$$

where n_c is equal to 1 if the horizontal and vertical motion are uncoupled, and is equal to 2 if they are fully coupled. In order to confine the horizontal emittance growth, we intensionally couple the horizontal and vertical motion. The growth rates at high energy become

$$\begin{bmatrix} \dfrac{1}{\sigma_p}\dfrac{d\sigma_p}{dt} \\ \\ \dfrac{1}{\sigma_x}\dfrac{d\sigma_x}{dt} \end{bmatrix} = \frac{Z^4 N}{A^2}\frac{\pi r_0^2 m_0 c^2 L_c}{16\gamma_T\epsilon_x\epsilon_y S_{rms}} \begin{bmatrix} n_b(1 - d^2)/d \\ \\ d/n_c. \end{bmatrix}, \qquad (\gamma \gg \gamma_T) \tag{3.10}$$

which is to the first order independent of the beam energy.

In order to evaluate the beam intensity lifetime, we use the Fokker-Planck equation to describe the evolution of particle distribution in the phase space. The general 6 dimensional (6-D) equation can be greatly simplified by the fact that the IBS growth time is typically much longer than the synchrotron-oscillation period, which is again much longer than the multiple collision relaxation time. In the case that the leading source of beam loss is in the longitudinal direction due to the limited voltage of the RF system, we further assume in the transverse directions a time-evolving Gaussian distribution. After averaging over the machine circumference and the synchrotron phase

for all the particles involved in the collision [8], we obtain a 1-D Fokker-Planck equation of the density function $\Psi(J)$ in the longitudinal direction in terms of the action variable J,

$$\frac{\partial \Psi}{\partial t} = -\frac{\partial}{\partial J}\left(F\Psi\right) + \frac{1}{2}\frac{\partial}{\partial J}\left(D\frac{\partial \Psi}{\partial J}\right), \text{ with } \begin{cases} J = 0: & -F\Psi + \dfrac{D}{2}\dfrac{\partial \Psi}{\partial J} = 0\,, \\ J = J_{max}: & \Psi = 0\,. \end{cases} \tag{3.11}$$

Here, the drift coefficient is given by the expression

$$F(J) = \oint \frac{2ds}{\pi R}\int_0^{\frac{1}{4}} dQ\, \left.\frac{\partial W}{\partial J}\right|_\phi^{-1}(Q,J)\int_{J_{min}}^{\hat{J}} \left.\frac{\partial W}{\partial J}\right|_\phi (Q',J')\left[A_F(\lambda_1)+A_F(\lambda_2)\right]\Psi(J')dJ' \tag{3.12}$$

and the diffusion coefficient is given by the expression

$$D(J) = \oint \frac{2ds}{\pi R}\int_0^{\frac{1}{4}} dQ \left[\left.\frac{\partial W}{\partial J}\right|_\phi^{-1}(Q,J)\right]^2 \int_{J_{min}}^{\hat{J}} \left.\frac{\partial W}{\partial J}\right|_\phi (Q',J')\left[A_D(\lambda_1)+A_D(\lambda_2)\right]\Psi(J')dJ' \tag{3.13}$$

where

$$A_F(\lambda) = -\frac{2Z^4 r_0^2 L_c E}{A^2\beta^2\gamma^4}\frac{I_F(\lambda)}{\sigma_x\sigma_y},\ A_D(\lambda) = \frac{Z^4 r_0^2 L_c E^2}{A^2\gamma^3 h\omega_s}\frac{I_D(\lambda)}{\sigma_x\sigma_y},\ \lambda_{1,2} = \frac{h\omega_s g}{\gamma\beta^2 E}(W \mp W'),\ g = \frac{1}{2}\sqrt{\frac{\beta\gamma\beta_{x,y}}{\epsilon_{x,y}}}, \tag{3.14}$$

ω_s is the revolution frequency,

$$\left.\frac{\partial W}{\partial J}\right|_\phi^{-1} = 8k\,\mathrm{K}(k)\cos 2\pi Q\,\left[1-4\xi\sin^2 2\pi Q + O(\xi^2)\right], \tag{3.15}$$

and $\xi = \exp\left[-\pi \mathrm{K}'(k)/\mathrm{K}(k)\right]$ and $\mathrm{K}'(k) = \mathrm{K}(\sqrt{1-k^2})$. The first integrals in Eqs. 3.12 and 3.13 represents the average over the machine lattice; the second integral represents the average over synchrotron-oscillation period; while the third integral describes particles of different action J' involved in the collision. The integration over J' is performed such that $k(J')\sin 2\pi Q' \approx \sin\left[\phi(Q,J)/2\right]$, extending from J_{min} to the bunch edge $\hat{J}$, with $k(J_{min}) \approx \left[\sin\phi(Q,J)/2\right]$. For a round beam with near constant $D/\beta_x^{1/2}$, we have

$$\begin{aligned} I_F(\lambda) &= 2g^2\mathrm{sgn}(\lambda)e^{-(D\gamma\lambda/2\sigma_x)^2}\left\{1-\sqrt{\pi}|\lambda|e^{\lambda^2}\left[1-\Phi(\lambda)\right]\right\}, \\ I_D(\lambda) &= ge^{-(D\gamma\lambda/2\sigma_x)^2}\left\{\sqrt{\pi}(1+2\lambda^2)e^{\lambda^2}\left[1-\Phi(\lambda)\right]-2|\lambda|\right\}, \end{aligned} \tag{3.16}$$

where Φ is the error function, and sgn(λ) is 1 if $\lambda \geq 0$, and is -1 if otherwise.

Starting from an initial distribution, Eq. 3.11 can be iterated to yield the time evolution of the longitudinal particle distribution, as shown in Fig. 3.20. Based on this information, evolution of the transverse beam dimension is obtained from the growth rate formulae given above. Beam loss through the RF bucket boundary is evaluated from the reduction of the integrated density $\Psi(J)$ over J. Typically, the longitudinal distribution under intra-beam scattering is Gaussian-like with zero density at the edge of the RF bucket, as shown in Fig. 3.20.

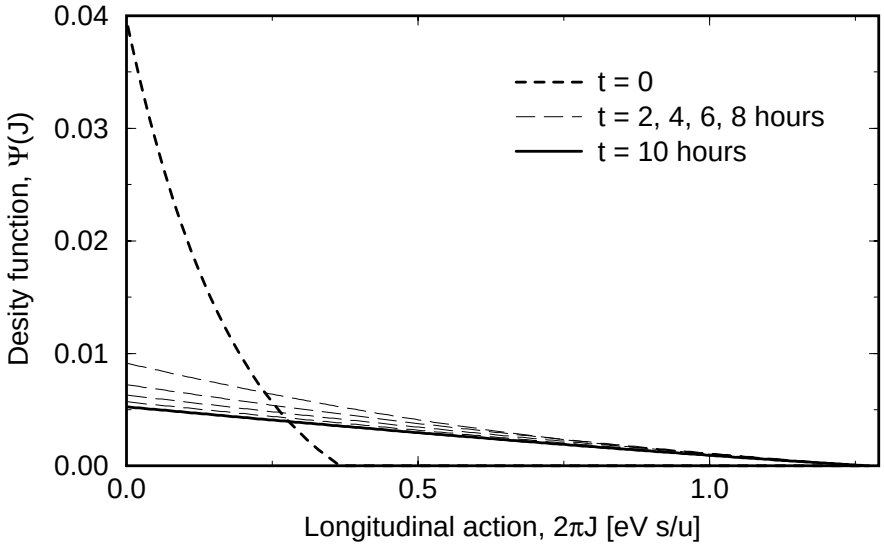

Figure 3.20: Evolution of the longitudinal density distribution under intra-beam scattering during the 10 hour storage in RHIC. The edge of RF bucket corresponds to 1.29 eV·s/u.

References

[1] J. Wei, *Intensity Dependent Effects in RHIC*, Proc. Workshop on Instabilities of High Intensity Hadron Beams in Rings, AIP Conference Proceedings 496, edited by T. Roser and S.Y. Zhang, (1999) p. 197.

[2] *Handbook of Accelerator Physics and Engineering*, edited by A. Chao and M. Tigner, World Scientific, Singapore, 1999.

[3] X-P. Li, A.M. Sessler, J.Wei, *Crystalline Beam in a Storage Ring: How Long Can It Last?* Proc. European Accelerator Conference, London, U.K. (June 1994) p. 1379 - 1381.

[4] A. Piwinsky, *Intra-Beam-Scattering*, CERN 92-01, Proc. CERN Accelerator School, Gifsur-Yvette, Paris, 1984, p405.

[5] J. Bjoken, S.Mtingwa, *Intrabeam Scattering*, Particle Accelerators **13**, 115 (1983).

[6] G. Parzen, *Intrabeam Scattering at High Energies*, Nucl. Instr. Meth. **A256**, 231 (1987); Proc. 1988 EPAC, Rome, p.821.

[7] J. Wei, *Evolution of Hadron Beams under Intra-beam Scattering*, Proc. 1993 Part. Accel. Conf., Washington, D.C. (1993) p.3653.

[8] J.Wei and A.G.Ruggiero, *Beam Life-Time with Intra-Beam Scattering and Stochastic Cooling*, Proc. 1991 Particle Accelerator Conference, San Francisco, p.1869.

3.6.7 Polarized Electron Sources For Electron-Ion Colliders

B. Matthew Poelker Poelker@jlab.org Jefferson Lab, Newport News, VA 23606 USA

Charles K. Sinclair Cornell University, Ithaca, New York, USA

Of the various schemes presently being considered to achieve a high luminosity electron-ion collider, those using either a linac or a linac plus circulator ring for the electron beam require a high performance polarized electron source. In the versions without a circulator ring, the polarized source must deliver an average current of highly polarized electrons several hundred times greater than the present state of the art. While the average current requirement is reduced significantly by the use of a circulator ring, it remains well above the best polarized source performance yet demonstrated. The charge limit phenomenon should not pose a problem for the single bunch charges under consideration, but it remains to be demonstrated that a polarized photocathode can support these bunch charges in a high average current situation. Lasers to illuminate the polarized photocathode are demanding in the linac plus circulator ring case, and are technically beyond reach in the linac only case. Thus, a highly polarized source for the linac only case will require the development of new photocathodes providing far higher quantum efficiency than presently available with existing high polarization photocathodes.

All present day polarized electron sources employ negative electron affinity photocathodes prepared on GaAs or similar semiconductors. Under illumination by circularly polarized light of wavelength close to the minimum direct bandgap, polarized electrons are emitted. Ordinary GaAs gives an electron polarization theoretically limited by degeneracy in the valence band to 50%, and in practice no better than about 40%. To obtain higher polarization, schemes to break this degeneracy are employed. The most common method is to grow a GaAs layer on a substrate of smaller lattice constant, resulting in a compressively strained GaAs layer. Various multilayer semiconductor structures, with or without strain, have also been demonstrated. With either scheme, the active photoemission layer is no more than one to three hundred nanometers thick. This results in low optical absorption, and a correspondingly low quantum efficiency. The very best polarized photocathodes used to date have provided polarization somewhat above 80% and maximum quantum efficiency of about 0.2% at the operating wavelength.

The extreme operating ranges of contemporary polarized sources are found at SLAC and Jefferson Lab. The polarized source at SLAC, operating at 120 kV DC, delivers high single bunch charges or sub-microsecond duration pulses containing up to about 6 x 10^{11} electrons at repetition rates up to 120 Hz, corresponding to an average current of about 12 μA [1]. At Jefferson Lab, CW beams with average currents as high as 270 μA have been delivered from a 100 kV DC gun at bunch repetition rates between 499 and 1497 MHz, corresponding to a fraction of a picocoulomb per bunch [2].

The injector of the Jefferson Lab FEL provides another useful data point. Although not a polarized electron injector, it employs a GaAs photocathode in a very high voltage DC gun, and provides an indication of what can be accomplished with such electron sources. This gun operates at $\sim$ 320 kV DC, and delivers up to 5 mA average current in either 74.85 MHz or 37.425 MHz bunch trains [3]. The FEL is presently being upgraded, and the gun is expected to deliver 10 mA average current at a 500 kV DC operating voltage.

While the emittance requirements for the electron source are not terribly demanding, preventing unacceptable emittance growth due to space charge will require care, particularly at the highest bunch charges. Guns with high electric field strength at the photocathode will be required. These high fields will be a problem with either DC guns, where field emission is a problem, or RF guns, for which CW operation poses significant thermal problems. It should be noted that GaAs photocathodes have never been operated in an RF gun, and developmental challenges will likely be encountered before this is done successfully.

It has proven difficult to achieve long photocathode operational lifetimes in polarized sources,

particularly at high average current. In the Jefferson Lab polarized source, the cathode life is limited only by ion back bombardment. The ions are produced on the residual gas in the cathode-anode gap. It is thus more reasonable to express the cathode life in terms of the number of coulombs delivered per unit illuminated area, rather than in clock hours. Presently, the Jefferson Lab source has demonstrated cathode lifetimes in excess of 2 x 10^5 coulombs/cm^2. The only practical way to increase this number is to reduce the vacuum pressure. This is a challenging task, as the pressure in typical polarized guns is already below about 10^{-11} mbar (and difficult to measure with precision). The payoff is large, however, and an R&D program for an electron-ion collider should devote resources to this topic. It is interesting to note that while the exact nature of the degradation caused by ion back bombardment is not understood, the quantum efficiency of a degraded cathode can be fully restored by a brief heat treatment and re-activation.

Semiconductor diode and Ti:sapphire lasers are presently used to illuminate the polarized photocathodes [4]. To support the high average current, high bunch charge operation of an electron-ion collider, laser development work will be required. If a circulator ring is employed, the polarized source need deliver only a few mA average current, requiring a laser power approaching 10 W for use with the present high polarization cathodes. Lasers providing this average power with the proper wavelength and time structure have not been demonstrated, but do not seem technically out of reach. Without a circulator ring, the required average current is about two orders of magnitude greater, and it seems quite unlikely that existing lasers can be developed to reach this power level with the necessary time structure and beam quality. Alternatively, one could use conventional GaAs photocathodes, with their much higher quantum efficiency, but with the penalty of much lower beam polarization. It is worth noting that while the addition of a circulator ring reduces the average power requirement for the laser, each optical pulse in the pulse train must have the same energy as in the case with no circulator ring.

The so-called charge limit phenomenon results from charge buildup at the surface of the photocathode. The field from this surface charge layer inhibits photoemission, limiting the charge that can be emitted. Recently, it has been demonstrated that a high dopant density in a thin layer at the cathode surface eliminates the charge limit effect for the bunch charges and time structure required for linear collider applications [5]. It remains to be demonstrated, however, that charge or current limiting effects do not occur at the much higher average currents required for the electron-ion collider. While the problem may be solved, a demonstration seems necessary, particularly in the case of the very large average currents required with no circulator ring.

It may prove possible to develop new photoemission cathodes that provide both high polarization and high quantum efficiency. For example, various chalcopyrite semiconductors are believed to have band structures without the problematic valence band degeneracy of GaAs. Recently, a proposal has been made for a specific chalcopyrite material to provide both high polarization and high quantum efficiency [6]. R&D to support the growth and evaluation of this material, and other possible candidate materials, should be supported. The currently active field of “spin-tronics”, which seeks to utilize the spin degree of freedom in semiconductors, is also worth considering. One goal of current R&D efforts in this area is the development a means to efficiently inject highly polarized electrons into GaAs. Although there are a great many challenges to developing a polarized source based on these ideas, were this effort to succeed, it might be the basis for a polarized source requiring no laser.

In summary, the best present day polarized electron sources fall short of meeting the polarized beam requirements for either the linac-ring or linac plus circulator ring-ring versions of the electron ion collider. R&D is required is several areas, such as improved ultimate vacuum pressures; DC or CW-RF guns capable of operating with very high cathode field strengths; higher average power lasers with appropriate RF time structure and operating wavelength; and high quantum efficiency,

high polarization photocathodes. Delivery of the required bunch trains at high average current should be demonstrated as well.

References

[1] T. B. Humensky et al., SLAC-PUB-9381, September 2002, submitted to Nuclear Instruments and Methods A.

[2] C. K. Sinclair, in Proceedings of the 1999 Particle Accelerator Conference, IEEE, Piscataway, NJ, 1999, p. 65. The measured cathode lifetime has steadily improved above the value reported in this paper.

[3] T. Siggins et al., Nucl. Instr. Meth. A **475**, 549 (2001).

[4] Matt Poelker and John Hansknecht, in "Polarized Gas Targets and Polarized Beams", AIP Conference Proceedings No. 421, R.J. Holt and M. A. Miller, eds. AIP, Woodbury, NY, 1998, p. 270. C. Hovater and M. Poelker, Nucl. Instr. Meth. A **418**, 280 (1998).

[5] K. Togawa et al., Nucl. Instr. Meth. A **414**, 431 (1998).

[6] A. Janotti and Su-Huai Wei, Appl. Phys. Lett. **81**, 3957 (2002)

3.6.8 Energy Recovering Linacs

L. Merminga merminga@jlab.org CASA, Jefferson Lab, Newport News, VA 23606 USA

D. R. Douglas douglas@jlab.org CASA, Jefferson Lab, Newport News, VA 23606 USA

G. A. Krafft krafft@jlab.org CASA, Jefferson Lab, Newport News, VA 23606 USA

Electron storage rings have fulfilled the needs of the accelerator community for high current applications for several decades with high efficiency and increasingly improved performance. They are at present however confronted by two fundamental limitations. The first is on the minimum available 6-dimensional phase space, which is determined by the equilibrium between radiation damping and quantum excitation. The second is on the maximum available beam lifetime, which is limited by the Touschek effect. In contrast, linear accelerators can deliver beams with small emittance, energy spread, and very short bunches; they have, however been limited to relatively low average currents, of order 1 mA, by prohibitive rf power requirements.

Energy recovering linacs (ERLs), in which the beam, after it has been used, is returned back to the rf cavities 180^0 out of phase where it is decelerated and returns its beam power back to the cavities as microwaves that are used for the acceleration of new bunches, promise to provide an interesting alternative. Energy recovering linacs combine characteristics of both storage rings and linacs, in that they can produce beams of linac quality – with emittance and energy spread determined by the source and with very short bunches (sub-picosecond) – yet they promise efficiencies approaching those of storage rings.

The highest power energy recovery experiment to date has taken place in the Jefferson Lab IR FEL, where a cw beam current of up to 5 mA has been accelerated to $\sim$50 MeV and energy recovered [1]. Energy recovery is used routinely in this system during its operation as a user facility. The Jefferson Lab IR FEL has been dismantled and an upgrade to 10 kW IR FEL and 1 kW UV FEL [2] are being installed. Commissioning of the JLAB FEL Upgrade is scheduled to commence in the spring of 2003.

Energy recovering linacs are contemplated for a variety of applications, including high energy electron cooling (see section above on Electron Cooling) and electron-ion colliders. This cooler will be driven by a 50 MeV, 100 mA ERL. ERLs for colliders are envisioned to operate in the 3-10 GeV energy range and they require average currents of order 100-200 mA. The parameters required by these ERL proposals are an extrapolation from today's demonstrated performance by one to two

orders of magnitude both in beam energy and in average current, and a number of technical issues need to be resolved in order for the feasibility of these designs to be demonstrated and for the ultimate limitations of ERLs to be understood. Several prototype facilities are being proposed to address and explore the technical feasibility of future ERLs. Among the proposed prototypes are: The Cornell/Jefferson Lab ERL Phase I, a 100 MeV, 100 mA ERL [3], the BNL/BINP electron-cooling prototype [4,5], the Jefferson Lab's 10 kW FEL Upgrade and its likely successor, the 100 kW IR FEL. We now proceed to discuss the technical challenges of the next generation ERLs, focusing on the superconducting rf linac-based schemes.

3.6.8.1 Accelerator Physics and Technology Challenges of Energy Recovering Linacs

Generation and Preservation of Low Emittance, High Current Beams

In order to take full advantage of the ERL technology, one should both generate and preserve a low emittance, high average current beam. As we saw in an earlier section, laser-driven, photoemission guns are considered likely source candidates [6], but technology development is required to demonstrate operation at the highest possible cathode voltage and to ensure adequate life time under high current conditions. Once the low emittance beam is generated, one needs to ensure its preservation first at the low energy regime where careful emittance compensation must take place against space-charge effects, and then in the linac and beam lines against wakefield affects, and in the recirculator against coherent synchrotron radiation-induced emittance degradation [7]. Other effects that could degrade the beam quality performance include ion effects and halo formation.

Longitudinal Beam Dynamics

The JLab FEL experience was that for proper energy recovery, longitudinal phase space manipulations were necessary [8]. Longitudinal phase space manipulations are also important for the proper operation of the electron cooling device. In the JLab IRFEL proper matching of the longitudinal phase space is required for high peak current (minimum bunch length) at the FEL and management of the large electron beam momentum spread, introduced by the FEL interaction, during energy recovery. Off-crest acceleration in the superconducting rf linac, together with non-zero momentum compaction in a chicane give rise to maximum compression at the wiggler. A second magnetic chicane (acting as a bunch decompressor) downstream of the wiggler is followed by a recirculation transport, which provides both a linear (R_{56}) and a quadratic (T_{566}) momentum compaction, the latter introduced by sextupoles. The sextupole-induced curvature on the longitudinal phase space of the bunch is essential to compensate the rf-induced nonlinearities, acquired during deceleration of the relatively long bunch. As a result, the bunch arrives at the energy recovery dump with relatively small momentum spread, and minimum beam loss.

Transverse Beam Dynamics

In addition to the transverse matching issues common to all types of accelerators, ERLs face the challenge_of preserving the quality of a high brightness beam during acceleration and the energy recovery of a potentially degraded beam phase space through common linac and transport channels. The linac optics in ERLs must ensure stability of both accelerating and decelerating beams as they traverse the same focusing channel, while they can be at very different energies, particularly at the two ends of the linac. Furthermore, the decelerating beam is adiabatically anti-damping, which leads to increase in the relative energy spread and betatron envelopes, and has the potential for scraping and beam loss. These issues are particularly accentuated in a high energy ERL with a long linac transport channel, such as required in the collider designs. In order to investigate transport beam dynamics aspects of energy recovery in large-scale systems, we have designed and proposed the experiment CEBAF-ER [9,10]. CEBAF-ER is a high energy demonstration of energy recovery and will take place at CEBAF. The experiment is described in the following section.

Collective Effects

In recirculating linacs, in general, the beam and the cavities form a feedback loop, which closes upon the return of the beam to the same cavity on a subsequent pass. The closure of the feedback loop between beam and cavity can give rise to instabilities, at sufficiently high currents, driven predominantly by the high-Q superconducting cavities. Energy recovering linacs, in particular, are more susceptible to these instabilities because they can support currents to reach the threshold of the instabilities. The following types of instabilities can occur:

1) The transverse Beam Breakup (BBU) instability, which results from the interaction of the beam with the cavity's transverse Higher Order Modes (HOMs) [11].

2) The longitudinal BBU instability that can result from the interaction of the beam with longitudinal HOMs [12].

3) The beam-loading type instabilities, which can arise from fluctuations of the cavity fields in the linac and can cause beam loss on apertures and phase oscillations [13].

Theoretical models of the instabilities have been developed and initial measurements on the JLab IR FEL are being used to benchmark codes and models [14,15,16,17]. At the present time, it appears that transverse BBU is the limiting stability mechanism, especially for srf linacs operating at relatively high rf frequency, 1.3 or 1.5 GHz [17]. It is expected that, selecting a lower rf frequency ($\sim$700-800 MHz), improving the HOM damping in multi-cell cavities and using bunch-by-bunch transverse feedback, similar to the one used in B-Factories, could result in stability threshold in the range of 0.5 - 1 A.

Superconducting RF Issues

Although energy recovery works well with pulsed beam, its potential is truly realized with cw beam (high average current). As a consequence, all the ERL applications proposed to date, require cw rf fields. Superconducting rf (srf) parameter optimization for ERLs in the multi-GeV energy range, which minimizes linac length and cryogenic power consumption, points towards gradients of $\sim$20 MV/m at Q_0 $\sim$1x10^{10}. This level of srf performance has not been demonstrated in cw, high average current operating conditions. Furthermore, R&D towards increasing the quality factor Q_0, of the cavities would directly reduce the ERL operating costs and increase the overall ERL efficiency. Further damping of transverse HOMs in multi-cell cavities is required to ensure stability against multibunch BBU instabilities, as discussed earlier.

Finally, efficient extraction of HOM generated by sub-picosend short bunches must be ensured. High average current and short bunch length beams in superconducting cavities can excite higher order modes which, in addition to beam stability consequences, could result in increased cryogenic load due to power dissipation in the cavity walls. The power in HOMs, primarily longitudinal, depends on the product of bunch charge, q, and average current, I_{ave}, and it is equal to $2qk_{||}I_{ave}$ where $k_{||}$ is the loss factor of the superconducting cavity and the factor of 2 accounts for the two beams in the cavity (accelerating and decelerating). The total power depends on the bunch length through the loss factor. At high currents and short bunches, the amount of dissipated power can be quite high. For example, for average current of 100 mA, bunch charge equal to 0.5 nC and $k_{||}$ =10 V/pC, the HOM power is approximately equal to 1 kW per cavity. Part of this power is expected to be extracted by HOM couplers and be absorbed in room temperature loads, part of it is expected to be absorbed by cooled photon absorbers placed between cavities or cryomodules. The excitation of high frequency HOMs by the short bunches can, in principle, degrade the cavity's quality factor, according to BCS theory, and result in increased power dissipation in the cryogenic environment [18]. Detailed measurements in the proposed ERL prototypes will be needed to demonstrate adequate efficiency of the power extraction schemes. ***RF Issues***

In superconducting cavities, in the absence of beam loading, the coupling optimization is dominated by the amplitude of microphonic noise [19]. For example, in the Cornell/Jefferson Lab

ERL, the optimum Q_{ext} is 2.6x10^7 assuming 25 Hz of microphonic noise. With this coupling, the required rf power is 8 kW per cavity! Clearly, higher Q_{ext} implies higher ERL efficiency. The question is what is the highest practical value of Q_{ext}. With the higher Q_{ext}, the rf control system design becomes more challenging, in the presence of microphonic noise-induced phase and amplitude variations that must be corrected, and a net beam loading vector, that may result either from beam loss of from phase errors.

3.6.8.2 Conclusions

Energy recovering linacs are an emerging and potentially powerful application of rf superconductivity for a wide variety of applications, including FELs, light sources, electron cooling devices and electron-ion colliders. The success of the JLab IRFEL energy recovering linac has demonstrated technical feasibility of the concept. Proposed ERL prototypes are expected to elucidate the ultimate limitations of energy recovering linacs.

References

[1] G. R. Neil, et al., *Physical Review Letters* Vol. 84, Number 4 (2000)

[2] D. R. Douglas, et al. *Proc. 2000 Linear Accel. Conf.*, p. 857 and *Proc. 2001 Part. Accel. Conf.*, p. 249

[3] I. Bazarov, S. Belomestnykh, D. Bilderback, K. Finkelstein, E. Fontes, S. Gray, S. M. Gruner, G. A. Krafft, L. Merminga, H. Padamsee, R. Helmke, Q. Shen, J. Rogers, C. Sinclair, R. Talman, and M. Tigner, CHESS Technical Memo 01-003 and JLab-ACT-01-04 (2001)

[4] V. Parkhomchuk, I. Ben-Zvi, "Electron Cooling for RHIC," BNL Report C-A/AP/47

[5] I. Ben-Zvi, et al. Proc. of PAC 2003

[6] C.K. Sinclair, Proc. of PAC 1999, p. 65

[7] R. Li, Proc. of PAC 1999, p. 118

[8] P. Piot, D. Douglas, G. Krafft, Proc. EPAC 2000, p. 1543 and *Phys. Rev. ST-AB*, 6, 030702 (2003)

[9] D. Douglas, JLab TN-01-018 (2001) and JLab TN-01-045 (2001)

[10] http://casa.jlab.org/research/cebaf_er/er.shtml

[11] J. J. Bisognano and R. L. Gluckstern, Proceedings PAC 1987, p. 1078

[12] J. J. Bisognano and M. L. Fripp, Proc. Linac Conference 1988, p. 388

[13] L. Merminga, P. Alexeev, S. Benson, A. Bolshakov, L. Doolittle and G. Neil, NIM A 429 (1999) 58-64

[14] G. A. Krafft and J. J. Bisognano, Proc. PAC 1987, p. 1356

[15] B. C. Yunn, Proc. PAC 1991, p. 1785

[16] L. Merminga, Campisi, Douglas, Krafft, Preble, Yunn, Proc. PAC 2001, p. 173

[17] L. Merminga, NIM A 483 (2002) 107-112

[18] L. Merminga, G. A. Krafft, C. W. Leemann, R. M. Sundelin, B. C. Yunn and J. J. Bisognano, Proc. Linac Conf. (2000)

[19] L. Merminga and J. Delayen, JLab Technical Note TN-96-022 (1996)

3.6.9 CEBAF-ER: An Experiment for Large Scale Demonstration of Energy Recovery

Chris Tennant tennant@jlab.org CASA, Jefferson Lab, Newport News, VA 23606 USA

Alex Bogacz bogacz@jlab.org CASA, Jefferson Lab, Newport News, VA 23606 USA

David R. Douglas douglas@jlab.org CASA, Jefferson Lab, Newport News, VA 23606 USA

High energy (multi-GeV), high current (hundreds of milli-Amperes) beams require gigaWatt-class RF systems in conventional linacs - a prohibitively expensive proposition. However, invoking energy recovery alleviates extreme RF power demands, improves linac efficiency and increases cost effectiveness. Jefferson Lab has demonstrated its expertise in the field of Energy Recovery Linacs (ERLs) with the successful operation of the IR FEL, where 5 mA of average beam current have been accelerated up to 50 MeV and the energy stored in the beam was recovered via deceleration and given back to the RF power source. To date this has been the largest scale demonstration of energy recovery.

Presently there are designs for several ERL based accelerator systems world-wide. These include designs for FELs (KAERI, BINP Accelerator-Recuperator), synchrotron light sources (Cornell/JLab ERL, ERLSYN, 4GLS, BINP MARS), electron cooling devices (BNL-BINP) and electron-ion colliders (ELIC, eRHIC). Some of the ERL-based accelerator applications that are being proposed require beam currents of the order of 100 mAs, while the beam energy for these applications ranges from the currently achieved 50 MeV up to 5 GeV. There are several important accelerator physics and technological issues that must be resolved before any of these applications can be realized. The JLab FEL Upgrade, presently under construction and designed to accelerate 10 mA up to 150-200 MeV and then subjected to energy recovery, and the proposed Cornell/Jlab ERL Prototype, designed to accelerate 100 mA up to 100 MeV and then decelerated for energy recovery will be ideal test beds for the understanding of high current phenomena in ERL devices. In an effort to address the issues of energy recovering high energy beams, Jefferson Lab has proposed a minimally invasive energy-recovery experiment utilizing the CEBAF accelerator [1]. The experiment is slated to begin at the end of March and its goal is to demonstrate the energy recovery of a 1 GeV beam. Until this proposed experiment, there were no plans aimed to address issues related to beam quality preservation in systems with large final beam energy (up to 1 GeV) or large energy ratio between final and injected beams (up to factors of 40-80).

A schematic representation of the CEBAF-ER (CEBAF with Energy Recovery) experiment is shown in Figure 3.21. Beam will be injected into the north linac at 45 MeV where it will be accelerated to 545 MeV. The beam will traverse arc 1 and then begin acceleration through the south linac where it will reach a maximum energy of 1045 MeV. Following the south linac, the beam will pass through a newly installed phase delay chicane (see Figure 3.22). The chicane was designed to create a path length differential of exactly $\frac{1}{2}$-RF wavelength so that upon re-entry into the north linac, the beam will be 180 degrees *out of phase* with the cavities and will subsequently be decelerated to 545 MeV. After traversing arc 1 the beam will enter the south linac - still out of phase with the cavities - and be decelerated to 45 MeV at which point the spent electron beam is sent to a dump. In this way the beam gives energy back to the RF system, which may be used to accelerate subsequent beam.

To gain a quantitative understanding of the beam behavior through the machine, an intense effort has been made towards planning measurements for CEBAF-ER [2]. One of the most critical is measuring the beam emittance - which serves as a figure of merit by characterizing the extent to which beam quality is preserved during energy recovery. A scheme has been implemented to measure the emittance of the energy recovered beam prior to being sent to the dump [3], as well as in the injector and in each arc. In this way we can understand how the emittance evolves through the machine. One of the performance limitations of high energy beams is beam halo or small regions of phase space outside the beam core. To study halo effects in the experiment, a tomographic scheme has been devised, scanning the phase advance as a means of exploring the phase space for halo particles (that is, those nominally at large angular displacement at the beam profile monitors). Furthermore, the halo will be measured both in the injector and in the beam dump to ascertain what effects energy recovery has on halo formation and evolution. In addition to the beam

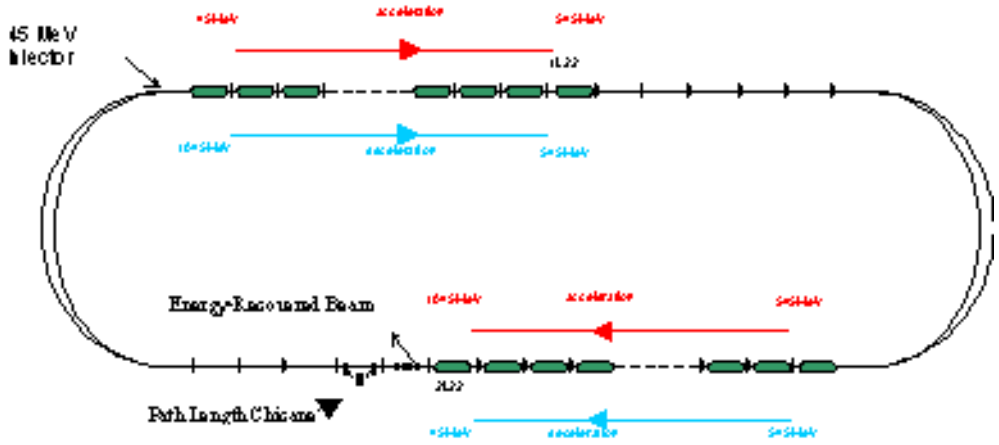

Figure 3.21: Schematic of CEBAF-ER.

based measurements mentioned above, another important class of measurements deals with the RF system's response to energy recovery. These measurements will test the RF system response by measuring the gradient and phase stability with and without energy recovery in several cavities throughout the north and south linac. Once satisfactory measurements have been obtained using the nominal 45 MeV injection energy, a parametric study exercising low injection to final energy ratios is planned. Based on the aforementioned measurements, at the conclusion of CEBAF-ER experiment, we should know enough about the behavior of the beam to be in a position to address the issues facing future ERL based machines; namely, those issues involving the energy recovery of very energetic beams.

References

[1] Bogacz A., Benesch J., Butler C., Chao Y., Chattopadhyay S., Dickson R., Douglas D., Guerra A., Hutton, A., Krafft G., Lauze R., May R., Merminga L., Neil G., Oren W., Spata M., Tennant C., Tiefenback M., White K., "CEBAF Energy Recovery Experiment", JLAB-TN-03-006, (2002).

[2] Tennant C., Chao Y., Douglas D., Tiefenback M., "Beam Characterization in the CEBAF-ER Experiment", Particle Accelerator Conference, (2003).

[3] Tennant C., "An Overview of Emittance Measurements for CEBAF-ER", JLAB-TN-03-004, (2003).

3.6.10 Electron Circulators for Linac-Ring EIC

Yaroslav Derbenev derbenev@jlab.org CASA, Jefferson Lab, Newport News, VA 23606 USA

Rui Li lir@jlab.org Jefferson Lab, Newport News, VA 23606 USA

3.6.10.1 Introduction

A high luminosity, 10^{33}/cm^2.s and above, and efficient spin manipulation of polarized beams are the basic requirements to the electron-light ion collider design [1]. Two possible schemes have been proposed: scheme with electron storage ring (ring-ring, or RR option) where electron beam polarized by the synchrotron radiation [2], and linac-ring (LR) scheme with electron beam delivered from polarized source and accelerated by a superconducting (SRF) linac under beam energy

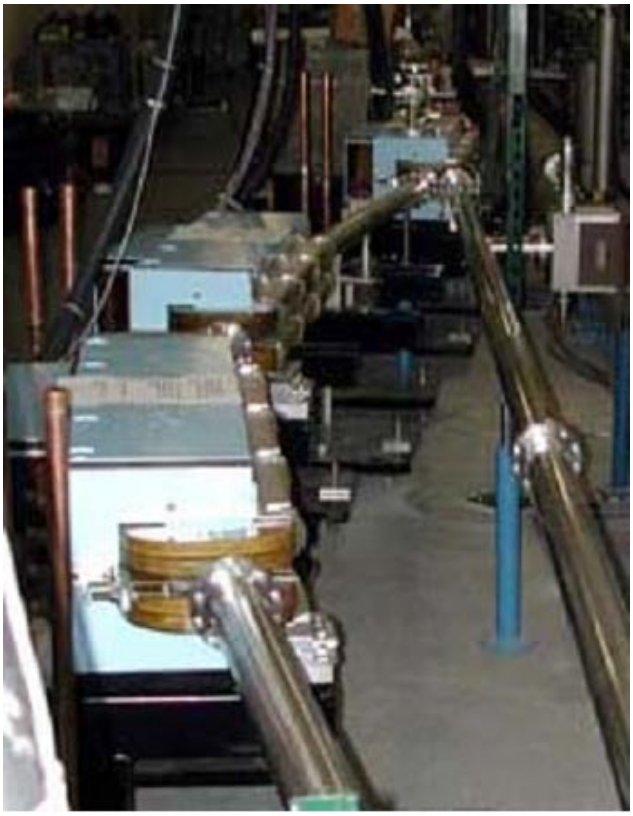

Figure 3.22: Path length chicane (to left) and straight ahead beam pipe.

recovery (ERL) [3]. A critical constraint of RR scheme is a complexity of a storage ring conditioning for radiative polarization and manipulating the electron spin. A challenge to LR option is the necessity to approach and operate a high current polarized electron source, injector and ERL. Use of circulator-collider ring (CR) for polarized electron beam in LR scenario was proposed as a way to release the RL scheme of this issue (LCR scenario) [3,4]. In this scenario, polarized electron bunches after acceleration in ERL are injected in a ring to perform a number of revolutions (typically, up to 100), colliding with ion bunches at interaction points and then returning to the linac in decelerating phase for energy recovery. The decelerated and accelerated bunch trains should overlap in order to reduce to a minimum the voltage deviation in SRF structure.

3.6.10.2 CR Advantages

Gain in electron current operating in EIC with CR, obviously, is equal to number of electron revolutions in CR. Maximum circulating current is limited by attainable charge per bunch and bunch spacing, but also (as in any scenario with high energy beam bent) by the syncrotron radiation power in bending magnets. Minimum number of revolutions is limited by the admissible value of average current in electron source or ERL, while the maximum one can be determined by the beam quality lifetime in circulator-collider. Electron spin can be firmly controlled by superconducting solenoids as Siberian Snakes installed in arcs and/or in ERL-CR transport line [4,5].

One can list the following features of LCR scheme with respect to the RR: ease spin handling (no crossing spin resonance, no quantum depolarization); spin rotators around the IP are not needed; spin is not sensitive to energy change; minimum beam emittance can be reduced; high order beam-beam effects are less important; a shorter bunch length and a larger circulating current

can be attained. With respect to the LR option, photo-injector is released of the loading by a high average current, and beam break-up and high order RF modes issues of ERL [6] are alleviated. The CR being designed and mounted in one tunnel with twisted spin (i.e. figure 8) ion ring could accommodate up to 4 interaction points [4]. Finally, when and if the multi-turn electron beam operation will not present any advantage, the CR can naturally be used as electron loop of a single path LR scheme.

3.6.10.3 ERL-CR Filling Pattern Options

In a simplest version, a bunch train almost the CR circumference as long after acceleration in ERL is injected into the ring, while, simultaneously, the previously circulated train is ejected and returned back to ERL for deceleration. Such filling pattern, obviously, is the easiest one concerning the requirements to the beam kicker device, but it may challenge one with a high current value in macro-pulse equal to the current circulating in collider, i.e. CR. A contrary to this pattern would be a CW current regime with bunch spacing ratio between ERL and CR equal to number of bunch revolutions in CR; this pattern challenges one with building up a very fast kicker (up to 3 GHZ frequency bandwidth). An optimum pattern design might compromise between the two ultimate versions.

Beam Quality Limits In CR

There are a few fundamental processes that limit beam quality in CR, although they will manifest less than in storage rings.

Quantum emittances in CR are decreased, with respect to those in storage ring, by a factor of ratio between duration of bunches circulation and radiation damping time of the ring.

High order non-linear beam-beam interaction is diminished, again due to the short time of electron bunches circulation in CR.

Coherent synchrotron radiation (CSR) [7,8] may increase the longitudinal emittance of short bunches delivered by electron linac.

The bursting of coherent synchrotron radiation has been observed on several storage rings [9-13], as a result of development of the microbunching instability in the bunch due to CSR impedances [14]. The threshold of this instability for a coasting beam with shielded CSR impedances [15] gives good account of the start up of the instability in simulation results [16] and observations. Simulation and observation also show that beyond the threshold, microbunching develops and reaches its peak in a fraction of damping time, before it gets relaxing by the radiation damping. An accurate threshold balance for bunched beam can be based on Haissinski approach [17] counting for particles synchrotron oscillations and Landau damping due to non-linearity of the CSR interaction forces. This logic also seems adequate in order to rely on it at estimation of the critical bunch length for a circulator ring. The increase of strength of the bunching RF field appears a basic recommendation for stabilization of injected bunches. This can be achieved by installation of SRF cavities in CR.

Note, that the value of the CSR power that shown in Table 3.11 can be strongly decreased by the vertical shielding. Also, both the critical bunch length and CSR power do not depend on particle mass and energy, thus, they can immediately be referred to heavy particle beams in a similar ring.

Conclusion

The circulator-collider ring concept seems advancing the linac-ring scheme of EIC with the possibility to base the luminosity design of level $10^{33}/\text{cm}^2$.s and above on the existing state of art of polarized electron sources or not far away of that. There seems not to be a significant technical issue in CR design other than building up the fast kickers for beam switching between ERL and CR In rest, a better understanding of beam-beam interaction and maintenance of short bunches in

Table 3.11: Estimated parameters of electron circulator-collider ring

Beam energy	GeV	7
Circumference	km	1.5
Bend radius in arcs	m	100
Compaction factor		$4x10^{3}$
Integrated 1.5 GHz SRF voltage amplitude	MV	100
Bunch spacing	cm	20
Number of electrons/bunch	10^{10}	1
Circulating beam current	A	2.5
Synchrotron tune		0.25
Energy acceptance	%	1.4
Critical bunch length (estimated value)	mm	1
Energy spread		$3x10^{-4}$
Number of bunch revolutions in the ring		100
Bunch storage time	ms	0.5
Radiation damping time	ms	10
Power of synchrotron radiation	MWt	4
CSR power (estimated value, non-shielded)	MWt	8

electron and ion rings with very strong bunching SRF fields requires more analysis and simulation.

References

[1] L.Merminga and J.Wei, this ICFA Beam Dynamics Newsletter
[2] A. Otboev et al., this ICFA Beam Dynamics Newsletter
[3] I. Ben-Zvi, L. Merminga, and Ya. Derbenev, this ICFA Beam Dynamics Newsletter
[4] L. Merminga and Ya. Derbenev, this ICFA Beam Dynamics Newsletter
[5] Ya. Derbenev, this ICFA Beam Dynamics Newsletter
[6] L. Merminga, et a., Proceeding of PAC Conference 1999
[7] Ya. Derbenev et al., TESLA-FEL 95-05, DESY Print, Hamburg (1995)
[8] J. Murphy et al., Proc. of IEEE PAC 1995, Dallas (1995)
[9] A. Anderson et al., Opt. Eng. 39, 3099 (2000)
[10] U. Arp et al., PRST-AB, Vol. 4, 054401 (2001)
[11] G. Carr et al., NIM A 463, 387 (2001)
[12] B. Podobedov et al., PAC 2001, p. 1921 (2001)
[13] J. Byrd et al., PRL 89, 224801 (2002)
[14] G. Stupakov and S. Heifets, PRST-AB, Vol. 5, 054402 (2002)
[15] R. Warnock and P. Morton, Part. Accel. 25, 113 (!990)
[16] M. Venturini and R. Warnock, PRL, Vol. 89, 224802 (2002)
[17] J. Haissinski, Nuovo Cimento Soc. Ital. Fis., B 18, 72 (1973)

3.6.11 IR Issues

Witek Krasny `Witek.Krasny@cern.ch` CERN

The design of the *Interaction Region (IR)* for the future Electron-Ion Collider (EIC) has to take into account large diversity of its physics program. From the IR design perspective, the physics program can be split into two domains: the large luminosity domain and the low luminosity domain. Each of them requires different optimization of the IR design. If only one IR will be

available, a staged IR design scenario could be implemented, at first for the initial, low luminosity phase, and subsequently, for high luminosity phase. The choice of Storage Ring versus Linac-Ring collider options have also an important impact on the IR design, in particular, if the spin rotators are incorporated into the IR design.

3.6.11.1 IR for physics-optimal ratio of beam energies

The low luminosity physics program can use comfortable, large β* $\approx$1-10 m design, allowing for easy implementation of the full acceptance detector. On the other hand, the high luminosity program, requiring small β* $\approx$ 0.1 m beam optics, has to be based on a limited-angular-acceptance detector - if exclusivity zones for the IR design and for the detector design are respected.

3.6.11.2 IR for physics-optimal ratio of beam energies

For the large ratio of the nucleon to electron beam energies, of $\approx$10, optimal for the physics program of the EIC collider, the electron and the proton beam optics can be, to a large extent, uncoupled facilitating the IR design.

3.6.11.3 Beam crossing angle and bunch frequency

The zero-beam-crossing angle, at the Interaction Point (IP), is optimal for the EIC physics program - in particular for its large β* part. Such a crossing angle could lead to parasitic bunch-bunch interactions at high bunch frequencies. They can be avoided either by inserting (evacuating) the electron beam very closely to the IP [1], or, by separating the electron and ion beams already within the central detector [2].

3.6.11.4 IR design for low emittance beams

The Laslet and the beam-beam tune-shifts impose fundamental limits on the beam sizes at the IP. Low emittance beams allow to minimize bunch sizes while preserving small beam divergence at the IP. If the ion beam divergence is kept below 0.1 mrad, a novel physics program, which uses accelerated ions as femto-detectors for studying the space-time structure of strong interactions, can be realized.

3.6.11.5 Synchrotron radiation at IR

Synchrotron radiation in the IR is not only the source of heat, which has to be evacuated, but, more importantly, a source of background, affecting the detector operation - in particular, the operation of its trigger and its tracker systems. The maximal allowed heat load and the maximal allowed radiation critical energy is proportional to the fourth power of electron beam energy and inversely proportional to the electron bending radius squared. Such a dependence imposes very important constraints on the IR design. Lower electron beam energy at the EIC collider, with respect to the HERA collider, allows for more flexibility in the IR design. This flexibility could be used: to reduce the distances over which beams are separated, thus facilitating the detector design; and/or to run higher current beams.

3.6.11.6 Beam insertion schemes

There exist two distinct concepts of the beam insertions.

Within the first one, proposed at the Yale workshop [1], electrons are inserted using a 3 m long 2.3 Tm dipole magnet placed at the distance of 1.5 m from the IP and generating a field of 0.76 T. The large deflection angle, generating sizable but tolerable synchrotron radiation, allows for early separation of th electron beam, providing necessary free space for the low angle particle spectrometer.

Within the second one, proposed at the BNL workshop [2], a small vertical deflection inside the main detector separates electrons from protons(ions). A Lambertson dipole is used to separate the electron beam, which passes the magnet in zero-field zone, from the proton (ion) beam. The main advantage of this insertion scheme is in reducing the strength of the synchrotron radiation - at the price of limiting the angular acceptance of the detector.

3.6.11.7 IR design and the luminosity measurement

The elastic radiative scattering ep(A) $\rightarrow$ ep(A) + γ could be used to measure the machine luminosity. The IR-design should facilitate measurement of the spectrum of photons produced at zero angle, by including in the design a dedicated, small radiation length exit window for zero-angle photons.

IR for full acceptance detectors - synergy of detector and IR designs

The optimal detector for the EIC experimental program should have a capacity of full event reconstruction, including measurements of the ion remnants. A design of such a detector [1,3] requires a close cooperation of the IR-designers and detector-designers. Beam insertion magnets have to be employed, simultaneously, as the spectrometer magnets. An optimal synergy has to be found while designing and implementing the large-aperture final-focus lens system and while integrating the beam-pipe detectors within the IR layout.

3.6.11.8 IR for a multi-beam collider

The ultimate challenge for the future, dedicated QCD research program is to design a full acceptance detector in the dedicated interaction region allowing for variable collision schemes: electron-proton, electron-ion, photon-proton, photon-ion, proton-proton and proton-ion; at variable center-of-mass energies.

Reference:

[1] M.W. Krasny, Nucl.Phys.Proc.Suppl.105:185-189,2002;

[2] B. Parker, Proceeding of the Electron Ion Collider Workshop at BNL, February 26-27, 2002,

[3] R. Holt et al., The Electron-Ion-Collider, White Paper submitted to the NSAC Long Range Planning Meeting, BNL, March 2001.

3.6.12 Study of The Beam-Beam Effects In ELIC

R. Li lir@jlab.org Jefferson Lab, Newport News, VA 23606 USA

B. C. Yunn yunn@jlab.org Jefferson Lab, Newport News, VA 23606 USA

K. Beard beard@jlab.org Jefferson Lab, Newport News, VA 23606 USA

To highlight the study of the beam-beam effect in the ELIC design, we first review the previous results of beam-beam effect in a linac-on-ring B factory, then move on to our present study of the beam -beam effect in a linac-on-ring electron-proton collider (ELIC).

The linac-on-ring collision scheme, where a linac beam collides with a storage ring beam, was earlier porposed [1] based on the idea that in such colliders the charge density for the storage ring beam is no longer limited by the beam-beam tune shift of the linac beam, hence a higher luminosity can be achieved. However, the consequently high charge density in the ring bunch together with the relatively low linac energy often leads to high (¿1) disruption for the linac bunch. The special feature of beam-beam interaction in a linac-ring collider is that the stored bunch undergoes collision with linac bunches with relatively high disruption which often comes in with jitters originated from the gun; thus the stability of the stored bunch and the corresponding beam-beam tune shift limit becomes an important issue for such new interaction regime.

The beam-beam effect in the early designs [2,3] of the linac-on-ring B factory was studied using a strong-strong beam-beam simulation code developed based on the macroparticle model [4,5]. The ring-ring version of the code was benchmarked with the simulation results on the flip-flop phenomena [6]. The code is then modified to study the linac-on-ring beam-beam effect for the CEBAF linac-on-ring B factory design. In this design, the beam-beam tune shift for the e^+ bunch is ξ_{y+}=0.05, and the disruption of the e^- bunch during collision is D_{y-}=273, indicating that the electron focal length is much shorter than the positron bunch length, and the electrons oscillate through the positron bunch during each collision [4]. In the initial test of the simulation, if one turns off the synchrotron oscillation of the stored bunch, due to high D_{y-}, one finds that kink instability was developed in the positron beam after few tens of collisions. This kink instability observed from simulation is explained analytically [7] using the linear beam-beam force model. It is found that in the collision process, the effects of offsets of previous positron slices are passed to trailing slices by the electrons via beam-beam interaction. After many turns, the offsets in the positron slices are cumulatively enhanced in a coherent manner. Further simulations show that the synchrotron oscillation of the positron bunch tends to have some suppressing effect on the kink instability. In fact, the inclusion of the synchrotron oscillation turns the above mentioned kink instability into the strong head-tail dipole instability, where the electron beam from the linac acts analogously to a transverse impedance. In simulations, the offsets of slices are usually introduced by numerical noises due to finite number of macroparticles. However, in reality, the e^- bunches from linac could fluctuate in intensity, transverse position, longitudinal position (timing) and possibly shape; so it is important to investigate the impact of this jitter of the linac beam on the stabilities of the storage ring beam. The destructive effect of jitter in the linac beam for a linac-ring B factory was first analyzed [8] using linear beam-beam force model, whereas the full nonlinear beam-beam simulation shows less destructive results [5].

The interest of the linac-on-ring collision scheme was renewed recently for proposals of the electron-light ion collider (ELIC) [9]. The advantage of using an energy-recovered linac for the electron beam is that it avoids the limitation of beam-beam tune shift inherent in a storage ring, pertains good beam quality and easy manipulation of polarization. These proposals were followed by a series of numerical and analytical studies on the stability of the stored ion bunch using linear beam-beam force model. The first of these approaches was done by Perevedentsev and Valishev [10], whose simulation study demonstrated that the betatron phase advance of the ion bunch through the interaction region could cause serious head-tail instability before the strong head-tail instability takes place. It also shows that the head-tail instability can be cured by introducing adequate chromaticity. Analyses [11] based on the linearized Vlasov equation also show that the linear beam-beam kick between electron and ion bunches acts like a broad-band transverse impedance to the dipole moment of the ion slices. For $\Lambda \equiv D_{y-}\xi_{y+}/\nu_s$, the analysis yields the transverse mode coupling threshold to be $\Lambda_{th} \approx 4$, where D_{y-} is the vertical disruption of the electron bunch, ξ_{y+} is the vertical beam-beam tune shift for the ion bunch, and ν_s is the synchrotron tune of the ion bunch. Similar threshold was also obtained by V. Lebedev [12] and B. Yunn [13]. For example, in

one such design [9], D_{y-}=4.6, ξ_{y+} =0.003, and ν_s = 0.00033, Λ=40 ¿¿ Λ_{th}.

It was later pointed out [14] that the betatron tune spread caused by the nonlinear beam-beam force introduces Landau damping to stablize the aforementioned head-tail or strong head-tail instability predicted by the linear beam-beam force model. To study this effect, the strong-strong simulation with full nonlinear beam-beam force previously used to study the beam-beam effect in the linac-on-ring B factory was recently modified to study the beam-beam effect in the linac-on-ring electron-ion colliders. Indeed, for the example of Λ=40, the growth of the beam transvese size is linear over several synchrotron oscillations with a much smaller growth rate compared to the exponential growth predicted by the linear beam-beam force model. These results are similar to the jitter effect studied earlier [5]. Further analytical and numerical studies of the linac-on-ring beam-beam interaction with the full nonlinear beam-beam force are underway so as to give useful input to designs of linac-on-ring colliders such as ELIC.

A circulator ring for the e^- bunch is proposed [15] to overcome the current limit on the production of a high average polarized electron current. In this scheme, the e^-bunch is recycled for collision in a circulator ring for a fraction of damping time. For such design the stability of both the e^- bunch in the circulator ring and the ion bunch in the storage ring should be carefully studied.

References:

[1] P. Grosse-Wiesmann, SLAC-PUB-4545, SLAC, 1988.

[2] J. Bisognano, *et. al.*, 1988 Linear Accelerator Conference, 1988.

[3] S. A. Heifets, G. A. Krafft and M. Fripp, Nuclear Inst. & Methods in Phys. Research, A295, p.286, 1990.

[4] J. R. Boyce, S. Heifets and G. A. Krafft, 1990 Linear Accelerator Conference, p.724, 1990.

[5] R. Li and J. J. Bisognano, *Phys. Rev. E* 48, 3965 (1993).

[6] S. Krishnagopal, private communication, 1992.

[7] R. Li, G. Krafft and J. J. Bisognano, CEBAF-TN-93-103 (http://tnweb.jlab.org/tn/1993), 1993.

[8] Y. Baconnier, CEERN PS/91-02(LP), 1991.

[9] L. Merminga and G. A. Krafft, V. A. Lebedev, Proceedings of the HEACC 2001 Conference, Japan (2001).

[10] E. A. Perevedentsev and A. A. Valishev, *Phys. Rev. Spec. Top*. **4**, 024403 (2001)

[11] R. Li, B. C. Yunn, V. Lebedev, J. J. Bisognano, 2001 Particle Accelerator Conference, Chicago (2001).

[12] V. Lebedev, private communication, 2001.

[13] B. Yunn, JLab-TN-01-017 (http://tnweb.jlab.org/tn/2001), 2001.

[14] Ya. S. Derbenev, private communication, 2002.

[15] Ya. S. Derbenev, 2002 European Particle Accelerator Conference, Paris, 2002.

4: Workshop and Conference Reports

4.1 International Workshop on Quantum Aspects of Beam Physics and Other Critical Issues of Beams in Physics and Astrophysics

Pisin Chen chen@slac.stanford.edu Stanford Linear Accelerator Center

The Joint 28^{th} ICFA (International Committee for Future Accelerators) Advanced Beam Dynamics and Advanced and Novel Accelerators Workshop on "**QUANTUM ASPECTS OF BEAM PHYSICS** – and Other Critical Issues of Beams in Physics and Astrophysics", was held in January 7-11, 2003, in Hiroshima, Japan. This was the third in the QABP workshop series. The first QABP workshop was launched in January 1998, in Monterey, California, and the second was held in October 2000, in Capri, Italy. Following the footsteps of the first two workshops, this one in Hiroshima was again a tremendous success.

The frontier of beam research points to increasingly higher energy, greater brightness and lower emittance beams with ever-increasing particle species. These demands have triggered a rapidly growing number of beam phenomena that involve quantum effects. With the significant advancement of laser and accelerator technologies, there is also a growing interest in using high energy, high intensity particle and photon beams for laboratory astrophysics investigations, as well as the application of beam physics expertise to astrophysics studies. Motivated by these exciting developments and prospects, and as part of the duties as a Panel member, in the fall of 1996 I proposed to Kohji Hirata (Graduate University for Advanced Research, Japan), then Chairman of the ICFA Advanced Beam Dynamics Panel, to organize such a workshop. The spontaneous enthusiasm on the proposed workshop around the world was overwhelming, and the first meeting in Monterey has made a history by giving birth to a new multi-disciplinary field of "quantum beam physics".

Over the past five years, this workshop series has passed its torch around the world, from the U.S. to Europe, and this time to Japan in Asia. Invariantly, these meetings had attracted a broad spectrum of experts from beam physics, astrophysics, particle physics, condensed matter physics, nuclear physics, atomic physics, and laser science, to explore a common frontier where their individual expertise and interests overlapped. This newly emerged subject basically covers the following general topics:

A. Quantum Fluctuations in Beam Dynamics;

B. Photon-Electron Interaction in Beam Production, Cooling, Monitoring;

C. Beam Phenomena under Strong Fields;

D. High Energy Astrophysics and Laboratory Astrophysics;

E. Quantum Methodologies in Beam Physics.

The progress of the field has been well documented by two volumes of the Monterey and the Capri workshop proceedings (more than 800 and 650 pages, respectively) published by the World Scientific under the same title "Quantum Aspects of Beam Physics" (ed. P. Chen).

About 70 physicists from China, Denmark, Georgia, Germany, India, Italy, Japan, Korea, Mexico, Mongolia, Russia, Taiwan, Ukrain, U.K., and U.S., had participated in the Hiroshima workshop. Unlike the first two workshops, the Hiroshima meeting was conducted in the symposium style. Other than one poster session, all the meetings were plenary. The Program Committee thought that the symposium style would allow participants to listen to all interesting talks. The concern, however, was the loss of opportunity for free exchange of ideas under such a format. To prevent such a drawback, the workshop had set-aside a block of time for round-table discussion at the end of each topical session. This was found to be a very welcome arrangement. In the end the

advantages of both workshop and symposium styles appeared to have preserved.

For the more traditional subjects, namely Topics A&E, H. Mais (DESY, Germany) gave a concise overview on the status of "Quantum Fluctuations in Beam Dynamics". V.N. Baier (BINP, Russia) emphasized the importance of coherent radiation in electron-positron colliders. R. Jaganathan (IMS) from India talked about quantum mechanics of electron beam transport through optical elements with curved axes. This was an extension from his earlier work using linear coordinates to curvilinear ones, which were more suitable for circular accelerators. M. Zeitlin (IPME, Russia) presented his deep mathematical insights into quasiclassical calculations for Wigner functions, and S. De Siena (Salerno, Italy) introduced his new "Stochastic-Hydrodynamic Model" for halo formation of charged particle beams.

Presentations within Topic B were largely dominated by the considerations of Compton scattering, its production as well as applications. F. Hartemann (LLNL) gave a nice overview on this, while many Japanese colleagues from Tokyo Metropolitan University, KEK, and Waseda University dwelled the subject further. There were also presentations on novel concepts of beam production, such as the "Low Emittance Laser-Plasma Electron Gun" by T. Tajima (JAERI-APRC, Japan). There were also novel ideas of producing polarized positron beams.

For Topic C, one focus was on the nature of the QED vacuum, in particular that under violent accelerations. As suggested by W. Unruh (1976), a particle "detector" undergoing a uniform acceleration should find itself surrounded by a thermal heat bath with a temperature, $kT = ha/2\pi\ c$, which is identical to the celebrated Hawking temperature for black hole radiation, except that the gravitational acceleration g in Hawking's case is replaced by the proper acceleration a of the particle detector. The meaning as well as the experimentation of this very fundamental phenomenon had been a controversial subject and a continuing discussion since the Monterey workshop. W. Unruh himself and D. Jackson, author of the classic textbook "Classical Electrodynamics", both attended the Monterey workshop and had a warm debate during that meeting. At the second workshop in Capri, J. Leinaas (Oslo, Norway), coauthor (with the late J. Bell) of a seminal paper on the subject, presented his side of the view. At the Hiroshima meeting, A. Ringwald (DESY, Germany) discussed the possibility of "boiling the vacuum" with an x-ray free electron laser, while H. Rosu (IPICyT, Mexico) reviewed possible experimental searches for Unruh effect. A. Yashin (SLAC, presented by P. Chen) reported on a new wave-packet approach to Unruh effect.

Other exciting subjects in beam physics under strong fields were best represented by the report on the observation of radiative cooling of positrons in a crystal, given by U. Uggerhoj (Aarhus U., Denmark). T. Esirkepov (JAERI, Japan) discussed a plasma-based scheme to achieve the Schwinger limit ($B_c \sim 4.4 \times 10^{13}$G) on Earth. It was unclear whether the scheme could indeed work, but it would be exciting if it did.

Perhaps the most exciting session(s) were that for Topic D. Spanning across a wide range of subjects, the session started with a somewhat controversial suggestion made by D. Dong (IHEP, Beijing) regarding gravitational-wave induced effects in storage rings beam dynamics. It was not clear why the GW induced effect could be so strong an effect on particle beams in storage rings. There was a very exciting development of J. Irwin (SLAC, presented by J. Ng), where the theoretical methodology in high energy particle beam optics was applied to investigate the cosmic gravitational lensing effects.

The center of focus of Topic D belongs to the issues related to ultra high cosmic rays (UHECRs). J. Matthews (Utah) reviewed experimental issues associated with UHECR detection, and explained the motivation for the "Fluorescence in Air Showers" (FLASH) experiment at SLAC. Y. Takahashi (U. Alabama) discussed the status of extremely high energy cosmic rays and suggested their possible non-conventional origins. P. Chen (SLAC) introduced a new model for UHECR based on the Alfven-shock induced plasma wakefield acceleration that occurred in the GRB fire-

ball. K. Reil presented the computer simulations efforts on this mechanism. The prominent H. Sato (Konan U., Japan) linked UHECR to the violation of Lorentz invariance, while P. W-Y. Hwang (CosPA, Taiwan) suggested the bridging of particle astrophysics and cosmology via UHECRs.

Additional astrophysical discussions mostly involved plasmas and strong fields. H. Li (LANL) discussed magnetic energy dissipation in force-free plasmas. S. -S. Xue (ICRA/U. Rome) talked about plasma oscillations in a strong electric field, while L. Vitagliano (ICRA/U. Rome) discussed evolution of a electron-positron-photon plasma around a collapsing star. Both works are relevant to the origin of gamma ray bursts (GRBs). Perhaps most interesting was the theory of neutrino-induced electroweak plasma instability presented by R. Bingham (RAL), who had coauthored this work with J. Dawson and H. Bethe in the early 90s. The theory could explain the long-standing issue of energy transport during supernova explosion through the collective plasma instability induced by the out-burst SN neutrinos.

With all these exciting developments, it was timely that H. Takabe (ILE, Osaka U.) promoted laboratory astrophysics using intense lasers, while J. S. T. Ng (SLAC) complimented this initiative by introducing laboratory astrophysics using high energy particle beams.

There were also several "Focused Forums" organized in this workshop. Specifically, there was a session that reviewed critical issues that faced future linear colliders and advanced accelerator concepts. E. Colby (SLAC) addressed critical issues for vacuum laser acceleration, and M. Uesaka (U. Tokyo) reviewed critical issues in plasma accelerators. S. Bulanov (JAERI) lectured on the radiation dominant laser-plasma interaction. There were also novel accelerator ideas presented by K. Nakajima (KEK/JAERI) on electron-positron pair-beam production and acceleration via ultra-strong laser-plasma interactions. A. Ogata (Hiroshima U.) suggested the use of macroscopic solid structure for accelerators. V. Telnov (BINP, Russia) discussed critical issues in linear colliders, while T. Takahashi (Hiroshima U.) reported on recent progress on photon-photon colliders. There was also the very important theoretical (as well as practical) issue of beam-size effect in bremsstrahlung in colliders, discussed by V.N. Baier (BINP).

One other Focused Forum was on "crystalline beams". U. Schramm (LMU, Munich) reported on the important experimental observations on crystalline beams. H. Okamoto (Hiroshima U.), on the other hand, concerned the dynamics of ultra-cold beams from the theoretical end. A. Noda (ICR, Kyoto U.) discussed an approach to achieve ultra-cold beams at LSR in Kyoto University.

In addition to the exciting scientific program, the social program of the Hiroshima workshop was wonderfully organized. Following the tradition of the QABP workshop series, which seeks to actively integrate science and culture, there was again an opening night music concert at the workshop, performed by concert marimbist, Ms. Hiroko Tsuji. Her repertoire extends from classical music of J.S. Bach to contemporary American and Japanese pieces. The excursion to the famous and sacred Miyajima island in the Hiroshima Bay was most memorable. Hiroshima is home to prestigious Sake breweries. The post-workshop visit to one of the famous breweries was very educational. Many foreign workshop participants also took extra time to visit the atomic bomb site and the memorial Piece Museum in Hiroshima.

None of these wonderful arrangements were possible without the dedication and outstanding organizational skill of Prof. Atsushi Ogata of the Hiroshima University. With the successful ending of the QABP03 Hiroshima meeting, the "trilogy" of workshops on "quantum beam physics" has by now come around the world in a full circle.

Six years ago, I designed the QABP workshop logo (a jumping whale overlaps with a vacuum-polarization Feynman diagram) under the inspiration that there was an interesting analogy between emerging whales from the sea and vacuum fluctuations in the Dirac "sea", and with the conviction that the ultimate understanding of the physical vacuum was one of the last frontiers in physics. In the interim, we saw the emergence of the notion of dark energy in cosmology, whose nature

is beyond anyone's comprehension. Although it is unclear which water will this "QABP whale" swim to next, it is clear that the subject will continue to be in the forefront of our pursuit.

More information can be found from the workshop home page at
http://home.hiroshima-u.ac.jp/ogata/qabp/home.html

4.2 Andy Sessler's 75th Birthday Celebration

Miguel Furman mafurman@lbl.gov Lawrence Berkeley National Laboratory

An event to celebrate Andy Sessler's many scientific achievements and humanitarian contributions, and his 75th birthday, took place on March 15, 2003 at LBNL. The event consisted of an afternoon symposium followed by a dinner in the LBNL cafeteria overlooking the San Francisco bay. The symposium speakers, who covered a subset of Andy's broad range of interests, were: Larry Jones (U. Michigan); Kwang-Je Kim (ANL); Simon Yu (LBNL); Bob Palmer (BNL); George Trilling (LBNL); Art Rosenfeld (CA Energy Commission); and Irving Lerch (APS). Andy's former student Phil Morton (retired from SLAC) served as master of ceremonies following the dinner. Don Prosnitz (LLNL) gave the main after-dinner talk. This was followed by brief remarks by relatives and friends of Andy's - and Andy himself gave a closing "coda." There were over 100 guests at the dinner, some of whom came from as far away as Japan for the event. A string quartet played classical music selections during the cocktail hour preceding the dinner. The event was fun, enlightening, and elegant.

Electronic proceedings of the symposium will be available, along with photos and digital movies. These will be posted in the Sessler Event website, http://mafurman.lbl.gov/sesslerevent/, which already contains the detailed program schedule and other information. A brief article covering the event and Andy's current interests and activities appeared in the March 21, 2003, issue of the LBNL Currents, http://www.lbl.gov/Publications/Currents/Archive/Mar-21-2003.html

In addition to the March 15 eventthe Accelerator and Fusion Research Division has established a new, ongoing, postdoctoral fellowship as a lasting tribute to Andy's accomplishments. Announcements inviting applications will soon appear in Physics Today and the CERN Courier.

5: Activity Reports

5.1 Design and Status of the Cooler Storage Ring in IMP

Jia-Wen Xia xiajw@impcas.ac.cn Institute of Modern Physics, China

(J.W. Xia, W.L. Zhan, B.W. Wei, Y.J. Yuan, M.T. Song, W.Z. Zhang, X.D. Yang)

5.1.1 Introduction

From May of 1993 to November of 1996, a new plan was proposed [1, 2] to upgrade the HIRFL [3] with a multi-functional Cooling Storage Ring (CSR) forming a HIRFL-CSR accelerator system shown in Fig. 1. This will greatly enhance the performances of HIRFL for those researches by using Radioactive Ion Beams (RIB) and high-Z heavy ion beams in the fields of nuclear physics and atomic physics. In July of 1998, the Chinese center government approved this plan, and on December 10 of 1999 the CSR project was started. The period from the beginning of 2000 to the summer of 2001 is the stage of the building construction, design optimization and prototype experiments. The machine fabrication is to be from 2001 to 2004, and 2005 is the installation and tuning time.

5.1.2 General Descriptions

HIRFL-CSR is a multipurpose Cooling Storage Ring system that consists of a main ring (CSRm), an experimental ring (CSRe), and a radioactive beam line (RIBLL2) to connect the two rings, shown in Fig. 5.1. The two existing cyclotrons SFC (K=69) and SSC (K=450) of the HIRFL will be used as its injector system. The heavy ion beams with the energy range of 8$\sim$30 MeV/μ from the HIRFL will be accumulated, cooled and accelerated to the high-energy range of 100$\sim$500 MeV/μin the main ring, and then extracted fast to produce radioactive ion beams (RIB) or highly charged heavy ions. The secondary beams (RIB or highly charged heavy ions) will be accepted and stored by the experimental ring for many internal-target experiments or high precision spectroscopy with beam cooling. On the other hand, the beams with the energy range of 100$\sim$1000MeV/μ will also be extracted from CSRm by using slow extraction or fast extraction for many external-target experiments.

Two electron coolers located in the long straight sections of CSRm and CSRe, respectively, will be used for beam accumulation and cooling

CSR intends to provide internal and external target beams for many physics experiments. One internal target in the long straight section of CSRe will be used for nuclear physics and highly-charged state atomic physics. Many external targets of CSRm will be used for nuclear physics, cancer therapy study and other researches.

The beam parameters and the major machine parameters of the CSR are listed in Table 5.1.

5.1.3 Operation scheme

5.1.3.1 Normal operation mode

CSR is a double ring system. In every operation cycle, the stable-nucleus beams from the injectors are accumulated, cooled and accelerated in the main ring (CSRm), then extracted fast to produce RIB or highly charged ions. The experimental ring (CSRe) can obtain the secondary beams once

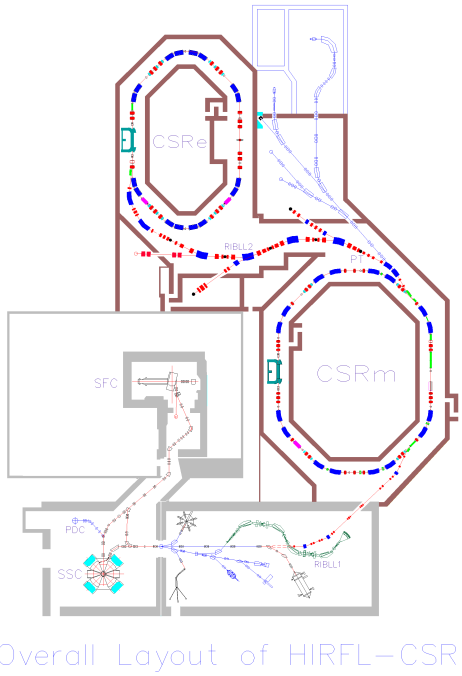

Figure 5.1: Overall layout of the HIRFL-CSR complex.

Table 5.1: Major parameters of the CSR.

	CSRm	**CSRe**
Circumference (m)	161.00	128.80
Ion species	Stable nuclei: C – U, RIB(A¡238)	Stable nuclei: C – U, RIB(A¡238)
Max. energy (MeV/u)	1100 (C^{6+}), 500 (U^{72+})	750 (C^{6+}), 500 (U^{90+})
Intensity (Particles)	10^5—10^9 (stable nuclei)	10^{3--9} (stable nuclei, RIB)
Bρ_{max} (Tm)	12.05	9.40
B$_{max}$ (T)	1.6	1.6
Ramping rate (T/s)	0.1–0.4	0.1–0.4
Repeating circle (s)	$\sim$ 17 s ($\sim$ 10 s for accumulation)	
Acceptance		Normal mode
A$_h$ (π mm-mrad)	200 (ΔP/P = $\pm$0.15 %)	150 (ΔP/P =$\pm$0.5%)
A$_v$(π mm-mrad)	30	75
ΔP/P (%)	1.25 (ε_h= 50 π mm-mrad)	2.6 (ε_h= 10 π mm-mrad)
E-cooler		
Ion energy (MeV/u)	8—50	25—450
Length (m)	4.0	4.0
RF system	Acceleration Accumulation	Capture
Harmonic number	1 16, 32, 64	1
f$_{min}$/f$_{max}$ (MHz)	0.24 / 1.81 6.0 / 14.0	0.4 / 2.0
Voltages (n $\times$ kV)	1 $\times$ 7.0 1 $\times$ 20.0	2 $\times$ 10.0
Vacuum pressure (mbar)	6.0 $\times$ 10^{-11}	6.0 $\times$ 10^{-11}

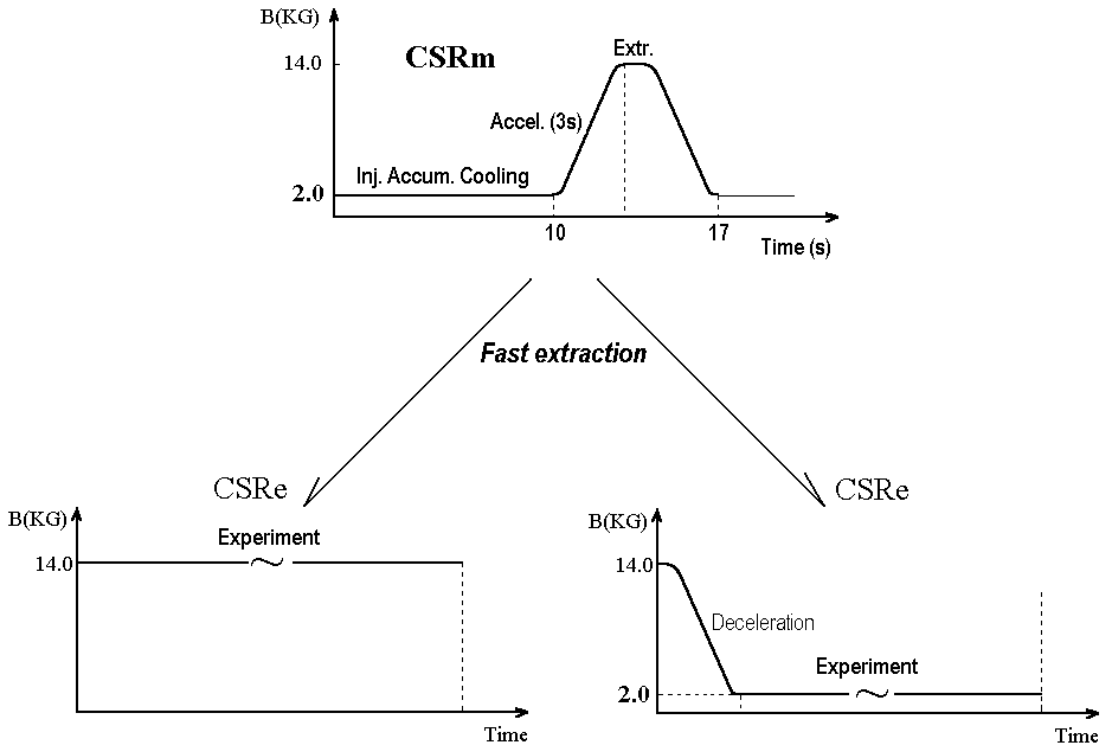

Figure 5.2: Magnetic field exciting procedure of CSR.

for every operation cycle. The accumulation duration of CSRm is about 10s. Considering the ramping rate of magnetic field in the dipole magnets to be 0.1∼0.4 T/s, the acceleration time of CSRm will be nearly 3s. Thus, the operation cycle is about 17s.

In CSRe, two operation mode will be adopt. One is the storage mode used for internal-target experiments or high precision spectroscopy with electron cooling. Another one is the deceleration-storage mode used for atomic-physics experiments. Fig. 5.2 shows the magnetic field exciting procedure of the two rings.

5.1.3.2 Injector system

The existing HIRFL [3] facility will be used as the injector system of CSR. It consists of two cyclotrons, the main accelerator SSC (Separated Sector Cyclotron, K=450) and the pre-accelerator SFC (Sector-Focusing Cyclotron, K=69). The light heavy ions, example C, N, O etc., can be injected into CSRm directly from SFC without the acceleration of SSC, but those heavy ions (A$>$40) should be accelerated by the combination of SFC and SSC before the injection. The mean extraction radius of SFC and SSC are 0.75m and 3.20m, respectively.

5.1.3.3 Beam accumulation

While heavy ion beams from HIRFL are injected into CSRm, the beam lifetime should be long enough for the beam accumulation in CSRm. Referring to the actually measured spectra of residual gases, in the case that the average pressure of CSR is assumed to be 6.0×10^{-11} mbar, the residual gas composition will be 85% of H_2 and 15% of N_2 and CO. According to the calculation [4], the REC (radiative electron capture) process in the electron cooler restricts the lifetimes of light heavy

Table 5.2: Parameters of the beam accumulation in CSRm.

	O^{6+}	O^{7+}	O^{7+}	Xe^{48+}	U^{72+}
Injector	SFC	SFC	SFC	SSC	SSC
Energy (MeV/u)	8	10	10	20	10
Current (pμA)	1	0.5	0.5	0.01	0.01
Current (pps)	6×10^{12}	3×10^{12}	3×10^{12}	6×10^{10}	6×10^{9}
Particles/Turn	2.5×10^{7}	1×10^{7}	1×10^{7}	1.5×10^{5}	2×10^{4}
Efficiency of strip.	90%			19%	15%
Method	STI	RFS	MMI	MMI	MMI
Cycle (ms)	1000	100	1000	250	100
Period (s)	10	10	10	10	10
Gain factor of MMI	40	2.8	5	5	5
Particles	1×10^{10}	2×10^{9}	4×10^{8}	5×10^{6}	1×10^{6}

ions (C–Kr) in CSRm, the electron capture from the residual gas molecule dominates the lifetimes of heavy ions (Xe–U), and the beam loss caused by Coulomb scattering can be negligible. In conclusion the beam lifetimes ($>$15s) are longer than the time of the beam accumulation ($\sim$10s) in CSRm.

Three method will be used in CSRm to accumulate the heavy ions up to $10^{6\sim10}$ in a short duration of 10s. The first is the Stripping Injection (STI) for those light heavy ions (A¡24). The second is the Multiple Multi-turn Injection (MMI) in the horizontal phase space with the acceptance of 150π mm mrad. The third one is the combination of the horizontal multi-turn injection and the RF Stacking [5] (RFS) in the momentum phase space. In the second method the horizontal acceptance is 50π mm mrad used for the multi-turn injection and the momentum acceptance is 1.25% for the RF stacking. During the accumulation, electron cooling will be used for the cooling of beam in order to increase the accumulation ratio and efficiency. Table 5.2 is the accumulation parameters for several typical ions.

5.1.4 Lattice

5.1.4.1 CSRm lattice

CSRm is a racetrack shape, as shown in Fig. 5.3, and consists of four identical arc sections. Each arc section consists of four dipoles, two triplets and one doublet. Eight independent variables for quadruple are used. The lattice of each arc section is given as follows,

$$\text{—— } L_1\text{——FDF–B–B–F—- } L_2\text{—DF–B–B–F}\tfrac{1}{2}\text{D}$$

Where, $2L_1$is a long-straight section with dispersion free for e-cooler or RF cavity. L_2 is a dispersion drift for beam injection or extraction. Fig. 5.4 is the distributions of the β-functions and the dispersion in CSRm, Table 5.3 is the lattice parameters of CSRm.

In the injection arc-section 3 bump magnets (BP1, BP2, BP3) will be used to move the closed orbit from center to the injection orbit in the horizontal plane, then injection beam will be deflected into the closed orbit by one static-electric septum (ES1) and one magnetic septum (MS1). During the multi-turn injection, the field of the 3 bumps will be reduced to zero isochronously, the closed orbit will move back to the center, and the horizontal acceptance (150π or 50π mm-mrad) will be filled by injection beam simultaneously. Fig. 5.5 is the orbits of the MMI.

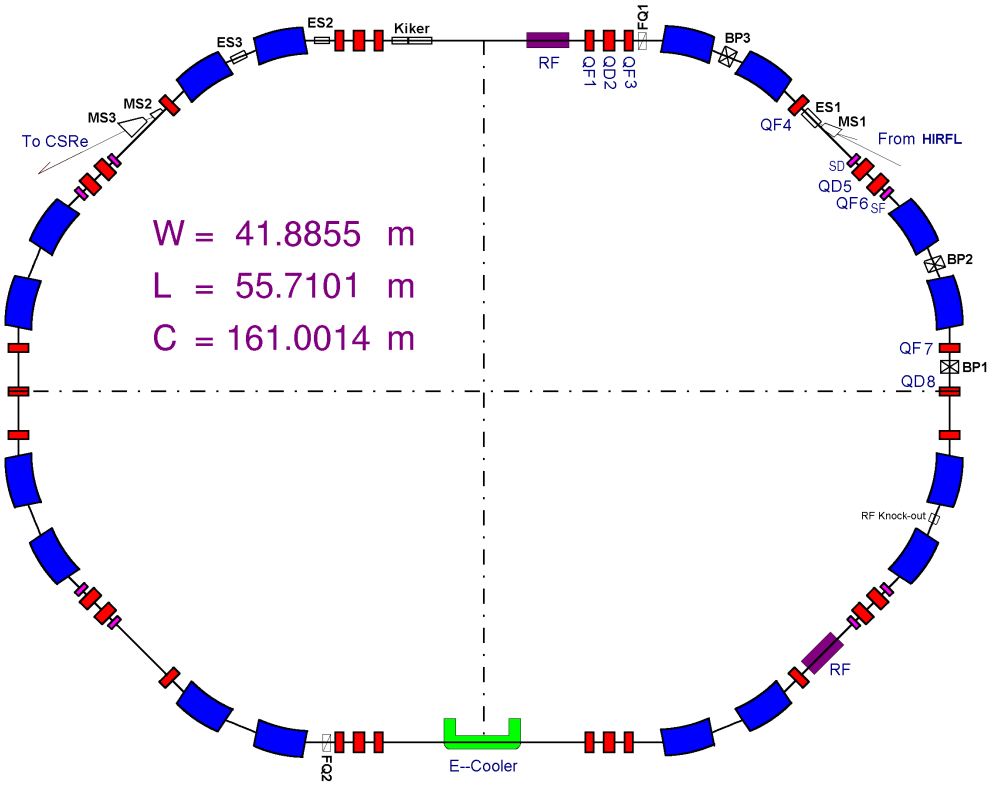

Figure 5.3: Lattice layout of CSRm.

For CSRm, fast and slow beam extractions should be done. In the extraction arc-section, five kicker modes will be used for the fast extraction, and two static-electric septum (ES2, ES3), two fast quadruples (FQ1, FQ2), two families of sextuple and six in-dipole coils will be used for the slow extraction of 1/3 order resonance. The two extractions will use one channel, and the final elements of the extraction are two magnetic septa (MS2, MS3).

For beam injection and extraction, the special vacuum chambers will be adopted to obtain large horizontal space.

In CSRm, 16 auxiliary coils in dipoles, two combined vertical and horizontal correctors and nine vertical correctors will be used for the global closed-orbit correction.

Table 5.3: Lattice parameters CSRm.

Transition gamma	γ_{tr}= 5.168
Betatron tune values	Qx / Qy = 2.63 / 2.61
Natural chromaticity	$Q'_x/Q'_y = -3.05 / -5.34$
Max. β-Amplitude	β_x/β_y=10.4/17.5 m (Dipole), β_x/β_y=13.5/32.2m (Quadruple)
Max. Dispersion	D_{max}(x)=3.2 m (Dipole, β_x=10.4m), D_{max}(x) = 4.6m (Quad., β_x=8.0 m)
Injection section	β_x=10.0 m, D_x= 4.0 m (Septum), β_x=11.9 m, D_x=3.9 m (Quadruple)
E-cooler section	β_x/β_y= 10.0/17.0 m , D_x= 0
RF station section	β_x/β_y= 10.0/6.4 m , D_x= 4.0

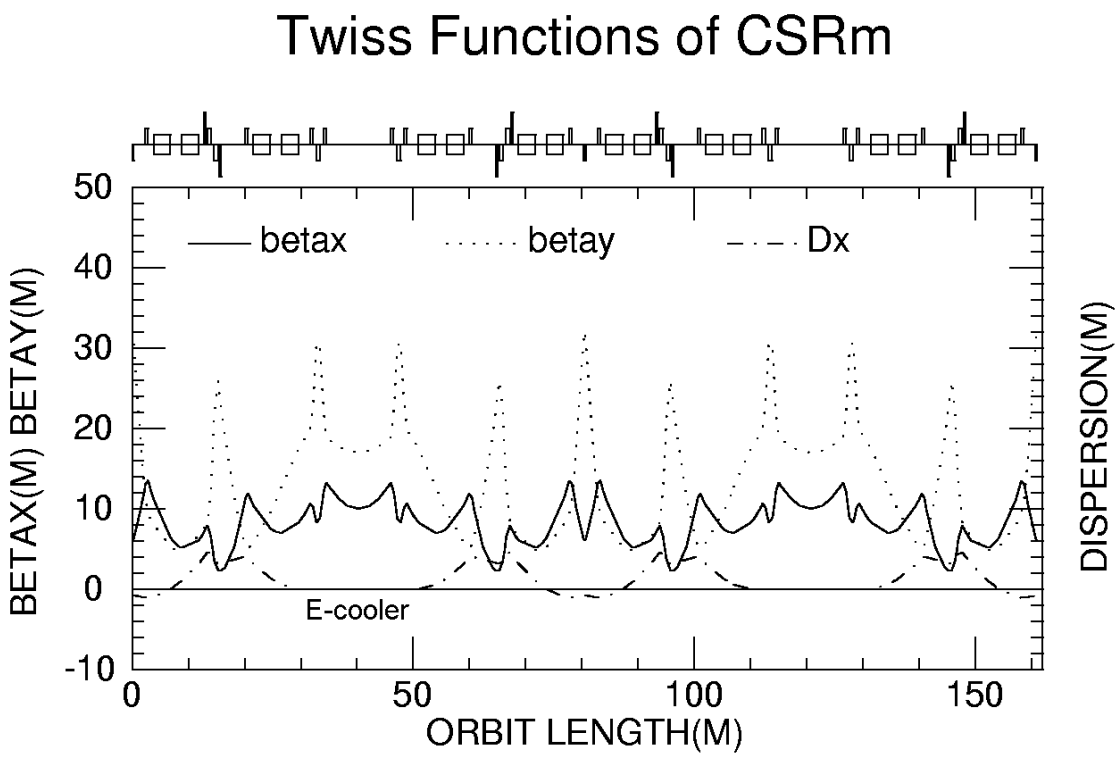

Figure 5.4: Distributions of the β and dispersion of CSRm.

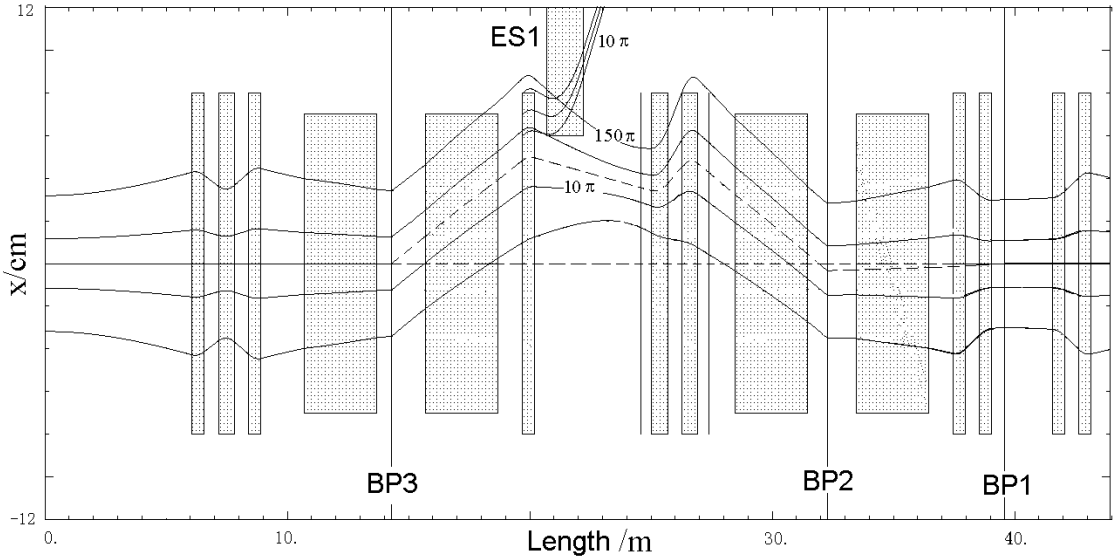

Figure 5.5: Orbits of the MMI in CSRm.

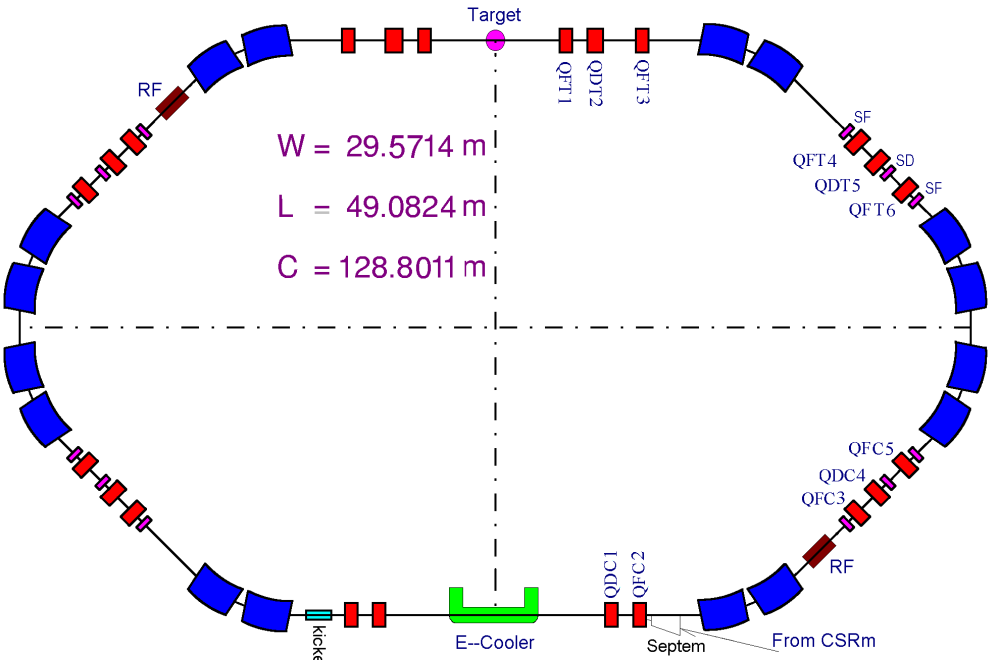

Figure 5.6: Lattice layout of CSRe.

5.1.4.2 CSRe Lattice

The layout of CSRe is shown in Fig. 5.6 It has a race track shape and consists of two quasi-symmetric parts. One is the internal-target part and another is the e-cooler part. Each part is a symmetric system and consists of two identical arc sections. Each arc section consists of four dipoles, two triplets or one triplet and one doublet. 11 independent variables for quadruple are used in CSRe. The lattice of the half ring is given as follows,

—L_T—FD-F–B-B–L_R–FD-F-B-B–B-B-F-DF–L_R–B-B–FD—-L_c—

Where, $2L_T$and $2L_C$ are the long-straight sections with dispersion free for internal target and e-cooler. L_R is the dispersion drift for RF cavities.

In CSRe, three lattice modes will be adopted for different requirements. The first one is the internal-target mode with small β-amplitude in target point and the large transverse acceptance (A_h=150πmm-mrad, A_v=75πmm-mrad) for internal-target experiments. The second one is the normal mode with a large momentum acceptance of ΔP/P = 2.6% for high-precision mass spectroscopy [6]. The third one is the isochronous mode with a small transition γ_{tr} that equals the energy γ of beam in order to measure the mass of those short-life-time RIB.

Table 5.4 shows the lattice parameters of CSRe for the three lattice modes, and Figs. 5.7-5.9 denotes the distributions of the β-functions and the dispersions for those modes.

The injection of CSRe is located in the zero-dispersion section of the e-cooler in order to accept the large momentum-spread ($\pm$1%) beams from RIBLL2 shown in Fig. 5.1 The single-turn injection will be adopted by using one magnetic septum and four modes of kicker. During the injection, four auxiliary coils in four main dipoles will be used to create the bump orbit for the injection, and the injection channel will pass through the fringe field of a dipole and two quadruples. For the three lattice modes, the gradient of the doublet quadruple nearly the injection septum should be maintained at the same value in order to obtain the same injection orbit. Fig. 5.10 shows the single-turn injection orbit of CSRe.

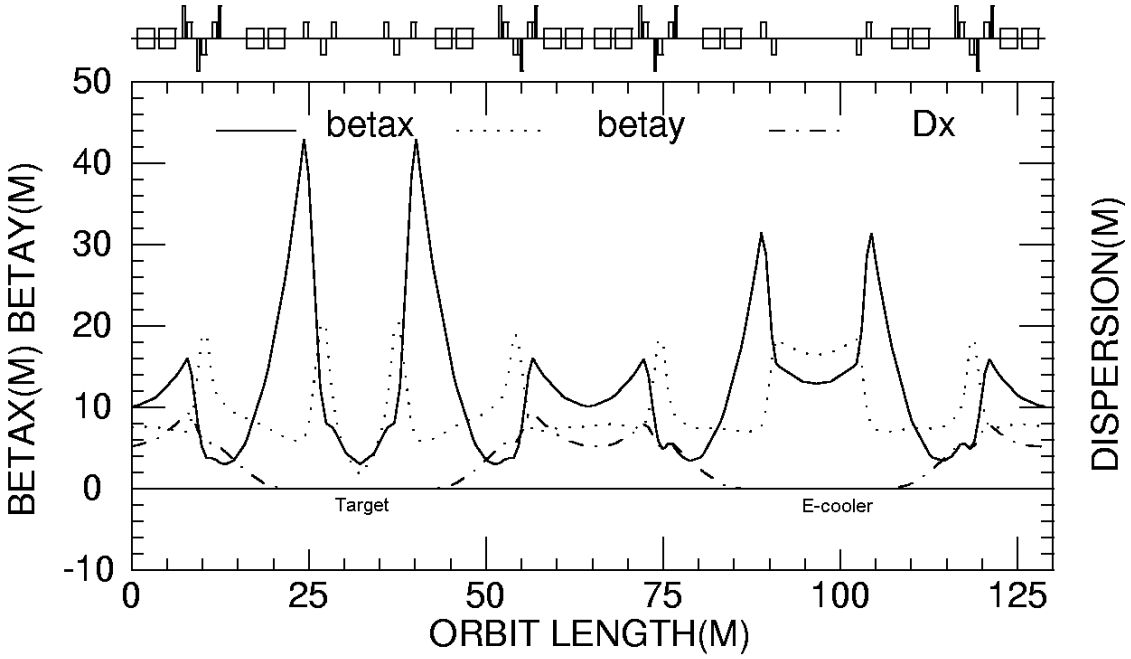

Figure 5.7: Tiwiss functions for the internal-target mode.

In CSRe, two families of sextuple will be used to correct the chromaticity, and 16 in-dipole coils, four double-direction correctors, six vertical correctors will be used for the global closed-orbit correction.

5.1.5 Subsystem

5.1.5.1 Magnets and correlative subsystems

All the magnetic cores of CSR will be laminated of 0.5mm-thick sheets of electro-technical steel with high induction and cold-rolled isotropy. Coils will be made of T2 copper conductor with hollow and insulated with polyimide stick tape and vacuum epoxy resin impregnating. In order to reach the necessary field uniformity at the different levels of the range of 1000Gs $\sim$ 16000Gs, a so-called modified H-type dipole was designed for CSRm. An air hole will be punched at the center of the pole to control the magnetic field flux flow at high magnetic fields[7], The magnetic field distribution on the median plane will be improved and a good field distribution in a wide field range can be obtained. In CSRe, the C-type dipole with a large useful aperture will be adopt for physics experiments.

All power supplies of the ring magnets will need DC and pulse operation modes, while high current stability, low current ripple, good dynamic characteristic are necessary requirements. Two types of supply, a traditional multi-phase thyristor rectifier for dipoles and a switching mode convertor for quadruples, will be adopted Table 5.5 displays the major parameters of magnets and its correlative power supplies and vacuum chambers.

5.1.6 Electron-cooler system

Two electron coolers will be equipped in CSRm and CSRe, respectively, for heavy ion beam cooling. In CSRm, e-cooling will be used for the beam accumulation at the injection energy range

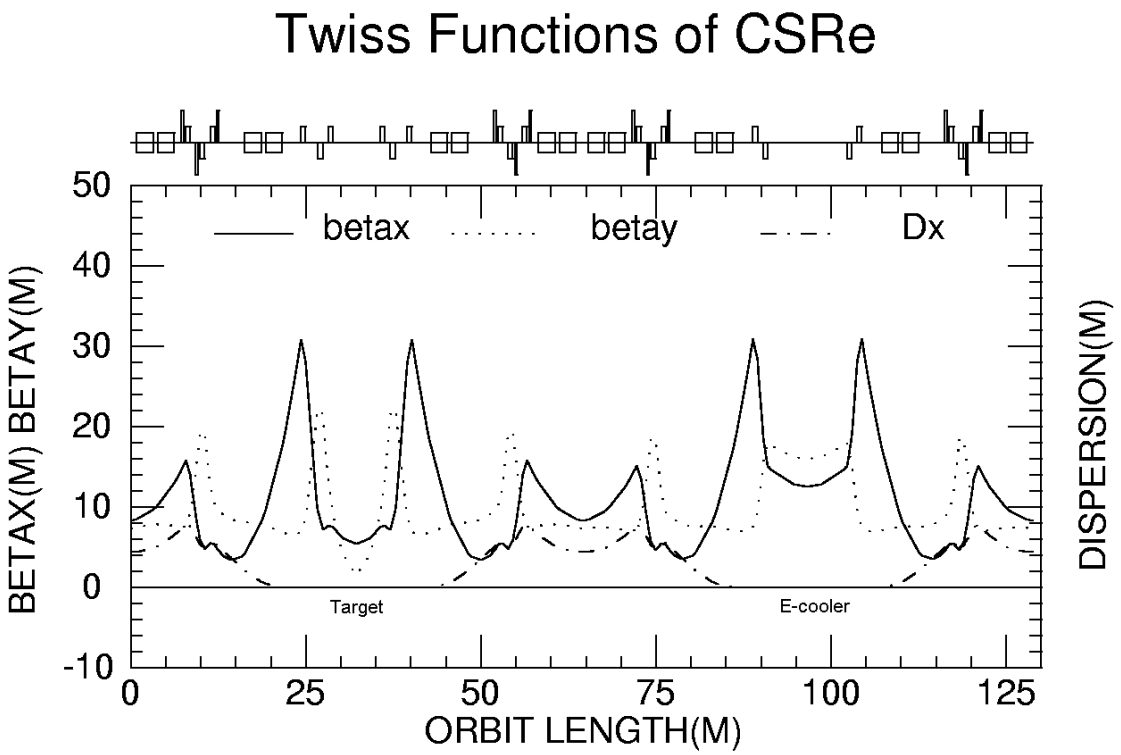

Figure 5.8: Tiwiss functions for the normal mode.

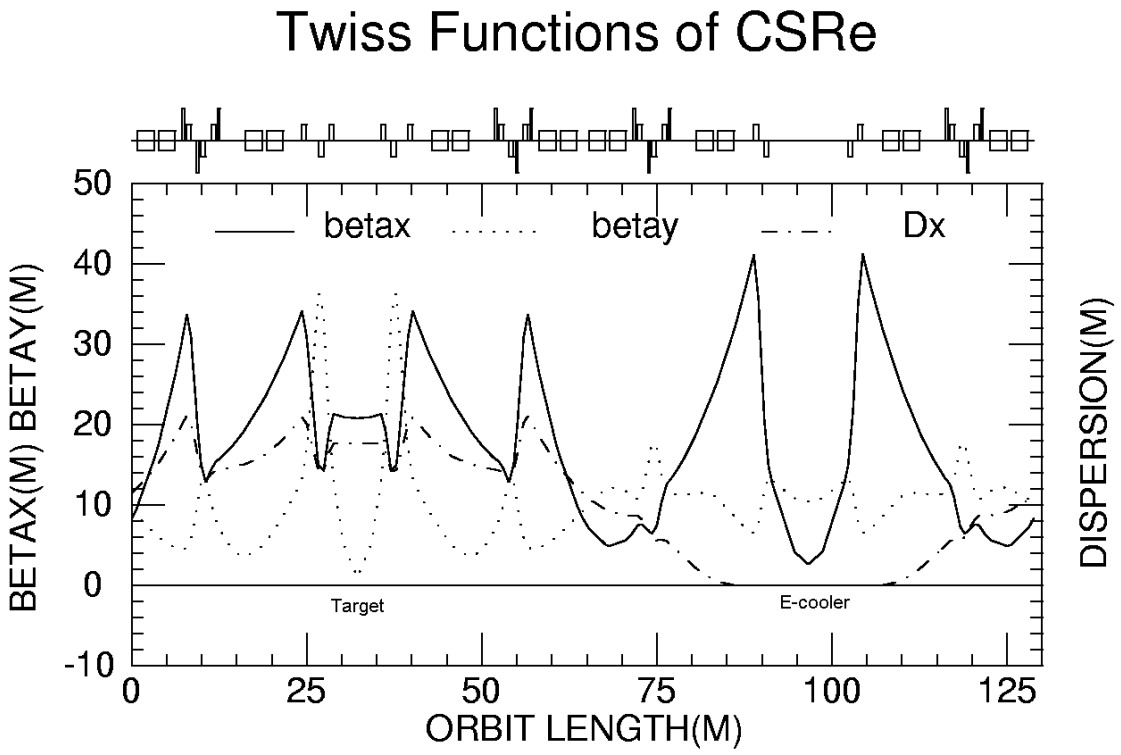

Figure 5.9: Tiwiss functions for the isochronous mode.

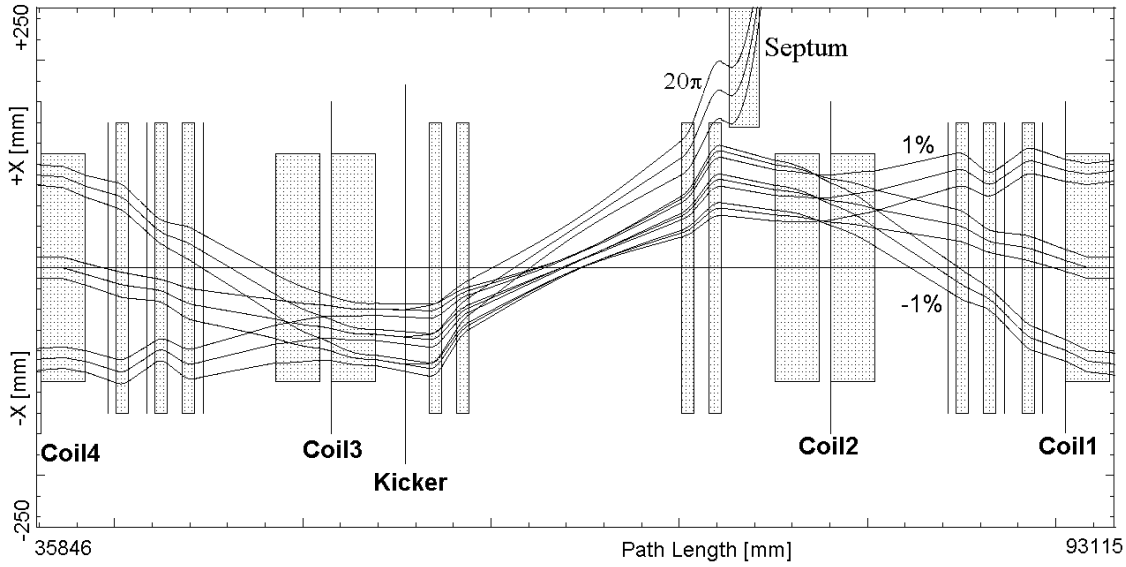

Figure 5.10: Single-turn injection orbit of CSRe.

Table 5.4: Lattice parameters of CSRe.

	Internal-target mode	**Normal mode**	**Isochronous mode**
Transition gamma	γ_{tr}= 2.457	γ_{tr}= 2.629	γ_{tr}= 1.395
Betatron tune values	Qx / Qy = 2.53 / 2.57	Qx / Qy = 2.53 / 2.57	Qx / Qy = 1.695 / 2.72
Natural chromaticity	$Q'_x/Q'_y = -3.70 \ / \ -3.55$	$Q'_x/Q'_y = -3.10 \ / \ -3.74$	$Q'_x/Q'_y = -1.57 \ / \ -3.25$
Max. β-Amplitude	β_x/β_y=25.7/8.7 m (Dipole) β_x/β_y=43.0/20.4 m (Quadruple)	β_x/β_y=17.6/8.2 m (Dipole) β_x/β_y=30.9/22.3 m (Quadruple)	β_x/β_y=28.1/12.2 m (Dipole) β_x/β_y=41.2/36.4 m (Quadruple)
Max. Dispersion	D_{max}(x)=7.9m(Dipole, β_x=14m) D_{max}(x)=9.4m(Quad. , β_x=16m)	D_{max}(x)=6.5m(Dipole, β_x=13m) D_{max}(x)=7.8m(Quad. , β_x=16m)	D_{max}(x)=18.5m (Dipole, β_x=28m) D_{max}(x)=21.2m(Quad. , β_x=34m)
Injection section	β_x= 30.8 m , D_x= 0 m (Septum) β_x=31.4m, D_x=0m (Quadruple)	β_x= 30.4 m, D_x= 0 m (Septum) β_x=30.9m, D_x=0m (Quadruple)	β_x= 40.8 m , D_x= 0 m (Septum) β_x= 41.2m, D_x= 0 m (Quadruple)
E-cooler section	β_x/β_y= 12.9/16.5 m , D_x= 0	β_x/β_y= 12.5/16.0 m , D_x= 0	β_x/β_y= 2.6/10.5 m , D_x= 0
Target	β_x/β_y= 3.0/1.7 m , D_x= 0	β_x/β_y= 5.4/1.5 m , D_x= 0	β_x/β_y= 20.8/1.0 m , D_x= 17.7m
RF station section	β_x/β_y= 4.0/8.3 m , D_x= 4.6	β_x/β_y= 4.0/8.4 m , D_x= 4.5	β_x/β_y= 19.0/11.5m , D_x= 15.0m

Table 5.5: Major correlative parameters of the magnets.

Dipole				Quadruple		
	CSRm	CSRe			CSRm	CSRe
Number×angle (deg.)	16×22.5	16×22.5		Number	30	22
Bending radius (m)	7.6	6.0		Gradient range (T/m)	0.3—10.0	0.3—7.0
Field range (T)	0.1–1.6	0.1–1.6		Bore diameter (mm)	170	240
Ramping rate (T/s)	0.1–0.4	0.1–0.4		Useful aperture (mm^2)	160×100	280×140
Air gap (mm)	80	84		ΔK/K	$\pm 1.5 \times 10^{-3}$	$\pm 1.5 \times 10^{-3}$
Useful aperture (mm^2)	140×60	220×70		Ideal length (m)	0.5, 0.65	0.65, 0.75
Homogeneity (ΔB/B)	$\pm 1.5 \times 10^{-4}$	$\pm 1.5 \times 10^{-4}$				
Vacuum. Chamber				Vacuum. Chamber		
Aperture (mm^2)	156×61	236×72		Aperture (mm^2)	180×110	285×150
Cross section	Rectangular	Rectangular		Cross section	Octagonal	Octagonal
Supply of dipole				Supply of quadruple		
Number	1	1		Number	30	22
Feeding mode	Series	Series		Feeding mode	Independent	Independent
Stability (at low cur.)	$\pm 1 \times 10^{-4}/8$h	$\pm 1 \times 10^{-4}/8$h		Stability (at low cur.)	$\pm 5 \times 10^{-4}/8$h	$\pm 5 \times 10^{-4}/8$h
Ripple (at low cur.)	5×10^{-5}	5×10^{-5}		Ripple (at Max. cur.)	3×10^{-6}	5×10^{-6}
Tracking precision	$\pm 3 \times 10^{-4}$	$\pm 3 \times 10^{-4}$		Tracking precision	$\pm 5 \times 10^{-4}$	$\pm 5 \times 10^{-4}$

of 8∼30 MeV/μ to increase the beam intensity. In CSRe, e-cooling will be used to compensate the growth of beam emittance during internal-target experiments or to provide high quality beams for the high-resolution mass measurements[6] of nuclei. Table 5.1.6 denotes the major parameters of the two e-coolers. The two coolers are the same with the only difference in the high voltage unit in order to reduce the time of development and the production cost of the devices.

Parameters	CSRm	CSRe
Ion Energy [MeV/u] Electron Energy [keV]	8-50 4-35	25-450 10-300
Electron beam current [A]	3 (1.0A@5.5keV)	
Cathode radius [cm]	1.25	1.25
Magnetic expansion factor	1- 4	1- 10
Max. field of gun region [kG]	2.4	5
Magnetic field of collector region [kG]	1.2	1.2
Magnetic field of cooling section [kG]	0.6-1.5	0.5-1.5
Length of cooling section [m]	4.0 effective length = 3.4m	4.0 effective length = 3.4m
Deflection angle of toroid [Deg.]	90 °	90 °
Deflection radius of toroid [m]	1.0	1.0

5.1.7 Project Status

In the summer of 2001 the building construction of CSR was finished and the injection beam line from HIRFL to CSRm was completed in the beginning of 2003. Several subsystems, two e-coolers, RF system, kickers, internal-target system and the Mg-jet monitors, are being designed and fabricated jointly by IMP and the Russian BINP. The major subsystems, magnet, power supply, vacuum chamber, control, beam diagnosis and so on, are being manufactured by several Chinese companies.

Reference

[1] B. W. Wei et al., HIRFL heavy ion cooler-storage ring proposal, Proc. of the Fifth China-Japan Joint Sym. on Acc. for Nuclear Sc. and Their App., Osaka, Japan, 1993, 162pp.

[2] J. W. Xia, et al., HIRFL-CSR Plan, Proc. of the 6th China-Japan Joint Symposium on Accelerators for Nuclear Science and Their App., Chengdu, China, Oct. 1996, 24pp.

[3] B. W. Wei, Results From Lanzhou K450 Heavy Ion Cyclotron, Proc. of 1989 Particle Acc. Conf., IEEE.

[4] Y. N. Rao et al., Lifetime of Ion Beam Stored in HIRFL-CSR, Proc. of the 14th Inter. Conf. on Cyclotrons and Their App., South Africa, 1995, 358pp.

[5] Y J. Yuan et al., Simulation of RF Stacking and Multiple Single-Turn Injection and Multi-turn Injection, Proc. of the 14th Inter. Conf. on Cyclotrons and Their App., South Africa, 1995, 479pp.

[6] B.Schlitt, Schottky Mass Spectrometry at the Heavy Ion Storage Ring ESR, GSI reports, DISS. 97-01, Se p. 1997.

[7] M.Umezawa, A new dipole bending magnet with improved magnetic field distribution, Proc. of the 11^{th} sym. on accelerator science and tech., Harima Science Garden city, 1999.

5.2 Ground Breaking for the Middle East Synchrotron Armenian Synchrotron

Time to Launch the African Synchrotron Research Programme

Sameen Ahmed Khan rohelakhan@hotmail.com

Jordan:

On 6 January 2003, King Abdullah of Jordan laid the cornerstone for the Middle East's *first* synchrotron known as SESAME: *Synchrotron-light for Experimental Science and Applications in the Middle East*. The ceremony took place in the presence of the UNESCO Director-General Koichiro Matsuura, members of the Jordanian government and international dignitaries including Werner Burkart, Deputy Director General of IAEA. Eight Founding Members have signed the statutes of SESAME and now form the *SESAME Council*, which will provide the annual operating budget. The founding countries are Bahrain, Egypt, Iran, Israel, Jordan, Pakistan, Palestine, and Turkey. Herwig Schopper was elected to continue as the President of the Council. SESAME Project was born in 1997 when Germany decided to decommission the fully functioning 800MeV BESSY-I synchrotron worth 60 million US$ and gift it to Middle East. The SESAME Project was put under the auspices of UNESCO in much the same way UNESCO assisted in the creation of CERN about half-a-century back. The *International Interim Council* met nine times since its formation in 1999, with assistance form several countries as *Observers*. The SESAME Council has replaced the Interim Council. Several non-Middle Eastern countries that were observers to the Interim Council (Armenia, Cyprus, France, Germany, Italy, Japan, Russia, Sweden, Switzerland, UK and USA) are expected to continue as Observers in the new Council. The remaining members of the Interim Council were: Greece, Morocco, Oman, and the United Arab Emirates who too will continue to participate. Kuwait is an Observer and Libya has requested to become one. More countries are expected to participate as full members or observers.

Entire BESSY-I was shipped to Jordan in June 2002. Now it is being upgraded in the range 2-2.5GeV. SESAME is located in Allaan, about 30Km from the Capital Amman. SESAME is expected to promote science and foster international cooperation. Planned research programmes include, structural molecular biology, molecular environmental science, surface and interface science, micro-electromechanical devices, X-ray imaging, archaeological microanalysis, materials characterization, and medical applications. Annual operating costs will be about US$3.5 million. With the continued progress it is expected that the research programs will start in 2007.

Armenia:

Armenia was envying to receive the BESSY-I from Germany, but Jordan was chosen to host the facility with Armenia as first runner-up. Then, Armenia switched its status from a full Member to an *Observer* and launched a campaign to build its own synchrotron, the CANDLE: *Center for the Advancement of Natural Discoveries using Light Emission*. CANDLE aims to build a 3.2GeV third-generation synchrotron from scratch in the Armenian capital Yerevan and is envisaged as an international regional facility. Americans of the Armenian decent have been very actively campaigning for the synchrotron facility in Armenia. Much of the credit for kindling CANDLE belongs to Iraqi-born Armenian-American 75-year-old property magnate in New Jersey. In 2002 the US Department of Energy awarded half a million US$ for the preparation of a Technical Design Analysis report for the CANDLE project. This report is under review by the National Science Foundation in Washington. Assuming a positive response, CANDLE may receive up to 15 million US$ as aid. If this funding is secured the construction can begin in 20004 and some of the planned fifty beamlines are expected to be operational by 2007. Construction of CANDLE is projected to be 48 million US$, with annual operating costs of 4 million US$. When constructed, CANDLE will be the only facility of its kind within a 2000km radius, serving numerous users from countries

of the former Soviet Union, parts of Europe, the Middle East and Asia.

Africa:

The continent of Africa is the only region, which is yet to even start its synchrotron programme. However, there is an excellent network of laser programmes across Africa. It would be relevant to mention the *African, Laser, Atomic, Molecular, and Optical Sciences Network* (LAM) operating under the directorship of Ahmadou Wagué. The LAM Network has 27 *Regional Coordinators* across Africa and *International Contacts* in 11 countries outside of Africa. The LAM has held six *International Workshop on Laser Physics and its Applications*, since May 1991.Another organization is the recently created *African Laser Center* (ALC). Both the organizations are working to promote the application of laser-based technologies in the fields ranging from environment to health care. The countries supporting these programmes include, France, Germany, Italy, Japan, Sweden and the USA. There are active and well organized Research Groups & Networks in a broad range of disciplines across Africa, which can definitely benefit immensely by employing synchrotrons. The question is not if Africa needs synchrotron radiation sources, but rather how to acquire these sources. It will be difficult for many of the fifty African countries to have synchrotron radiation sources of their own. It is essential to focus on the need to launch the *African Synchrotron Radiation Programme* (AfSRP), which shall assist in coordinating *African Participation* in SESAME and other synchrotron facilities all over the world. At the same time ASRP can play a pivotal role in creating SR facilities in Africa. Given the cost and the lead-time in designing a new facility, we need to start preparing straightaway. In few years the ASRP can evolve into an *African Synchrotron Radiation Facility* (AfSRF). This will eventually set a trend for several other disciplines such as *High-Energy Physics*, *Space Exploration*, *Fusion Research*, to name a few.

Further Reading:

[1] Sameen Ahmed Khan, **Jordan to host Middle East synchrotron**, *ICFA Beam Dynamics Newsletter*, **22**, 6-7 (August 2000).

[2] Sameen Ahmed Khan, **Synchrotron Radiation (in Asia)**, ATIP Report No. **ATIP02.034**, 28 pages (21 August 2002). (The Asian Technology Information Programme, Tokyo, Japan, 2002).

[3] SESAME Website: http://www.sesame.org.jo/

[4] CANDLE Website: http://www.candle.am/

[5] Susan M. Reiss, **Launching a New Laser Center in Africa**, *Optics & Photonics News*, **13** (4), 16-17 (April 2002); LAM Website: http://www.lamnetwork.org/

[6] African Scientific Network: http://www.physics.ncat.edu/∼michael/asn/

5.3 Spallation Neutron Source Front-End Recommissioning

A. Aleksandrov sasha@ornl.gov SNS Project, ORNL

(A. Aleksandrov and S. Henderson)

5.3.1 Introduction

The Spallation Neutron Source (SNS) accelerator system will deliver a 1 GeV, 1.44 MW proton beam to a liquid mercury target for neutron scattering research [1]. The SNS Project, a collaboration of six national laboratories (Argonne, Brookhaven, Jefferson, Lawrence Berkeley, Los Alamos and Oak Ridge) is expected to begin operations in 2006.

The Front-End System (FES) for the SNS accelerator, designed and built by LBNL, is a 2.5-MeV linac injector consisting of the following major subsystems: an rf-driven H- ion source, an electrostatic Low Energy Beam Transport line (LEBT), a 402.5 MHz RFQ, a Medium Energy

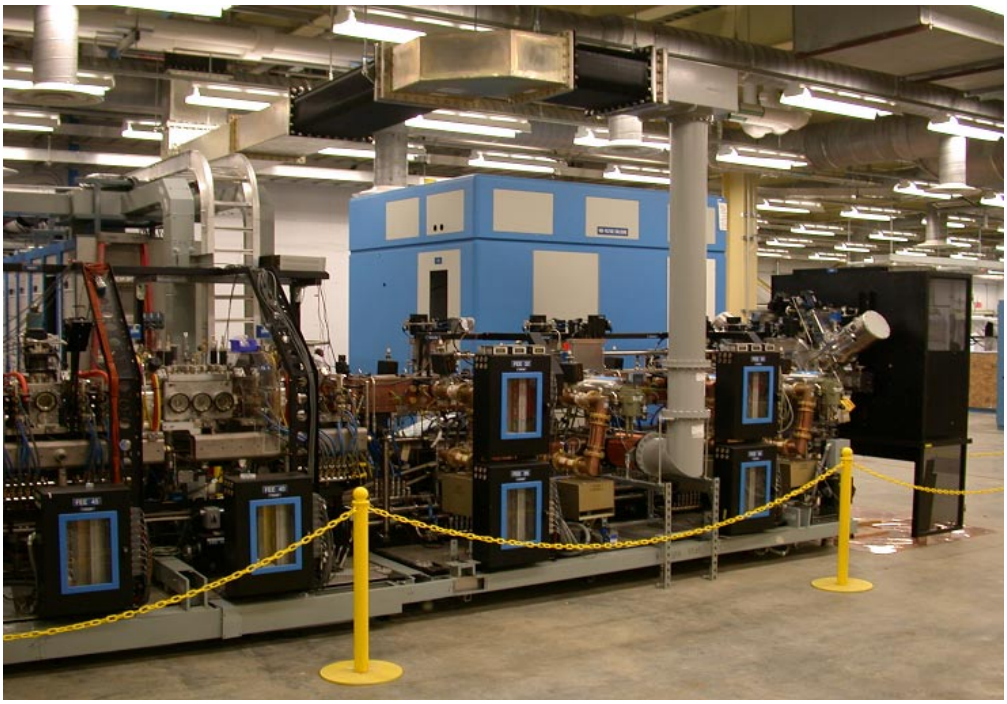

Figure 5.11: SNS Front End system installed in the Front End building at the SNS site in Oak Ridge.

Beam Transport line (MEBT), a beam chopper system and a suite of diagnostic devices [2]. The FES is required to produce a 38-mA pulsed current beam at 2.5 MeV with 6% duty factor and appropriate chopped beam structure with chopper on to off beam current ratio of 10^{-4}.

The FES was successfully commissioned at LBNL, where nominal beam output parameters were achieved [3].

5.3.2 Front End System Recommissioning at Oak Ridge

The FES was shipped to Oak Ridge and installed at the SNS site (Figure 1) in the summer of 2002. Extensive recommissioning at ORNL was performed in a two-month period ending January 31, 2003. A number of technical systems were new to the ORNL FES installation, namely the high-power RF, low-level RF and controls systems, and therefore were commissioned for the first time at ORNL. The Front-end recommissioning was an important milestone for the SNS project as it demonstrates the first accelerated beam on the SNS site and also marks the beginning of the 2 $^1/_2$ year phased commissioning program of the accelerator systems.

The primary beam parameter goals of peak current and transverse emittance were both achieved [4]. The maximum beam current achieved at the MEBT output was 51 mA , far exceeding the design specification of 38 mA. Figure 2 shows a typical commissioning beam pulse with approximately 17 mA peak current and 100 μsec width. Transverse normalized emittances at the MEBT output, measured in a variety of beam conditions, were less than the baseline specification of 0.3 π mm-mrad. A measured vertical emittance scan recorded at the design beam current of 38 mA is shown in Figure 3.

Two choppers are employed, one which chops the 65 keV LEBT beam, and another, shorter-risetime chopper in the MEBT whose function is to clean the edges of the beam gap left by the slower LEBT chopper. The design extinction ratio of the LEBT chopper of 1% was demonstrated,

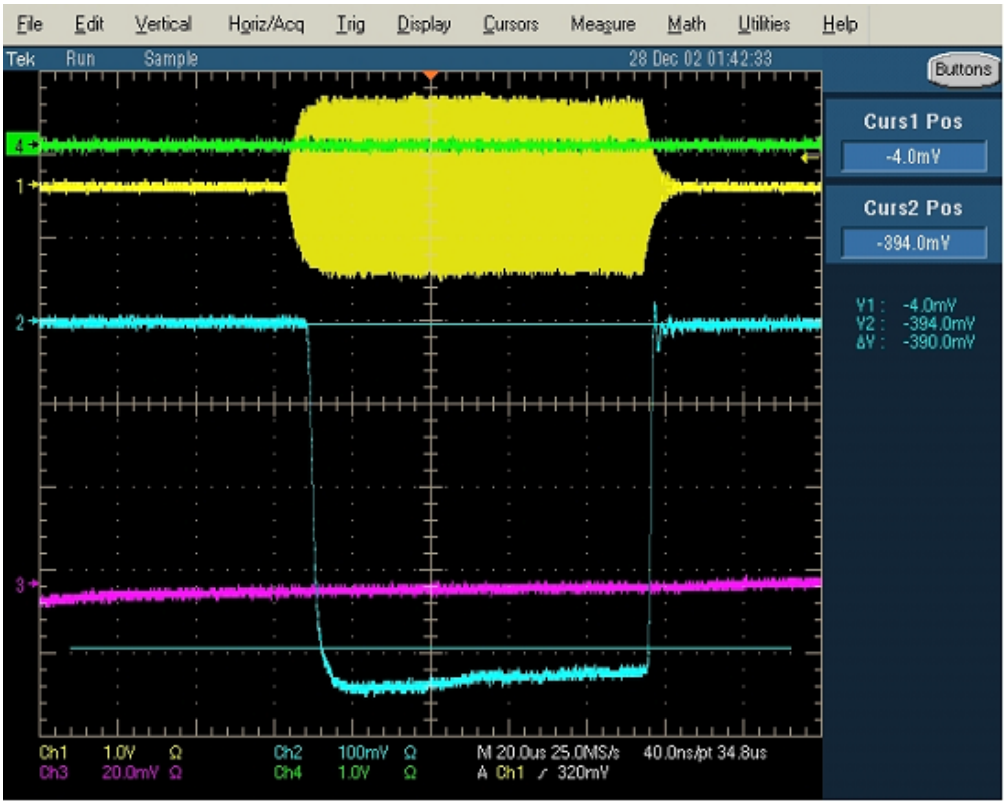

Figure 5.12: Oscilloscope snapshot of a beam pulse at the MEBT beam stop (lower trace), RFQ RF pulse (upper trace).

as shown in Figure 4. The MEBT chopper system, designed to achieve an extinction ratio of 10^{-4}, was not tested due to hardware difficulties.

The main beam parameter goals were achieved at reduced duty factor, typically 0.05-0.1%, limited administratively by hardware concerns. A maximum duty factor of 0.5% was achieved with full 1 msec pulse length but reduced repetition rate. The nominal 6% repetition rate was achieved during the FES commissioning at LBNL.

In addition, two novel diagnostic systems were successfully tested. A laser-based diagnostic [5] capable of performing both transverse profile measurements and Beam-In-Gap measurements was successfully deployed and tested. A dynamic range of 10^5 in beam intensity was measured [6]. Additionally, a prototype Fast Faraday Cup was tested and used to measure a bunch length of 140 psec at the MEBT output.

Following the completion of Front-End commissioning, two of the six Drift Tube Linac tanks will be installed in spring 2003, with commissioning studies of the Front-End and the first DTL tank beginning in the summer of 2003.

References

[1] Spallation Neutron Source (SNS), ICFA Beam Dynamics Newsletter, No. 21, pp.10-24

[2] R. Keller et al., “Progress with the SNS Front-End Systems,” Proc. PAC 2001.

[3] R. Keller et al., “Commissioning of the SNS Front-End Systems at Berkeley Lab,” Proc. EPAC 2002.

[4] A. Aleksandrov et al., “Commissioning of the SNS Front-End Systems at Oak Ridge,” to be presented at PAC 2003.

[5] S. Assadi et al., “The Spallation Neutron Source Diagnostics: Initial Integration and Com-

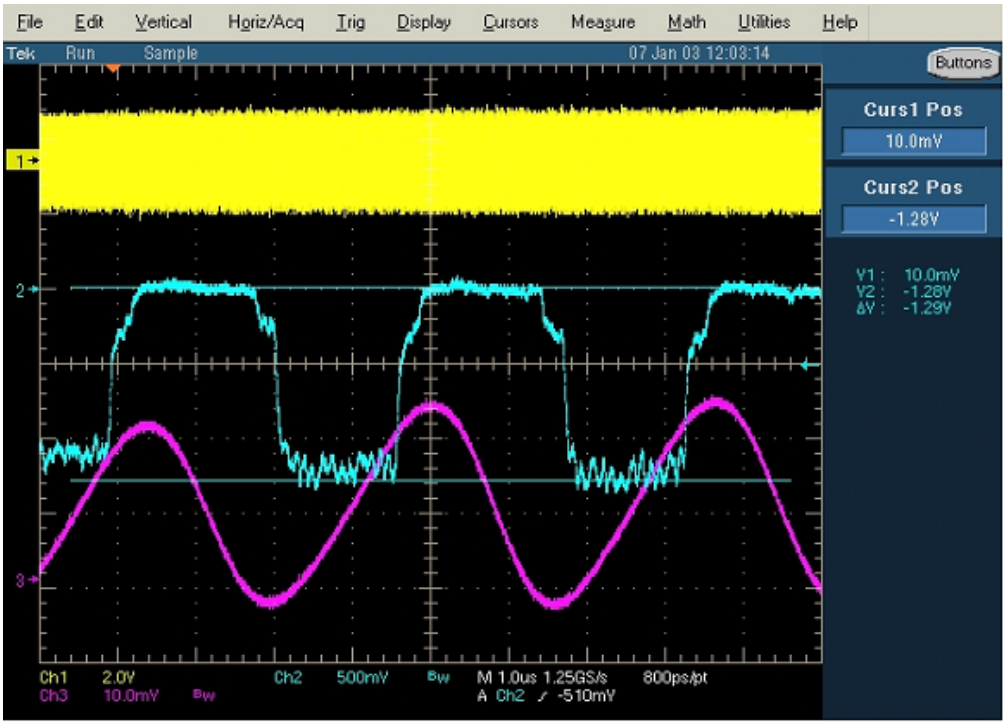

Figure 5.13: Measured transverse phase space at the MEBT exit.

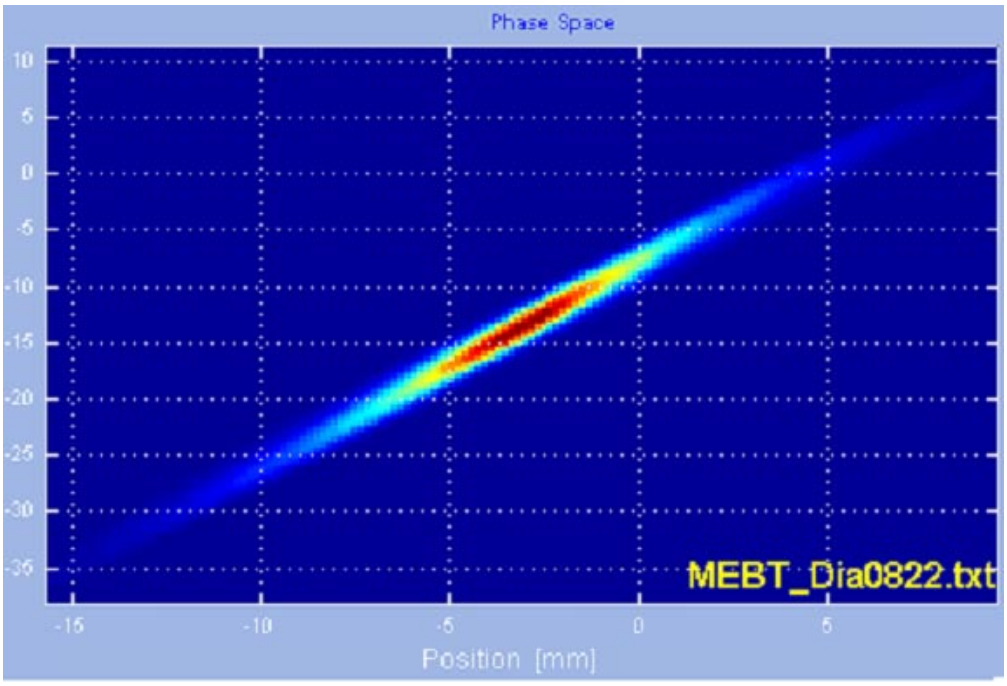

Figure 5.14: Oscilloscope snapshot of chopped beam at the MEBT beam stop (meander trace).

missioning Progress Report," to be presented at PAC 2003.

[6] A. Aleksandrov et al., "Beam in Gap measurements at the SNS Front-End," to be presented at PAC 2003.

5.4 Beam Dynamics Activity at Hiroshima University

Hiromi Okamoto okamoto@sci.hiroshima-u.ac.jp Hiroshima University, Japan

(H. Okamoto and A. Ogata)

The Beam Physics Group (BPG) at Hiroshima University was organized in October 1998, as a new group belonging to the Graduate School of Advanced Sciences of Matter (AdSM). Since then, efforts have been made to initiate various theoretical and experimental research programs of beam physics. BPG is now playing an important role in the Japanese beam-physics community [1]. In this report, the overview of recent research activities at BPG is presented.

5.4.1 Space-Charge-Dominated Beam Physics

5.4.1.1 Resonance analysis

We have explored the collective behavior of space-charge-dominated beams, employing approximate analytic approaches and multi-particle simulation codes. In particular, a systematic theoretical investigation of resonant beam instabilities has been performed for the last couple of years.

By solving the Vlasov-Poisson equations for a one-dimensional beam, we found that the beam becomes unstable when

$$\nu_c - \delta\nu_x < \nu_x < \nu_c + \delta\nu_x, \tag{5.1}$$

where ν_x is the depressed single-particle tune, $\nu_c = -[k_1 - k_2 + \nu_x B_0(m_1 F_{m_1 m_1} - m_2 F_{m_2 m_2})]/(m_1 - m_2)$, and $\delta\nu_x = 2\nu_x\sqrt{|m_1 m_2|}\,|B_{k_1-k_2}|\,|F_{m_1 m_2}|\,/\,|m_1 - m_2|$ (k_1, k_2, m_1 and m_2 are all integers) [2]. Here, B_n's are lattice-dependent Fourier coefficients, and $F_{mn} = -32/[(m-n)^2 - 1][(m+n)^2 - 1]$ for $m + n = \text{even}$ (otherwise, $F_{mn} = 0$). It has been demonstrated that this condition explains self-consistent multi-particle simulation results fairly well. In many cases, severe instability is caused by the coupling of $+m$ and $-m$ modes. Putting $m_1 = -m_2 = m(> 0)$ in Eq. (5.1), we obtain the resonance condition

$$\Omega_m \equiv m(\nu_0 - C_m \Delta\nu) = \frac{n}{2}, \tag{5.2}$$

where Ω_m is the tune of the mth-order coherent mode, ν_0 is the bare tune, $\Delta\nu = \nu_0 - \nu_x$, and C_m's are certain constants [3]. It is probably informative to mention that nonlinear collective resonances can be excited even without nonlinear external driving force, in other words, without magnetic field imperfections.

Resonance calculations for circulating two-dimensional beams have also been done numerically. Since we now have momentum dispersion, the contribution from closed-orbit distortion should be separated first in order to investigate the instability of pure betatron motion; denoting the dispersion function of nth order as $D_x^{(n)}$, we can write $x = \tilde{x} + \sum_{k=1}^{\infty} D_x^{(k)} W^k$ where x is the horizontal spatial coordinate of a particle, $\tilde{x}$ is the amplitude of the betatron oscillation about a specific closed orbit, and W is the energy deviation from its design value. The betatron Hamiltonian is

then given by

$$\begin{aligned}\tilde{H} &= \frac{\tilde{p}_x^2+\tilde{p}_y^2}{2}+\frac{1}{2}(K_x-K_{sc}\xi_{20})\tilde{x}^2+\frac{1}{2}(K_y-K_{sc}\xi_{02})\tilde{y}^2 \\ &\quad -\frac{K_{sc}\xi_{40}}{24}\left[\tilde{x}^4+4D_x^{(1)}W\tilde{x}^3+6(D_x^{(1)})^2W^2\tilde{x}^2\right]-\frac{K_{sc}\xi_{04}}{24}\tilde{y}^4 \\ &\quad -\frac{K_{sc}\xi_{22}}{4}\left[\tilde{x}^2+2D_x^{(1)}W\tilde{x}+(D_x^{(1)})^2W^2\right]\tilde{y}^2+\cdots, \end{aligned} \tag{5.3}$$

where we have assumed the same notation as used in Ref. [4]. Equation (5.3) strongly suggests the existence of *dispersive resonances*. We have actually confirmed, through particle-in-cell simulations, that such a novel resonance mechanism does affect the beam quality.

In order to improve the quality of a beam, we often introduce some cooling device in a storage ring. Since the tune is gradually depressed as the beam temperature becomes lower, the operating point may cross resonance stopbands. It is thus important to figure out whether a resonance can interrupt the cooling process. Systematic numerical simulations showed that the effective tune is locked at a low-order stopband if the cooling force is weak [5]. It is almost impossible to go beyond a wide second-order stopband even if the cooling force is considerably strengthened.

5.4.1.2 Proposal of trap experiments

The experimental exploration of space-charge effects is obviously a tough job to carry out. There are many practical reasons for that. For example, it is not easy to observe the dynamic behavior of a moving beam at a sufficient resolution in a non-destructive manner. We face many limitations not only because the beam is traveling at great speed but also owing to various noise sources that complicate measurement data. Besides, lattice parameters and initial beam conditions are not so flexible in general, which means that we cannot survey a wide range of parameter space. To overcome these difficulties, we proposed a new experimental scheme utilizing non-neutral plasma traps [6]. Two types of trap configurations, i.e. a radio-frequency quadrupole trap (Paul trap) and a solenoidal trap, were considered. The reason why these trap systems can be used for the study of charged-particle beams in accelerators is quite simple; a beam seen from the rest frame is almost equivalent to a single-species plasma in a trap [6, 7]. In fact, charged particles in a long Paul trap obey the Hamiltonian

$$H_{trap}=\frac{p_x^2+p_y^2}{2}+\frac{1}{2}K(\tau)(x^2-y^2)+\frac{q}{m_0c^2}\phi(x,y;\tau), \tag{5.4}$$

where q and m_0 are, respectively, the charge state and rest mass of the particles, the independent variable is $\tau = ct$ with c being the speed of light, and $K(\tau)$ is a periodic function proportional to the radio-frequency voltages applied to the electrodes. Clearly, Eq. (5.4) has the form identical to the well-known Hamiltonian of betatron motion in a linear transport system. Since the scalar potential ϕ satisfies the Poisson equation just like in the case of charged-particle beams, the trap system can reproduce collective phenomena equivalent to those in a beam transport channel. It is even possible to emulate the behavior of bunched beams with various aspect ratios by using segmented electrodes [8]. Needless to say, there are many advantages in trap experiments: First of all, a trap is much more compact and cheaper than an accelerator system and is completely free from radio-activation due to particle loss. Secondly, the observation of the plasma behavior can be done very easily because the plasma centroid is at rest in the laboratory frame. If we choose a proper species of ions and apply a laser, extremely high-resolution measurements become feasible since each ion emits photons. Thirdly, various fundamental parameters such as tune depression

are well controllable in a very wide range. By changing the pulse pattern of $K(\tau)$, we can imitate arbitrary lattice structures and can even give a controlled mismatch to the plasma [6, 8].

5.4.2 Phase Transition of Ion Beams

As already demonstrated experimentally, a single-species plasma confined in a trap system undergoes a sort of phase transition when it is exposed to a strong cooling force. At low-temperature limit, the plasma reaches a unique ordered state that is called a *Coulomb crystal*. Provided that the line density of the plasma is low, the resultant crystalline structure is the one-dimensional *string* where all particles are aligned along a straight line at the same intervals. By increasing the line density, we can transform it into the two-dimensional *zigzag* configuration and, eventually, into a three-dimensional *shell* configuration. Recalling the dynamical analogy between a trap and a beam transport channel as discussed in the last section, we expect that a similar phenomenon may take place even in a cooler storage ring. Molecular dynamic simulations have actually shown that it is possible to crystallize a fast stored beam, at least, in principle [9]. At BPG, the nature of this *crystalline beam* has been extensively studied. In a crystalline ground state, the trajectories of individual particles are strongly correlated; the transverse spatial coordinates of each particle in a coasting crystalline beam can be expressed as

$$x = C_x D_x(s), \qquad y = C_y D_y(s), \tag{5.5}$$

where D_x and D_y are periodic functions of the path length s while C_x and C_y depend on which particle we see [10]. The orbit functions D_x and D_y satisfy the coupled differential equations

$$\begin{cases} D_x'' + K_x(s)D_x - \dfrac{\alpha}{D_x + D_y} = \dfrac{1}{\rho}, \\ D_y'' + K_y(s)D_y - \dfrac{\alpha}{D_x + D_y} = 0, \end{cases} \tag{5.6}$$

where ρ is the local curvature of the design orbit and α is a constant proportional to the beam perveance. Equation (5.5) clearly indicates that the emittance of a crystalline beam is exactly zero. Note, however, that the thermodynamic temperature is generally non-zero owing to the breathing motion induced by alternating gradient focusing.

Provided that a longitudinal radio-frequency field is present, the motion of a crystalline beam becomes more complex due to the existence of momentum dispersion. Even a string crystal comes to exhibit an oscillatory behavior when it is bunched [11], whereas the single-particle coordinates (x, y, z) still satisfy formulae similar to Eq. (5.5); i.e. $x = C\hat{D}_x$, $y = 0$ and $z = C\hat{D}_z$, where C is a particle-dependent constant while $\hat{D}_x$ and $\hat{D}_z$ are s-dependent periodic functions universal among all particles.

To our best knowledge, laser cooling is currently the only means for us to reach a crystalline state, considering the acceptable thermal noise level. However, the dissipative force generated by a laser light has been known to operate only in the longitudinal direction of beam motion. In order to extend the powerful laser-cooling force to the transverse degrees of freedom, we have been testing the *resonant coupling method* [12]. It has been verified that the coupling scheme can significantly improve the transverse cooling efficiency [13]. For a further study of this three-dimensional laser-cooling scheme, we are now developing a new simulation code in which the realistic photon pressure can be taken into account.

The dispersive effect peculiar to a storage ring imposes a special demand upon the nature of cooling force for stabilizing crystals. Since the revolution frequencies of all particles forming a crystalline beam are identical, a longitudinal laser must provide such a cooling force as to give a

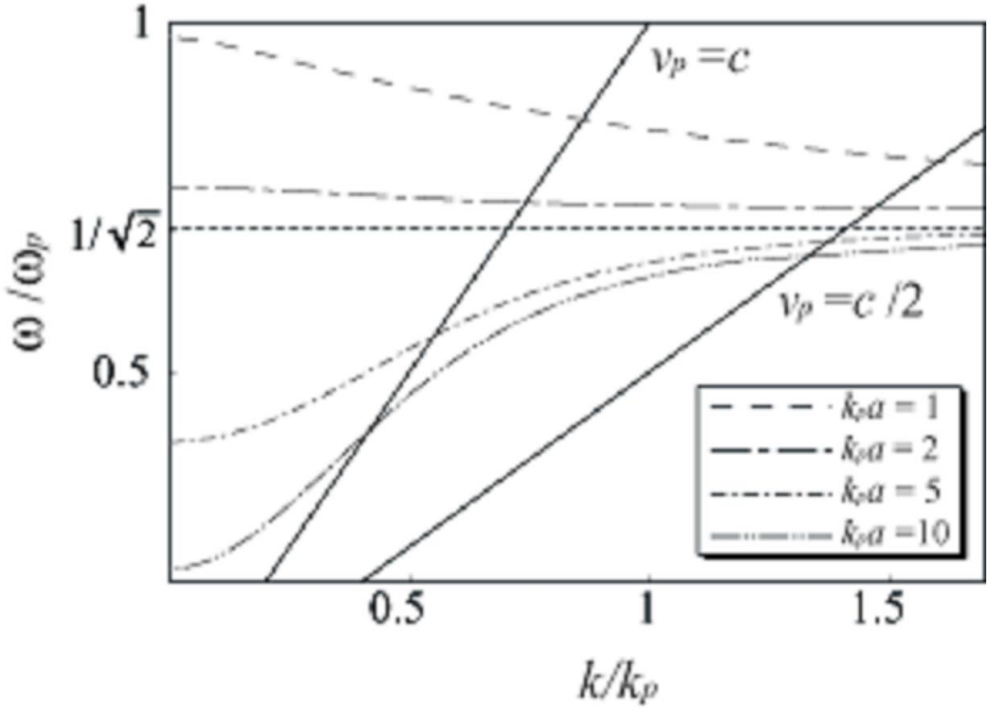

Figure 5.15: Dispersion diagram of plasmons.

greater average velocity to a radially outer particle. This is often referred to as *tapered cooling* [14]. If too powerful a conventional laser is applied, multi-dimensional crystalline structure could be destroyed because the *untapered* friction simply equalizes the longitudinal velocities of all particles. To develop a practical method for generating a tapered light seems to be the most important future issue toward our final goal.

5.4.3 Study of Compact Accelerators

It is over fifteen years ago that the idea of using solid structures for particle acceleration was discussed by several researchers [15]. Nevertheless, no proof-of-principle experiments have been performed yet. One primary reason is that the power source appropriate for this purpose is not available. Recently, we have considered the application of artificial macroscopic structures, instead of natural solids, such as a photonic band-gap crystal. The characteristic size of an accelerator structure can then be enlarged to the order of 1μm, much greater than the typical lattice constant of a solid [16].

An alternative, even simpler possibility is the use of a tiny cylindrical hole in a solid [17]. By injecting a laser light into the hole, we can excite strong *plasmons* along the inner surface if the aperture size is comparable to the laser wavelength. The potential of the plasmons can be utilized to accelerate charged particles [18]. The conversion efficiency of the laser power to the accelerating field is expected to be rather high; e.g., a MW laser should suffice for attaining a gradient of GeV/m level. This scheme is, in some sense, similar to laser wake-field acceleration in a hollow channel and also to a dielectric linac. However, the *plasmon linac* could supply a beam of nanometer in transverse size (though the attainable beam current would be low). Figure 5.15 shows the dispersion diagram of a typical plasmon linac whose aperture radius is a. ω_p is the plasma frequency and the corresponding wave number has been denoted by $k_p = \omega_p/c$. The frequencies

of all modes approach the surface plasmon-polariton frequency $\omega_p/\sqrt{2}$ as the wave number k increases. The two straight lines in the picture represent the dispersion of the accelerating waves whose phase velocities are $v_p = c$ and $c/2$. To accelerate an electron beam traveling nearly at the speed of light, we simply use a laser that has the frequency at the intersection between the plasmon dispersion curve and the $v_p = c$ line.

Suppose a plasmon linac made of silver. When $k_p a = 10$ and $v_p = c$, the required aperture radius and laser wavelength are, respectively, 227 nm and 344 nm. In this case, an acceleration gradient of 45.0 GeV/m is achievable with a 1 MW laser according to our estimate. The effective acceleration length is, however, only about 4.3 μm, which means that the total energy gain is less than 200 keV. This is basically due to the ohmic loss that raises the temperature of the linac and may eventually destroy the whole structure. One possible way to minimize this heating effect is to operate the linac in an extremely low-temperature atmosphere. At 10 K, for instance, the resistivity of silver becomes 1400 times smaller than that at room temperature. Consequently, the acceleration length and energy gain are increased to 6.1 mm and 273 MeV, respectively. Further, the power loss at $r = a$ could be kept below the damage threshold of silver unless the repetition rate is too high.

5.4.4 Laser-Matter Interactions

For the last several years, there has been growing interest in interactions between high-intensity lasers and matters. In particular, the generation of multi-MeV ions by the irradiation of a high-power ($>$ 10 TW), short-pulse ($<$ 1 ps) laser has attracted worldwide attention [19]. If an analogous effect is realizable by a laser of much lower power, that gives us a possibility of developing a compact ion source for diverse purposes. At BPG, we have been doing experiments in which very thin plastic and metal foils are irradiated with a relatively low-power laser (1 TW) having a pulse width (50 fs) shorter than hitherto experiments [20]. The wavelength and pulse frequency of our laser are 800 nm and 10 Hz. Two types of materials (mylar and aluminum) whose thickness are mostly less than 10 μm have so far been used as a target. It was found that the intensity threshold of ion generation is $10^{17}\mathrm{W}\cdot\mathrm{cm}^{-2}$ in the "forward" region (In what follows, we call the laser-illuminated side "backward" and the other side "forward"; see Fig. 5.16); particles produced below this threshold had no charge. By contrast, no such threshold was observed as to the particle generation toward the backward direction. The most energetic particles were usually protons in both directions, and the highest energy detected at the laser power of $10^{17}\mathrm{W}\cdot\mathrm{cm}^{-2}$ was about 550 keV. Figure 5.17 shows the dependence of the number of particles generated in the backward direction on the thickness of an aluminum foil. While the beams are largely composed of ions (especially protons) regardless of the foil thickness, we recognize that a weak signal from neutral particles is always present.

As far as we know, there has been no detailed report on the generation of neutral particles in laser-irradiation experiments. Our current understandings of this interesting effect are as follows [20]: 1) neutral particles are produced mainly in the forward direction, and the divergence angle is much less than that of ions, 2) there seems to be some connection between the origin of them and contaminants of the target surface, 3) the intensity of a neutral beam tends to increase as the target foil becomes thicker, 4) according to our spectroscopic data, hydrogen atoms are the most probable candidate; if we assume so, systematic measurements with CR39 track detectors suggest that the maximum energy is beyond 1 MeV. The mechanism of neutral-beam generation has not been understood yet.

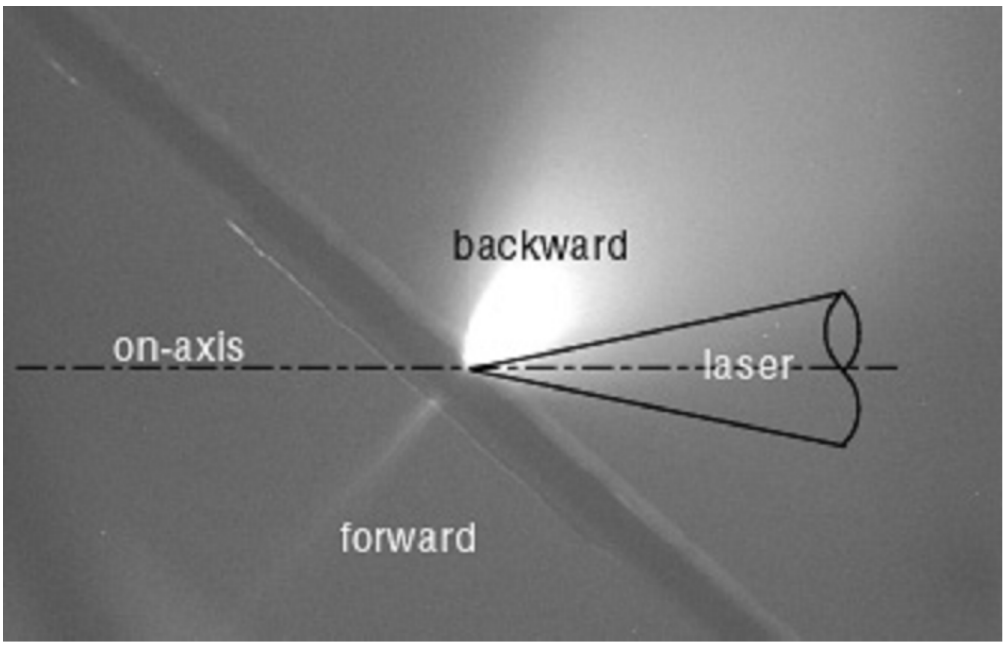

Figure 5.16: Photograph taken at the moment of laser irradiation to an Al foil of 3 μm in thickness. A laser is coming from the right side. The target foil is tilted by 45 degrees with respect to the laser axis.

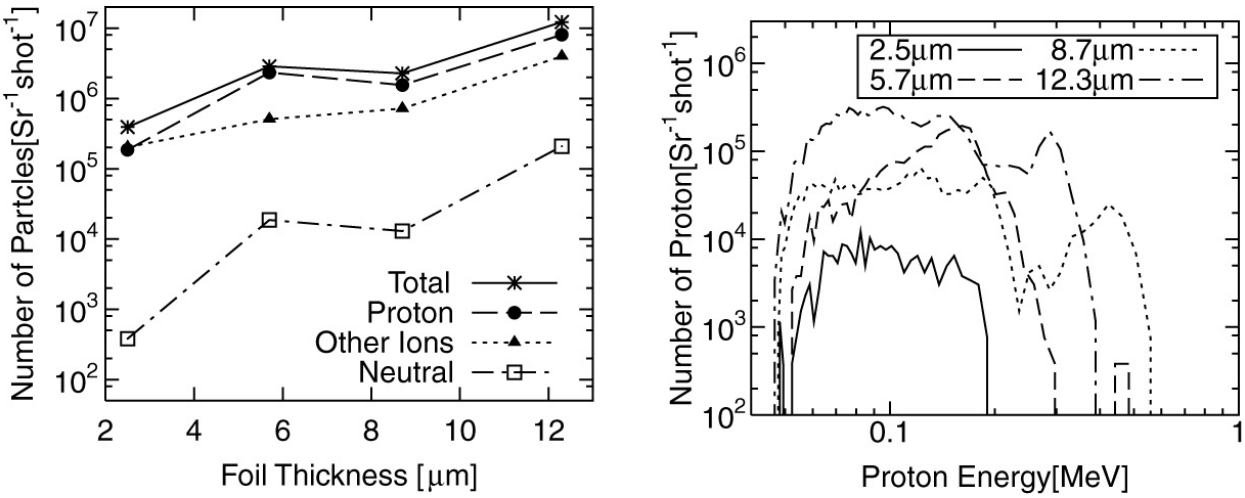

Figure 5.17: Dependence of the number of particles produced in the backward direction on the thickness of mylar foils. The intensity of the laser used in these experiments is $2 \times 10^{17} \mathrm{W} \cdot \mathrm{cm}^{-2}$.

References

[1] The homepage of the Japanese Beam Physics Club can be found at http://www-acc-theory.kek.jp/BP/BPclub.html (only in Japanese); See also: H. Okamoto, The Japanese beam physics club and its recent activities, *ICFA Beam Dynamics Newsletter* No.12 (1996) p.10.

[2] H. Okamoto and K. Yokoya, "Parametric resonances in intense one-dimensional beams propagating through a periodic focusing channel", Nucl. Instr. Meth. A482 (2002) p.51.

[3] Note that the famous coherent resonance condition given by Sacherer can be written as $\Omega_m = n$. Therefore, according to Eq. (5.1), we have, at least, twice as many resonance stopbands as he predicted.

[4] H. Okamoto and S. Machida, "Particle beam resonances driven by dispersion and space charge", Nucl. Instr. Meth. A482 (2002) p.65.

[5] K. Okabe and H. Okamoto, "Emittance limitation in cooled hadron beams", Hiroshima University Preprint HUBP-02/02 (2002), to be published in Jpn. J. Appl. Phys.

[6] H. Okamoto, "On dynamical analogy between linear beam transport channels and plasma trap systems", Hiroshima University Preprint HUBP-01/98 (1998); H. Okamoto and H. Tanaka, "Proposed experiments for the study of beam halo formation", Nucl. Instr. Meth. A 437 (1999) p.178.

[7] Later, the same idea was re-emphasized by Davidson et. al. in Phys. Plasmas 7 (2000) p.1020.

[8] H. Okamoto, Y. Wada and R. Takai, "Radio-frequency quadrupole trap as a tool for experimental beam physics", Nucl. Instr. Meth. A 485 (2002) p.244.

[9] J. Wei, X.-P. Li and A. M. Sessler, Phys. Rev. Lett. 73 (1994) 3089.

[10] H. Okamoto, "Single-particle orbit equation in crystalline beams", Phys. Plasmas 9 (2002) p.322.

[11] H. Okamoto, Y. Yuri and K. Okabe, "Oscillating Coulomb chain in a storage ring", Phys. Rev. E 67, 046501 (2003); Y. Yuri and H. Okamoto, "Effect of a longitudinal radio-frequency field on crystalline beams", J. Phys. Soc. Jpn. 71 (2002) p.1003.

[12] H. Okamoto, A. M. Sessler and D. Möhl, "Three-dimensional laser cooling of stored and circulating ion beams by means of a coupling cavity", Phys. Rev. Lett. 72 (1994) p.3977; H. Okamoto, "Transverse laser cooling induced through dispersion at an rf cavity", Phys. Rev. E 50 (1994) p.4982.

[13] T. Kihara et. al., "Three-dimensional laser cooling method based on resonant linear coupling", Phys. Rev. E 59 (1999) p.3594.

[14] J. Wei, H. Okamoto and A. M. Sessler, "Necessary conditions for attaining a crystalline beam", Phys. Rev. Lett. 80 (1998) p.2606; H. Okamoto and J. Wei, "Theory of tapered cooling", Phys. Rev. E 58 (1998) p.3817.

[15] T. Tajima and M. Cavenago, "Crystal x-ray accelerator", Phys. Rev. Lett. 59 (1987) p.1440; Chen and R. J. Noble, "Channeled particle acceleration by plasma waves in metals", in R.A. Calligan, Jr. and J. A. Ellisn (eds), Relativistic Channeling, Plenum, New York, (1987) p.517.

[16] A. Ogata, "Use of macroscopic solid structure in accelerators", to be published in Proc. 3^{rd} QABP Workshop.

[17] J. Takahara et al., "Guiding of a one-dimensional optical beam with nanometer diameter", Opt. Lett. 22 (1997) p.475.

[18] N. Saito and A. Ogata, "Plasmon linac", J. Plasma Fusion Res. 78 (2002) p.613.

[19] E. L. Clark et al., "Measurements of energetic proton transport through magnetized plasma from Intense Laser Interactions with Solids" Phys. Rev. Lett. 84 (2000) p.670 ; A. Maksim-

chuk et al., “Forward ion acceleration in thin films driven by a high-intensity laser”, Phys. Rev. Lett. 84, (2000) p.4108; R. A. Snavely et al., “Intense high-energy proton beams from petawatt-laser irradiation of solids”, Phys. Rev. Lett. 85 (2000) p.2945.

[20] Y. Wada, T. Kubota and A. Ogata, “Neutral beam generation by laser irradiation of thin foils”, in K. Nakajima and M. Deguchi (eds), Sciences of Superstrong Field Interactions, no.634 in AIP Conf. Proc. (2002) p.329.

5.5 ORBIT: Beam Dynamics Calculations for High-Intensity Rings

Jeffrey A. Holmes holmesja1@ornl.gov Oak Ridge National Laboratory

(J.A. Holmes, S. Cousineau, V. Danilov, S. Henderson, A. Shishlo, ORNL, Oak Ridge, TN 37831, USA; Y. Sato, Indiana University, Bloomington, IN 47405, USA; W. Chou, L. Michelotti, F. Ostiguy - FNAL, Batavia, IL 60510, USA)

5.5.1 Overview

High-intensity proton rings are characterized by low energy, high intensity beams, and by low loss requirements. Satisfying the beam-loss requirements necessitates a detailed understanding of beam dynamics in this regime. At high intensity, collective effects due to space charge and wakefields strongly affect the beam behavior, and single particle models do not suffice. Also, because of the complexity of collective phenomena for bunched beams in high-intensity rings, a computational approach is productive for theoretical studies and indispensable in solving detailed design and engineering problems.

Recognizing this, the SNS Accelerator Physics Group at ORNL, with help from colleagues at BNL, undertook the development of an object-oriented general-purpose code, ORBIT [1,2]. More recently, accelerator physicists at Fermilab have joined in to the ORBIT development. ORBIT began as a C++ rewrite of ACCSIM [3], developed under the SuperCode driver shell [4], but has since undergone extensive independent development, which will be described here.

ORBIT is a computer code designed specifically for beam dynamics calculations in high-intensity rings. Its intended use is the detailed simulation of realistic accelerator problems, although it is equally applicable to idealized situations. ORBIT is a particle-in-cell tracking code in 6D phase space that transports bunches of interacting particles through a series of nodes representing elements, dynamic effects, or diagnostics that occur in the accelerator lattice. ORBIT has been designed to simulate real machines: it has detailed models for strip-foil injection including painting, scattering, and nuclear processes; RF focusing and acceleration; transport through various magnetic elements; alignment and field errors, closed obit calculation, and error correction; longitudinal and transverse impedances; longitudinal, transverse, and three-dimensional space charge forces; feedback stabilization of instabilities; beam-in-gap cleaning, collimation, and limiting apertures; and the calculation of many useful diagnostic quantities.

Recent improvements include an interface to the BEAMLINE/MXYZPTLK library of accelerator maps; an in-code set of symplectic single particle trackers, including a hard edge fringe field model; the error, closed orbit, and correction models; the feedback model; and the inclusion of energy loss and nuclear processes in the foil stripping model. As with all ORBIT modules, these new models have been benchmarked against both analytic tests and other computer calculations. An electron cloud model is currently under development.

ORBIT is an object-oriented code, written in C++ with a scripting interface to facilitate interactive programming. Its basic classes are herds, which are groups of particles, and nodes, which

operate on the herds. A conversion of the SuperCode scripting interface to the standard scripting language, Python, is nearly complete. ORBIT supports parallel computing using MPI. The ORBIT code is an open source, powerful, and convenient tool for studying beam dynamics in high-intensity rings.

5.5.2 ORBIT Models

The equations used to transport particles in ORBIT are derived from a Hamiltonian formulation using the usual accelerator expansion. The horizontal direction is represented by x and p_x, the vertical direction by y and p_y, and longitudinal phase space by the phase angle ϕ and the energy deviation dE from a specified closed orbit reference particle. The independent variable is the machine location s.

The original ORBIT constructed lattices by reading output files from MAD [5] or DIMAD [6], by direct specification, or by specifying a uniform focusing channel. None of these methods is symplectic above the first order. While these capabilities still exist, two approaches to provide symplectic nonlinear transport have been completed. The first is the development of an in-code collection of Teapot-style symplectic maps for drifts, bends, quadrupoles, multipoles, and solenoids. These maps, which can be invoked with or without hard edge fringe fields, have been benchmarked against independent MathCad calculations and, for some cases, against UAL [7]. The second approach has been the creation of an interface to the powerful BEAMLINE/MXYZPTLK library of accelerator maps [8].

ORBIT now contains a complete set of magnet alignment and field error routines. These have been benchmarked against independently programmed MATLAB models. Errors can be applied either to individual or to selected sets of elements. In conjunction with the development of the error package, a closed orbit calculator has been added to ORBIT along with two new classes of nodes, BPM nodes and dipole corrector nodes. BPM nodes are diagnostic calculators that provide the horizontal and/or vertical beam centroid values over specified longitudinal portions of the beam. Dipole corrector nodes are simply thin lens kickers that are connected to an optimizer. The optimizer adjusts the dipole corrector kick strengths to minimize the BPM node signals in a least squares sense. The routine has been tested and found to work well, but the resulting improvement of beam quality depends on the number and placement of corrector nodes.

ORBIT can inject particles turn-by-turn or utilize a complete distribution specified at the start. A variety of distributions can be generated internally. Any externally generated distribution can also be read in. Injection painting is treated with user-defined time-dependent closed orbit bumps. ORBIT contains an injection foil model that keeps track of foil hits and applies transverse kicks based on multiple Coulomb scattering. A recent improvement to the foil model involved the incorporation of energy loss and nuclear elastic and inelastic scattering. These models were taken from the ORBIT collimation routines described below. Particles that miss the foil at injection, undergo nuclear inelastic scattering, or slow to kinetic energies below 20 MeV are removed from the beam.

The RF cavity model provides longitudinal kicks based on a specified time-dependent waveform with multiple harmonics. For nonaccelerating cases, the synchronous phase is assumed to be zero, and only the harmonics and time-dependent voltages need to be specified. For accelerating cases, the harmonics, voltages, and time-dependent dipole fields must be specified. The model uses this information to calculate the synchronous phase and the resulting kicks. The transverse phase space is also adjusted to conserve normalized emittance.

The 2.5D space charge model is implemented as a series of kicks separated by other transport operations. Particles are binned in a 2D rectangular grid using a second order distribution scheme. The potential for the distributed charges is then solved on the transverse grid using a fast FFT

solver. Conducting wall (circular, elliptical, or rectangular beam pipe) boundary conditions are then imposed using a method described in Ref. [9]. Particle kicks are obtained from second order interpolation of the potential, completing what might be called a "quasi-symplectic" evaluation. Finally, the kicks are weighted by the local longitudinal density to account for bunch factor effects; this is the reason we call the model 2.5D. There is also an alternative direct force (momentum-conserving) solver without beam pipe that uses a method described in Ref. [10].

The 3D space charge model is a simple generalization of the 2.5D routine. Particles are distributed to a 3D rectangular grid using a second order scheme. Typically, for rings, the longitudinal spacing greatly exceeds the transverse spacing. The potential is solved as a 2D problem using the distributed charges and fast Fourier transforms on the transverse grid for each longitudinal slice. Conducting wall boundary conditions (circular, elliptical, or rectangular beam pipe) are used to "tie together" the transverse solutions into a 3D potential. Particle kicks are obtained by interpolating the potentials in 3D using a second order "quasi-symplectic" interpolation scheme.

ORBIT treats longitudinal impedances and/or space charge in a fashion similar to ESME [11]. The longitudinal impedance is represented in terms of harmonics of the fundamental ring frequency. Particles are binned longitudinally and the binned distribution is Fourier transformed. The space charge contribution to the impedance is combined with the external impedance. The Fourier transformed distribution is multiplied by the impedance to give the longitudinal kicks to the particles. For many rings, the synchrotron period is much longer than a turn, and it is sufficient to evaluate the longitudinal impedance and space charge kicks once each turn. More frequent evaluations may be required for rings having higher synchrotron frequencies.

Transverse impedances are also treated as localized nodes in ORBIT. The validity of this approach requires the element length to be short compared to the betatron oscillation wavelength. Otherwise, multiple impedance nodes are required. As with the longitudinal impedance, the transverse impedance is represented by its Fourier components, but now the appropriate frequencies are the betatron sidebands of the ring frequency harmonics. For both impedance models, the formulation incorporates velocities below the speed of light. Particle kicks are obtained by convolution of the beam current dipole moment with the impedance. In evaluating the beam current it is assumed that the dipole moment evolves from the previous turn through a simple betatron oscillation.

The feedback stabilization routine monitors the transverse beam moments at specified locations over a selected number of turns and applies corrective kicks based on a specified gain. The model has been successfully applied to demonstrate the stabilization of an instability due to a model extraction kicker impedance in the SNS.

Circular, elliptical, rectangular, or racetrack apertures are defined in ORBIT. The apertures can be set either to allow particles to pass through and simply tabulate the hits, or to remove the particles from the beam and tabulate the loss locations.

ORBIT contains a detailed collimation model. Collimator shapes include the aperture shapes, single or multiple edges at arbitrary angles, and also a rectangular plate collimator that can be used for beam windows or foils. The physics includes multiple Coulomb scattering, ionization energy loss, nuclear elastic and inelastic scattering, and Rutherford scattering for a number of materials. The cross sections in the model are energy dependent, but no account is taken of showers of secondary particles or radiation. Monte Carlo algorithms are used for particle transport inside the collimator, and step sizes are carefully adjusted near collimator boundaries. There is also a beam-in-gap cleaning model consisting of fixed small amplitude kickers with programmable sequences of polarity. By properly programming the polarity sequences of the kickers, the beam-in-gap can be resonantly cleaned.

A list of useful diagnostics in ORBIT includes the following: dumps of particle coordinates, tunes, or emittances at any point/node in the ring; histograms of particle distributions in x, y,

phi, and emittance; rms emittances or beam moments versus turn or versus position; statistical calculation of beta functions; longitudinal harmonics of the beam centroid, and dumps of positions and times of lost particles. Because of the recent development of 3D models in ORBIT, we have extended many of our diagnostics to act as functions of longitudinal position.

The present emphasis in ORBIT code development is on completion of the conversion of the ORBIT user interface and driver shell from SuperCode to Python. This work has been mostly completed, using the boost.python library, but some details remain to be treated. Because of all the recent code developments it is also necessary to substantially revise the ORBIT documentation, and this is planned for the near future.

5.5.3 ORBIT Applications

ORBIT has been applied to a variety of problems associated with high intensity rings. Among the basic ring physics problems that have been studied using ORBIT are halo growth due to the parametric resonance [12], emittance exchange due to intrinsic space charge coupling resonances [13], the integer envelope resonance [14], comparison of longitudinal and transverse impedance stability thresholds with analytic calculations [15], and transverse impedance induced halo growth [16]. Extensive application has been made in the design and analysis of the SNS Ring. ORBIT has been used to study and optimize injection painting schemes; to examine the effects of space charge and impedances on losses; to determine stability limits posed by ring impedances; to study the option of an SNS synchrotron; to aid in design of the collimation and beam-in-gap cleaning systems; to demonstrate a potential feedback stabilization kicker; and to conduct a ring fault analysis. The results of a number of these studies, particularly the ring impedance, collimation, and beam-in-gap calculations had a strong influence on the SNS Ring design. ORBIT has also been successfully applied to a number of other rings including the CIS at Indiana University and PSR at Los Alamos National Laboratory. In the PSR studies, ORBIT obtained systematic agreement with measured beam profile broadening due to space charge over a wide range of parameter values [14]. Because of the understanding of PSR beam dynamics gained with the use of ORBIT, correction of the n=4 lattice harmonic, which is the driving term behind the beam broadening, is under study. ORBIT was used to study space charge effects at injection in the Fermilab Proton Driver Study II [17]. More recently, ORBIT is being applied to study space charge effects during injection into the Fermilab Booster Ring. This study is of importance because the Booster is the intensity bottleneck in the Fermilab accelerators, and because a significant fraction of the losses in the Booster occur during the first three milliseconds.

In addition to the Booster calculations, recent applications of ORBIT focus on the use of the new and computationally demanding physics modules to study and reoptimize injection scenarios as realistically as possible in the SNS Ring. Basic among these studies will be a foil to target simulation of the entire injection, accumulation, and ring to target transport. This simulation will actually consist of a whole series of calculations to differentiate and understand the effects of different model assumptions for foil scattering, single particle transport, fringe fields, errors and error correction, space charge, impedances, and collimation. In addition to all these variations, we are interested in optimizing the injection with respect to losses and beam-on-target, which requires varying the painting scheme, lattice tunes, chromaticities, and collimation scraper settings.

These SNS Ring studies have already begun. Initially we consider the SNS lattice with bare tunes (ν_x, ν_y) = (6.23,6.20), no chromaticity correction, and 1.44 MW beam power, which corresponds to final injection charge of 1.5*10^{14} particles. One of the first tasks was to determine the computational requirements imposed by convergence of the space charge model. For the SNS Ring, with bunch length in excess of 160m and slow longitudinal variation in longitudinal den-

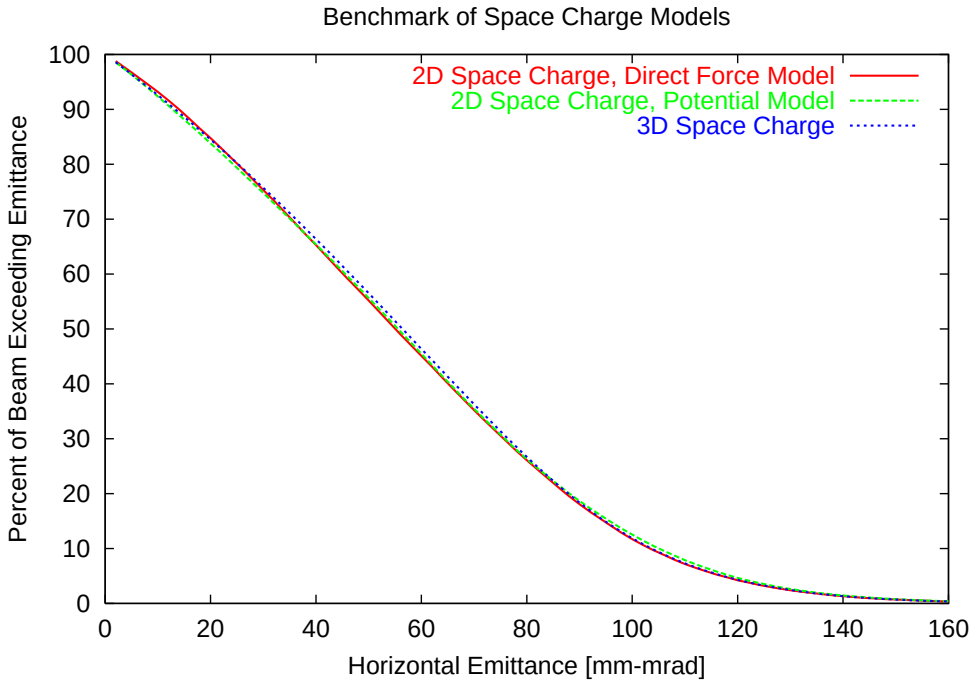

Figure 5.18: Percentage of beam with emittance exceeding the value indicated for the 2.5D direct force solver (red) with 159000 particles, the 2.5D potential solver (green) with 530000 particles, and the 3D solver (blue) with 1590000 particles.

sity, we anticipate that the 2.5D transverse and separate longitudinal space charge model will be accurate unless transverse impedance effects become important. The space charge convergence tests were conducted with the transverse impedance set to zero. For all three space charge models, the grid resolution and the number of particles were varied until convergence was achieved. The resulting grid sizes and numbers of particles were 64x64 mesh and 159000 particles for the 2.5D direct force space charge solver, 256x256 mesh and 530000 particles for the 2.5D potential space charge solver, and 256x256x64 mesh and 1590000 particles for the 3D solver. The difference in requirements between the 2.5D direct force and potential solvers is a result of the necessity of taking a derivative to obtain the force when the potential solver is used. Even with these parameters, the 3D solver is not fully converged, but significantly larger calculations are prohibitive on locally available resources. Figure 5.18 shows the horizontal emittance profiles of the final accumulated beam for the converged cases of the three space charge models, and it is clear that unless the transverse impedance generates instabilities that necessitate a 3D treatment, either of the 2.5D models is adequate.

In order to determine if the 3D space charge treatment is necessary, the transverse impedance was set to that of the ring extraction kicker, which is the dominant impedance in the ring, and a 3D space charge calculation was conducted. The results indicated transverse stability at 1.44 MW, so the 2.5D direct force transverse space charge model was the choice for further studies. Figure 5.19 shows the transverse beam distribution at the end of injection. In this calculation, the 2.5D transverse space charge model was employed using a 128x128 mesh and 159000 particles. The calculation was carried out using the in-code symplectic tracker with hard edge fringe fields, longitudinal space charge, and the longitudinal impedance of the extraction kicker and the RF cavities. It should also be mentioned that the parameters of the correlated injection painting scheme

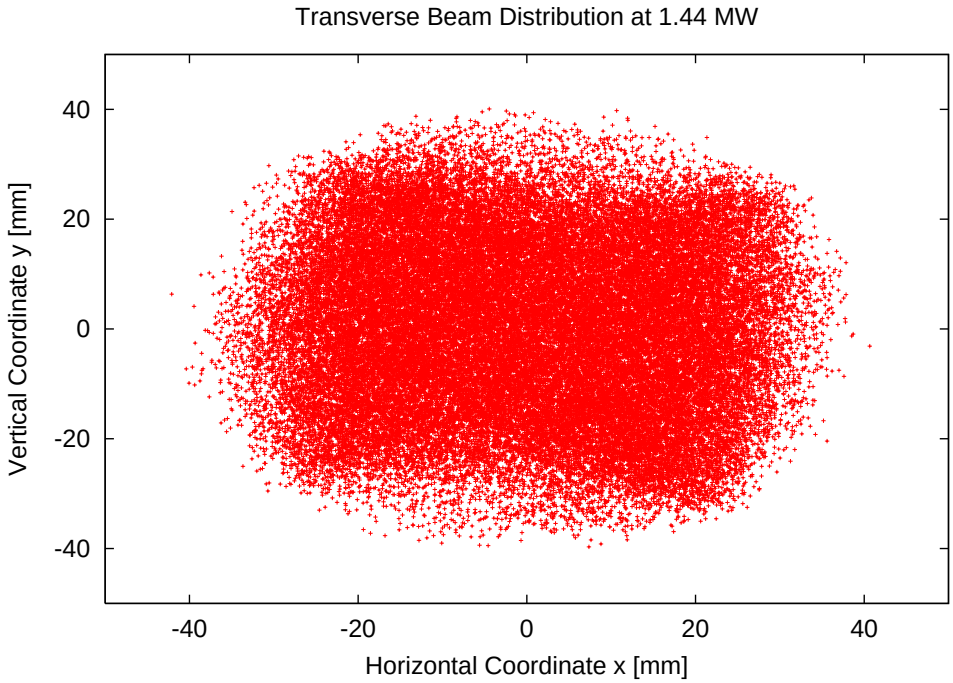

Figure 5.19: Transverse beam distribution at the end of accumulation for 1.44 MW beam power.

were adjusted to give an optimal beam profile at 1.44 MW.

Such results were used to determine the placement of the adjustable collimation beam scrapers to collect at most 1.0*10^{-3} of the beam in a controlled fashion, thus preventing uncontrolled beam loss. With placement of the primary scrapers at 140-162 pi-mm-mrad, less than 1.0*10^{-4} of the beam is scraped in this case, but collimation efficiency for the scraped beam is above 90%. Figure 5.20 shows the results of a power deposition calculation, using the ORBIT collimation package, for losses around the ring due to collimated beam. Because such a small portion of the beam was lost in the dynamic calculation, this collimation calculation was carried out by artificially forcing emittance growth to generate beam/scraper interaction. The power deposition scale is based on a normalization of 1.0*10^{-3} of the 1.44 MW beam impacting the scrapers. The results here show that the SNS collimation system collects about 90% of the scraped beam as controlled loss.

Another important consideration is the beam footprint on the target. Engineering considerations require at least 90% of the beam to land in a 20cm x 7cm rectangle on the target face with a maximum current density not exceeding 250mA/mm^2. We use ORBIT to transport the final accumulated beam through the Ring to Target Beam Transport line and through the target window, modeled as a solid 4mm steel collimator, and finally to the target. Figure 5.21 shows a contour plot of the beam current on target as calculated by ORBIT. For this case, 94% of the accumulated beam falls into the 20cm x 7 cm rectangle and the peak beam current is 248mA/mm^2.

We are now extending this initial work to include a comprehensive study of alignment and field errors in bends and quadrupoles. We expect this to lead to greater beam losses than in the initial calculations presented here. The plan is to examine these losses and then to apply the correction module to reduce the losses. As these studies progress, they will be expanded to other working points, to higher beam intensities as well, and to other injection schemes, such as round beams.

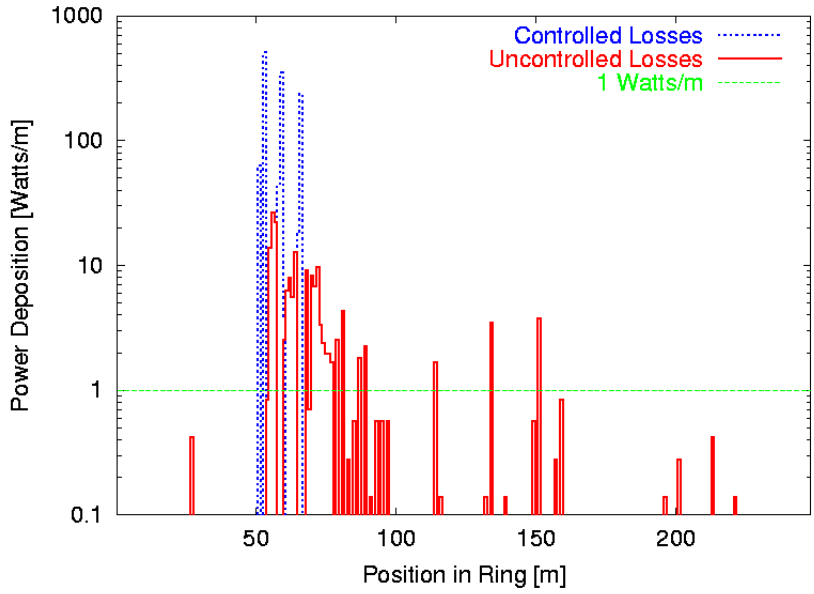

Figure 5.20: Controlled and uncontrolled beam losses in the SNS Ring, as calculated by the ORBIT collimation model.

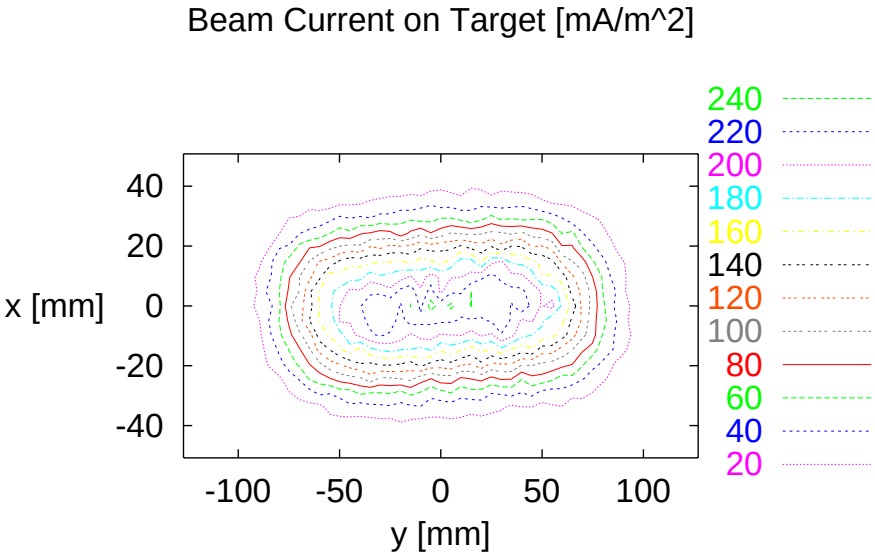

Figure 5.21: Beam current on target as calculated by ORBIT.

5.5.4 Open Code

Finally, we emphasize that ORBIT is an open code. An up to date version of the source code can be obtained upon request from Jeff Holmes (jzh@ornl.gov), and a user manual, instructions for building ORBIT, and some simple examples are available at

http://www.sns.gov//APGroup/Codes/Codes.htm.

The information on the web site is out of date, but we plan to rectify this over the coming months.

Acknowledgement

We wish to acknowledge the assistance of a number of collaborators and contributors during the development of ORBIT. These include J. Abrams, J. Beebe-Wang, M. Blaskiewicz, S. Bunch, A. Fedotov, J. Galambos, F. Jones, SY Lee, A. Luccio, R. Macek, J. MacLachlan, J. Wei, and K. Woody.

SNS is managed by UT-Battelle, LLC, under contract DE-AC05-00OR22725 for the U.S. Department of Energy. SNS is a partnership of six national laboratories: Argonne, Brookhaven, Jefferson, Lawrence Berkeley, Los Alamos, and Oak Ridge.

References

[1] J. Galambos, J. Holmes, D. Olsen, A. Luccio, and J. Beebe-Wang, ORBIT Users Manual, http://www.sns.gov//APGroup/Codes/Codes.htm

[2] J. Galambos, S. Danilov, D. Jeon, J. Holmes, D. Olsen, J. Beebe-Wang, and A. Luccio, in Proceedings of the 1999 Particle Accelerator Conference, (New York, 1999) 3143.

[3] F. Jones, Users' Guide to ACCSIM, TRIUMF Design Note, TRI-DN-90-17 (1990), http://www.triumf.ca/compserv/accsim.html

[4] S. W. Haney, Using and Programming the SuperCode, http://www.sns.gov/APGroup/Codes/Codes.htm

[5] H. Grote and F. Christoph Iselin, The Mad Program, Version 8.19, User's Reference Manual, CERN/SL/90-13, (Geneva, 1996).

[6] See ftp://csftp.triumf.ca/pub/CompServ/dimad/

[7] N. Malitsky, http://www.ual.bnl.gov/

[8] L. Michelotti, MXYZPTLK and BEAMLINE: C++ Objects for Beam Physics, AIP Conf. Proc. No. 255 (Proc. Advanced Beam Dynamics Workshop on Effects of Errors in Accelerators, Their Diagnosis and Correction, Corpus Christi, Texas, 1992.

[9] F. W. Jones, in Proceedings of the 2000 European Particle Accelerator Conference, (Vienna, 2000) 1381.

[10] R. W. Hockney and J. W. Eastwood, Computer Simulation Using Particles, Institute of Physics Publishing (Bristol: 1988).

[11] J. A. MacLachlan, Longitudinal Phase Space Tracking with Space Charge and Wall Coupling Impedance, Fermi National Accelerator Laboratory, FN-446, (1987).

[12] J. A. Holmes, V. V. Danilov, J. D. Galambos, D. Jeon, and D. K. Olsen, *Phys. Rev. Special Topics – AB* **2,** (1999) 114202.

[13] A. V. Fedotov, J. A. Holmes, and R. L. Gluckstern, *Phys. Rev. Special Topics – AB* **4,** (2001) 084202.

[14] S. Cousineau, J. Holmes, J. Galambos, A. Fedotov, J. Wei, and R. Macek, submitted to *Phys. Rev. Special Topics – AB*.

[15] K. Woody, J. A. Holmes, V. Danilov, and J. D. Galambos, in *Proceedings of the 2001 Particle Accelerator Conference*, (Chicago, 2001).

[16] V.Danilov, J. Galambos, and J. Holmes, in *Proceedings of the 2001 Particle Accelerator Conference*, (Chicago, 2001).

[17] G.W. Foster, W. Chou, E. Malamud, "Proton Driver Study II (Part 1)," Fermilab-TM-2169, (2002).

5.6 UAL Open Source Project

Nikolay Malitsky malitsky@bnl.gov Brookhaven National Laboratory

Richard Talman talman@lns61.tn.cornell.edu Cornell University, Ithaca, New York, USA

5.6.1 Introduction

Unified Accelerator Libraries (UAL[1]) software has been introduced as an open accelerator simulation environment providing support for many-to-many associations between diverse accelerator algorithms and diverse accelerator applications. Recently, UAL has been successfully applied to the development and study of the SNS Ring realistic beam dynamics model[2][3][4] including a complex combination of several physical effects and dynamic processes (such as injection painting, field errors, space charge effects, impedances, fringe fields, misalignments, etc.). The SNS and previous applications have confirmed the major UAL conceptual solutions and have encouraged us to transform this software into an Open Source project[5]. The major efforts have been releasing documentation and consolidation of UAL modules based on the Accelerator Propagator Framework (APF)[6]. At this time, the documentation encompasses User Guide[7], API specification of C++ classes, Perl User interface, and a collection of feature-illustrating examples. Also APF has been implemented to enhance the UAL infrastructure by providing a uniform mechanism for development and integration of accelerator algorithms. The key part of this approach is the Accelerator Propagator Description Format (APDF) that provides physicists a mechanism for switching among simulation models within their applications.

5.6.2 SNS Ring Application

The need to reduce beam losses to parts per ten thousand in the SNS high intensity proton accelerator complex have introduced a new level of requirements and expectations for beam dynamics studies. Realistic predictions at this level of precision demand a close reproduction of a complex combination of effects and dynamic processes in the accelerator simulation model. To address these tasks, the SNS Ring Accelerator Physics Group developed the SNS Ring package based on the UAL simulation environment[5]. Topics to which the package has been applied include:

- optimization of injection painting schemes;

- nonlinear effects arising from kinematics terms, magnet imperfections, and fringe fields;
- dynamic aperture and diffusion map studies;
- effect of space charge during transverse painting;
- tune spreads from space charge, chromaticity, and other nonlinearity in combination;
- intensity limitation and choice of working point dictated by imperfection resonance crossing in the presence of space charge;
- half-integer coherent resonance crossing;
- collective instability due to transverse coupling impedance;
- halo development and beam loss modeling.

These intensive studies required the deployment of the UAL software on parallel clusters. The original architecture was comfortably fitted to the Message-Passing Interface (MPI) parallel environment without any changes of existing modules. Then the time consuming algorithms were implemented as extensions (C++ shared libraries) and combined with other sequential and parallel components.

5.6.3 Accelerator Propagator Framework

The extensibility of the UAL environment is provided by its main architectural principle: separation of propagators from accelerator elements. This approach enables one to apply a variety of different simulation modules to the same accelerator lattice. Having initially rejected any implicit linkage between algorithm and element, the Accelerator Propagator Framework defines a mechanism for connecting accelerator elements with propagators tailored to each particular simulation model. In order to describe the structure of the simulation model, we have introduced the Accelerator Propagator Description Format (APDF). One can consider the APDF file to be a complement to the MAD lattice file. Its structure and relationship to elements and algorithms are indicated in Fig. 5.22.

Just as the initial lattice description unwinds into a (long) ordered list of all elements in the lattice, the propagator builder associates an appropriate propagator with every element in this list. But, as Fig. 5.22 indicates, default associations permit the APDF file to be quite brief. Some of the possible algorithms are indicated in the figure. ”MltTracker” and ”DriftTracker” implement pure, element-by-element, kick tracking, for example through elements ”qd1” and ”sd1”, by virtue of their element type being either ”quadrupole” or ”sextupole”. ”SectorTracker” implements concatenated, matrix or nonlinear mapping, for example from just before element ”d1” to just before element ”qf1”. Tracking algorithm can also be associated with element based on the element name; for example the ”BPM” algorithm is associated with element ”bpm1” in Fig. 5.22 Like the MAD format, APDF addresses a spectrum of applications ranging from small special tasks to full-scale, realistic model encompassing heterogeneous algorithms and special effects. Some possible modeling scenarios are indicated in Table1, which is intended to be self-explanatory.

Fig. 5.23 shows run-time output from an APDF-based simulation corresponding to application 1 in the table. It is a multiparticle simulation of energy ramping through transition of a bunch of protons. At the transition crossing the RF phase is shifted by π. Most of these scenarios have been applied within UAL in the past, but only as proprietary applications. The APDF provides these capabilities without any additional programming effort.

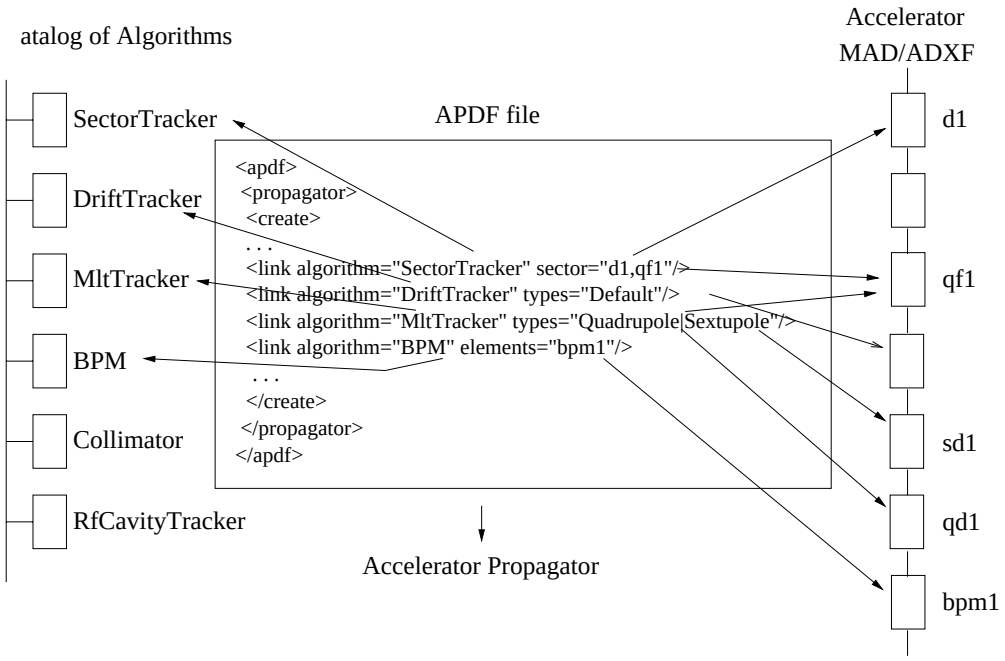

Figure 5.22: Figure illustrating the APDF-defined linkage between accelerator elements (or sectors) on the right to propagation elements on the left.

Table 5.6: Example simulation APF scenarios

	Application	Accelerator propagator
1	Longitudinal beam dynamics	2D sector matrices + RF tracker
2	Linear transverse lattice functions	4D sector matrices
3	Fast online tracking with chromatic effects (Fast Teapot)	6D sector matrices with chromatic extensions + selected quad, sext RF trackers
4	Instumentation modeling, such as tune or beam transfer function	#3 + propagators for selected active diagnostic devices, such as shaker or AC dipole
5	Dynamic aperture, halo, IR background investigation	element-type associations
6	Special localized effect, such as beam-beam, wall impedance or ions	#3 or #5 + propagator for special effect
7	Near-symplectic large amplitude modeling	octupole order maps for imperfections, kick tracking for explicit magnets
8	Full-scale “realistic” model	all of the above

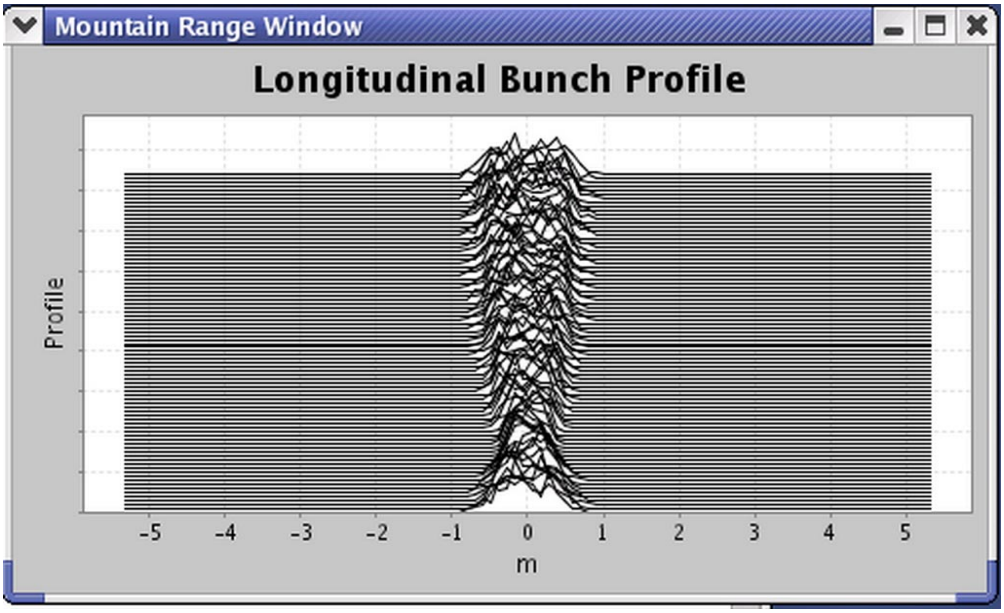

Figure 5.23: Mountain range plot simulating energy ramping through transition.

5.6.4 UAL Architecture

The organization of the UAL components is indicated schematically in Fig. 5.24
At this time, the APF-based modules included in UAL are:

- ZLIB: nmumerical library for differential algebra
- PAC: Platform for Accelerator Codes
- TEAPOT: Thin Element Program for Optics and Tracking
- ACCSIM : Accumulator Simulation Code
- TIBETAN : Longitudinal Phase Space Tracking Program

Modules that are partially supported and are under active development are

- ICE: Incoherent and Coherent Effects
- AIM: Accelerator Instrumentation Module
- SPINK: tracking code for polarized particles in a circular accelerator

The Application Programming Interface (API), written in Perl, provides a universal shell for integrating and managing all project extensions. Consolidation of C++ interfaces has also created a basis for supporting Swig-based interfaces to other script languages (e.g. Python).

References

[1] N. Malitsky and R. Talman, Unified Accelerator Libraries, AIP 391, 1996.

[2] N.Malitsky et al, *Application of UAL to High-Intensity Beam Dynamics Studies in the SNS Accumulator Ring*, EPAC 2002.

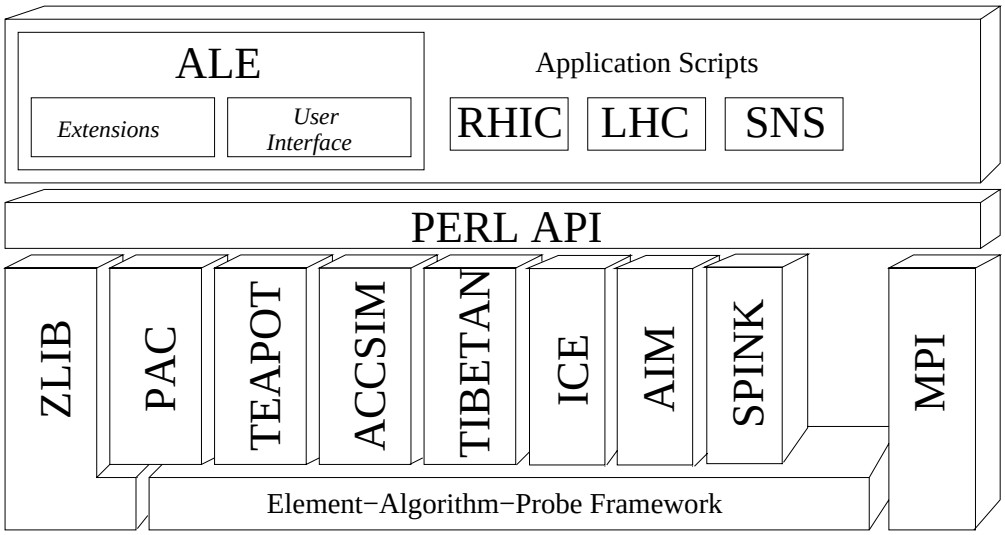

Figure 5.24: UAL architecture. The figure represents dependency metaphorically, by gravity; codes appearing higher up are supported by (that is, use) codes further down. The upper levels of the figure indicate control via scripting language (PERL).

[3] A.V.Fedotov et al. *Effect of Nonlinearities on Beam Dynamics in the SNS Accumulator Ring,* EPAC00, p. 1492.

[4] A.V.Fedotov et al. *Excitation of Resonances Due to the Space Charge and Magnet Errors in the SNS Ring,* PQC01, p. 2878.

[5] See http://www.ual.bnl.gov. References to original reports and publications are contained in the User Guide accessible from that source.

[6] N. Malitsky and R. Talman, *The Framework of Unified Accelerator Libraries,* ICAP98, Monterey, 1998.

[7] N. Malitsky and R. Talman, UAL User Guide, BNL Formal Report 71010-2003, 2002

5.7 New Doctoral Theses in Beam Dynamics

5.7.1 Sarah M. Cousineau

Author: Sarah M. Cousineau (cp3@ornl.gov), Spallation Neutron Source Project, Oak Ridge National Laboratory

Institution: Indiana University

Title: Understanding Space Charge and Controlling Beam Loss in High Intensity Synchrotrons

Date: December 2002

Supervisor: Prof. Shyh-Yuan Lee (shylee@indiada.edu),

Abstract: Future high intensity synchrotrons will require unprecedented control of beam loss in order to comply with radiation safety regulations and to allow for safe, hands-on maintenance of machine hardware. A major cause of beam loss in high intensity synchrotrons is the space charge force of the beam, which can lead to beam halo and emittance dilution. This dissertation presents a comprehensive study of space charge effects in high intensity synchrotron beams.

Experimental measurements taken at the Proton Storage Ring (PSR) in Los Alamos National Laboratory and detailed simulations of the experiments are used to identify and characterize resonances that affect these beams. The collective motion of the beam is extensively studied and is shown to be more relevant than the single particle dynamics in describing the resonance response. The emittance evolution of the PSR beam and methods for reducing the space-charge-induced emittance growth are addressed. In a separate study, the emittance evolution of an intense space charge beam is experimentally measured at the Cooler Injector Synchrotron (CIS) at Indiana University.

This dissertation also investigates the sophisticated two-stage collimation system of the future Spallation Neutron Source (SNS) high intensity accumulator ring. A realistic Monte-Carlo collimation simulation is developed and used to optimize the SNS ring collimation system parameters. The finalized parameters and predicted beam loss distribution around the ring are presented. The collimators will additionally be used in conjunction with a set of fast kickers to remove the beam from the gap region before the rise of the extraction magnets. The gap cleaning process is optimized and the cleaning efficiency versus momentum spread of the beam is examined.

5.7.2 Vahid Ranjbar

Author: Vahid Ranjbar (ranjbar@fnal.gov), Fermi National Accelerator Laboratory

Institution: Indiana University

Title: Increasing Proton Polarization in AGS and RHIC

Date: December 2002

Supervisor: Prof. Shyh-Yuan Lee (shylee@indiada.edu),

Abstract: Polarized protons were accelerated in AGS and RHIC up to 100 GeV during the 2002 polarized proton run. We examined some of the major sources of depolarization in both the AGS and RHIC. In the AGS uncorrected depolarization due to weak intrinsic resonances and coupled spin resonances result in a net loss on the order of 40%. We studied in detail the responses of these resonances to tune, skew quadrupole strength and partial snake strength and compared them against predictions given by an enhanced version of DEPOL.

Three solutions to the remaining weak and coupled spin resonances in the AGS were examined. An 11.4% partial solenoidal snake successfully flipped the spin during an intrinsic resonance crossing, the first time a strong partial snake has been tested in this way. Next we re-examine the proposal to add a family of 12 quadrupoles to the 15th lattice location in the AGS to suppress the weak intrinsic resonances and proposed the addition of a second family of six skew quadrupoles in the 15th location to suppress the coupled spin resonances.

In RHIC higher order snake resonances were observed and measured for the first time. Their location and behavior appeared consistent with current snake resonance theory. Finally using the measured multipole fields along a fixed surface and current, a full field map was developed for RHIC's Siberian snakes. These field maps were used to help control and calibrate the orbit and spin tune in RHIC.

6: Forthcoming Beam Dynamics Events

6.1 29th ICFA Advanced Beam Dynamics Workshop: Beam Halo Dynamics, Diagnostics, and Collimation (HALO'03)

Jie Wei jwei@bnl.gov Collider-Accelerator Department, Brookhaven National Laboratory, Upton, NY 11973, USA

The 29th ICFA Advanced Beam Dynamics Workshop on Beam Halo Dynamics, Diagnostics, and Collimation, in conjunction with the 3rd Workshop on Beam-Beam Interactions, will be held during the week of May 19-23, 2003 (immediately following the week of the 2003 US Particle Accelerator Conference), at Gurney's Inn, located at the eastern end of Long Island, New York, approximately 100 km from Brookhaven National Laboratory. There will be three working groups: halo dynamics (e.g., space charge, magnetic nonlinearities, resonance excitation, beam-beam, intra-beam scattering, instabilities and electron cloud, noise and diffusion processes, analytical and simulation techniques), halo diagnostics (e.g., diagnostics requirements, instrumentation design and performance, machine protection, experimental machine studies), and halo collimation (e.g., lattice design, betatron and momentum collimation design, scraper and collimator design, material tests, machine tests). We intend to publish both the plenary and contributed papers as American Institute of Physics (AIP) Proceedings.

Details of the HALO'03 workshop appear on the web at

http://www.sns.bnl.gov/halo03

Details of the Beam-beam'03 workshop appear on the web at

http://www.rhichome.bnl.gov/AP/BeamBeam/Workshop03

Some general information of the Gurney's Inn is on the web at

http://www.gurneys-inn.com/Welcome.htm

The four-day workshop is planned in 14 sessions. All three working groups of the HALO'03 workshop and the Beam-Beam workshop share five plenary sessions. Nine parallel sessions, organized independently by the chairs of each working group, also include joint sessions between various working groups.

The working group chairs are:

1) HALO'03 Beam dynamics: I. Hofmann (GSI), A. Fedotov (BNL)

2) HALO'03 Diagnostics: K. Wittenburg (DESY), P. Cameron (BNL)

3) HALO'03 Collimation: N. Mokhov (FNAL), A. Drees (BNL)

4) Beam-Beam: Y. Cai (SLAC), T. Sen (FNAL)

International Advisory Committee:

R. Baartman (TRIUMF)	krab@triumf.ca;
W. Barletta (LBNL)	WABarletta@lbl.gov;
A. Chao (SLAC)	achao@SLAC.Stanford.EDU;
I. Gardner (RAL)	I.S.K.Gardner@rl.ac.uk;
H. Haseroth (CERN)	Helmut.Haseroth@cern.ch;
S. Holmes (FNAL)	holmes@fnal.gov;
N. Holtkamp (ORNL)	holtkamp@ornl.gov;
R. Macek (LANL)	macek@lanl.gov;
R. Maier (FZJ)	r.maier@fz-juelich.de;
H. Okamoto (U. Hiroshima)	okamoto@sci.hiroshima-u.ac.jp;
C. Pagani (INFN)	carlo.pagani@mi.infn.it;
G. Rees (RAL)	G.H.Rees@rl.ac.uk;
T. Shea (ORNL)	shea@ornl.gov;
R.H. Siemann (SLAC)	siemann@SLAC.Stanford.EDU;
A.N. Skrinsky (BINP)	A.N.Skrinsky@inp.nsk.su;
W.T. Weng (BNL)	weng@bnl.gov;
H. Wiedemann (SLAC)	wiedemann@SLAC.Stanford.EDU;
F. Willeke (DESY)	Ferdinand.willeke@desy.de;
J.-W. Xia (IMP)	xiajw@impcas.ac.cn;
	and the ICFA Beam Dynamics Panel member.

Program Committee:

J.M. Brennan (BNL)	brennan@bnl.gov;
W. Chou (FNAL)	chou@fnal.gov;
Y. Fedotov (IHEP)	fedotov_yu@mx.ihep.su ;
R. Garoby (CERN)	roland.garoby@cern.ch;
S. Henderson (ORNL)	henderson@ornl.gov;
I. Hofmann (GSI)	i.hofmann@gsi.de;
J.-M. Lagniel (CEA)	jean-michel.lagniel@cea.fr;
N. Mokhov (FNAL)	mokhov@fnal.gov;
Y. Mori (KEK)	yoshiharu.mori@kek.jp;
A. Mosnier (CEA)	amosnier@cea.fr;
C. Prior (RAL)	C.R.Prior@rl.ac.uk;
T. Raubenheimer (SLAC)	tor@slac.stanford.edu;
T. Roser (BNL)	roser@bnl.gov;
F. Ruggiero (CERN)	francesco.ruggiero@cern.ch;
H. Schmickler (CERN)	Hermann.Schmickler@cern.ch;
K. Takayama (KEK)	takayama@post.kek.jp;
H. Thiessen (LANL)	hat@lanl.gov;
R. Wanzenberg (DESY)	rainer.wanzenberg@desy.de;
R. Webber (FNAL)	webber@fnal.gov;
J. Wei (Chair, BNL)	jwei@bnl.gov

Local Organizing Committee:

P. Cameron	Cameron@bnl.gov;
M. Campbell	maryc@bnl.gov;
A. Drees	drees@bnl.gov;
A. Fedotov	Fedotov@bnl.gov;
N. Franco	franco@bnl.gov;
J. Hauser	hauser@bnl.go;
L. Hoff	hoff@bnl.go;
P. Manning	pmanning@bnl.gov;
S. LaMontagne	stephl@bnl.gov;
W. McGahern	wmcgahern@bnl.gov;
D. Raparia	Raparia@bnl.gov;
N. Simos	simos@bnl.gov;
J. Wei (Chair)	jwei@bnl.gov;
D. Zadow	zadow@bnl.gov

Sponsorship: Brookhaven National Laboratory, Brookhaven Science Associates, Spallation Neutron Source Project, US Department of Energy, ICFA Panel on Beam Dynamics

6.2 Third Workshop on Beam-Beam Interactions

Wolfram Fischer wfischer@bnl.gov Collider-Accelerator Department, Brookhaven National Laboratory, Upton, NY 11973, USA

A workshop on beam-beam effects in collider rings will be held near Brookhaven National Lab from May 19 to 23th, 2003 in conjunction with the 29th Advanced ICFA Beam Dynamics Workshop HALO'03. A single registration fee allows participants to attend both workshops. The workshop follows directly the PAC'03 conference in Portland, Oregon.

The workshop will review progress in the understanding of beam-beam effects in hadron and lepton collider rings. The organization parallel to the HALO'03 workshop offers the unique opportunity to discuss the role of beam-beam effects in halo formation, as well as means to detect and remove halos.

Workshop topics to be discussed include:

Beam-beam limits, especially coherent limits and their effects on existing and future hadron colliders Beam-beam compensation techniques, particularly for long-range interactions Beam-beam study tools in theory, simulation, and experiment

Workshop web page: http://www.rhichome.bnl.gov/AP/BeamBeam/Workshop03/

Beam-Beam Workshop Committee:

Y. Cai (SLAC)	yunhai@slac.stanford.edu;
W. Fischer (BNL)	wfischer@bnl.go;
M. Furman (LBNL)	MAFurman@lbl.gov;
W. Herr (CERN)	Werner.Herr@cern.ch;
M. Minty (DESY)	michiko.minty@desy.de;
F. Pilat (BNL)	pilat@bnl.gov;
T. Sen (FNAL)	tsen@fnal.gov;
R. Talman (Cornell)	talman@lns61.tn.cornell.edu ;
K. Yokoya (KEK)	kaoru.yokoya@kek.jp

6.3 Workshop on e^+e^- in the 1-2 GeV range: Physics and Accelerator Prospects

(ICFA Mini-workshop - Working Group on High Luminosity e+e- Colliders)

The Workshop, sponsored by Istituto Nazionale di Fisica Nucleare (INFN), Università di Cagliari and Università di Sassari, will be jointly organized by INFN-LNF, INFN-Roma1, Università di Sassari and will be held on **10-13 September 2003** at Alghero (SS), Italy. The aim of the Workshop is to discuss the physics issues and to address the strategies and the problems towards higher luminosities in the energy range between 1 and 2 GeV. Particular attention will be devoted to possible future upgrades of DAFNE. Physics topics will include precision measurements of nucleon form factors, low energy spectroscopy, physics of hypernuclei, tests of fundamental symmetries through rare kaon decays, gamma-gamma interactions. The Workshop is organized in plenary sessions and working groups. The expected attendance is about one hundred participants. All the relevant information is available on the Workshop Website:

http://www.lnf.infn.it/conference/d2/

Please, check regularly the content of the website to be informed of the latest information concerning the workshop.

7: Announcements of the beam Dynamics Panel

7.1 ICFA Beam Dynamics Newsletter

7.1.1 Aim of the Newsletter

The ICFA Beam Dynamics Newsletter is intended as a channel for describing unsolved problems and highlighting important ongoing works, and not as a substitute for journal articles and conference proceedings that usually describe completed work. It is published by the ICFA Beam Dynamics Panel, one of whose missions is to encourage international collaboration in beam dynamics.

Normally it is published every April, August and December. The deadlines are 15 March, 15 July and 15 November, respectively.

7.1.2 Categories of Articles

The Beam Dynamics Newsletter particularly encourages contributions from smaller institutions and countries where the accelerator physics community is small.

The categories of articles in the newsletter are the following:

Announcements from the panel.

Reports of Beam Dynamics Activity of a group.

Reports on workshops, meetings and other events related to Beam Dynamics.

Announcements of future Beam Dynamics-related international workshops and meetings.

Those who want to use newsletter to announce their workshops are welcome to do so. Articles should typically fit within half a page and include descriptions of the subject, date, place, Web site and other contact information.

Review of Beam Dynamics Problems: this is a place to bring attention to unsolved problems and should not be used to report completed work. Clear and short highlights on the problem are encouraged.

Letters to the editor: a forum open to everyone. Anybody can express his/her opinion on the beam dynamics and related activities, by sending it to one of the editors. The editors reserve the right to reject contributions they judge to be inappropriate, although they have rarely had cause to do so.

Editorial.

The editors may request an article following a recommendation by panel members. However anyone who wishes to submit an article is strongly encouraged to contact any Beam Dynamics Panel member before starting to write.

7.1.3 How to Prepare a Manuscript

Before starting to write, authors should download *the latest* model article file, in Microsoft Word format, from the Beam Dynamics Panel home page

http://wwwslap.cern.ch/icfa/

It will be much easier to guarantee acceptance of the article if the latest model is used and the instructions included in it are respected. These model files and instructions are expected to evolve with time so please make sure always to use the latest versions.

The final Microsoft Word file should be sent to one of the editors, preferably the issue editor, by email.

The editors regret that LaTeX files can no longer be accepted: a majority of contributors now prefer Word and we simply do not have the resources to make the conversions that would be needed. Contributions received in LaTeX will now be returned to the authors for re-formatting.

In cases where an article is composed entirely of straightforward prose (no equations, figures, tables, special symbols, etc.) contributions received in the form of plain text files or simply formatted Word files may be accepted at the discretion of the issue editor.

Each article should include the title, authors' names, affiliations and e-mail addresses.

7.1.4 Distribution

A complete archive of issues of this newsletter from 1995 to the latest issue is available at

http://wwwslap.cern.ch/icfa/

This is now intended as the primary method of distribution of the newsletter.

Readers are encouraged to sign-up for to electronic mailing list to ensure that they will hear immediately when a new issue is published.

The Panel's Web site provides access to the Newsletters, information about Future and Past Workshops, and other information useful to accelerator physicists. There are links to pages of information of local interest for each of the three ICFA areas.

Printed copies of the ICFA Beam Dynamics Newsletters are also distributed (generally some time after the Web edition appears) through the following distributors:

Weiren Chou chou@fnal.gov North and South Americas

Helmut Mais mais@mail.desy.de Europe* and Africa

Susumu Kamada Susumu.Kamada@kek.jp Asia** and Pacific

* Including former Soviet Union.

** For Mainland China, Chuang Zhang (zhangc@bepc3.ihep.ac.cn) takes care of the distribution with Ms. Su Ping, Secretariat of PASC, P.O.Box 918, Beijing 100039, China.

To keep costs down (remember that the Panel has no budget of its own) readers are encouraged to use the Web as much as possible. In particular, if you receive a paper copy that you no longer require, please inform the appropriate distributor.

7.2 ICFA Beam Dynamics Panel Members

The views expressed in this newsletter do not necessarily coincide with those of the editors. The individual authors are responsible for their text.

Caterina Biscari	caterina.biscari@lnf.infn.it	LNF-INFN, Via E. Fermi 40, Frascati, Italy
Swapan Chattopadhyay	swapan@jlab.org	Jefferson Lab, 12000 Jefferson Avenue, Newport News, VA 23606, USA
Pisin Chen	chen@slac.stanford.edu	SLAC, P.O. Box 4349, MS26, Stanford, CA 94309, USA
Weiren Chou	chou@fnal.gov	FERMILAB, MS 220, P.O.Box 500, Batavia, IL60510, USA
Yoshihiro Funakoshi	yoshihiro.funakoshi@kek.jp	KEK, Oho, Tsukuba, IBARAKI 305-0801, Japan.
Kohji Hirata	hirata@soken.ac.jp	Sokendai, the Graduate Univ. for Advanced Studies, Shonan Village, Hayama, Miura, Kanagawa, 240-0193, Japan
Sergei Ivanov	ivanov_s@mx.ihep.su	Institute for High Energy Physics, Protvino, Moscow Region, 142281 Russia
John M. Jowett	John.Jowett@cern.ch	CERN, CH-1211 Geneva 23, Switzerland
Kwang-Je Kim	kwangje@aps.anl.gov	Argonne Nat. Lab., Advanced Photon Source, Accelerator Systems Division, 9700 S. Cass Avenue, Bldg 401/C4265, Argonne, IL 60439
Alessandra Lombardi	Alessandra.Lombardi@cern.ch	CERN, CH-1211 Geneva 23, Switzerland
Helmut Mais	mais@mail.desy.de	DESY, Notkestrasse, 85 D-2000, Hamburg 52, Germany
Olivier Napoly	Olivier.Napoly@cea.fr	DAPNIA-SEA, CEA Saclay, 91191 Gif/Yvette CEDEX, France
David Rice	dhr1@cornell.edu	Cornell University, 271 Wilson Lab, Ithaca, NY 14853-8001, USA
Yuri Shatunov	Yu.M.Shatunov@inp.nsk.su	Acad. Lavrentiev prospect 11, 630090 Novosibirsk, Russia
Jie Wei	wei1@bnl.gov	BNL, Bldg. 911, Upton, NY 11973-5000, USA
JiuQing Wang	wangjq@mail.ihep.ac.cn	IHEP, CAS, BEPC National Laboratory, P.O. Box 918, 9-1, Beijing 100039, China